Effects of riparian vegetation on meandering rivers

MSc. Thesis Earth sciences
Track: Earth, surface and water
Roy Teske BSc. 3345939
Version 2
September 2012-February 2013
Supervisor: dr. M.G. Kleinhans
2nd supervisor: W.M. van Dijk MSc.

Abstract

Vegetation that is present, along meandering river systems, is known as riparian vegetation. Riparian vegetation cover has been recognised to affect the strength of the banks and the hydraulic resistance of the floodplain. The river in turn has affects the riparian pattern formation. A more thorough understanding of the specific contributions of vegetation in relation to meandering river dynamics is beneficial for re-meandering projects and flood risk control measurements in real systems. In recent experimental scale meandering rivers alfalfa sprouts were used to change width depth ratios and channel patterns. The effects of vegetation on an already meandering system have not been investigated. The main aim of this thesis is to evaluate the effects of riparian vegetation on the hydraulic roughness of the floodplain, self-formed meandering river pattern and river dynamics. To isolate the hydraulic roughness effects and bank strength of vegetation a new annular flume setup was used. The effect on channel patterns was investigated using a 3x10 m flume. The scaling of the hydraulic resistance was determined by conducting measurements in a 4x52 m long with a full scale natural vegetation cover. The effect of vegetation on the meandering river patterns was a reduction of the bank erosion with a change in bank failure mechanics. These changes resulted in asymmetric sharp meander bends. The hydraulic resistance of vegetation in scale experiments proved difficult to quantify. It was strongly influenced by the flume specific vegetation cover condition and linked to the morphologic development. An approximate quantitative scaling in terms of resistance values was found with a real natural vegetation cover in a controlled flume environment. The dominant effects of riparian vegetation in the scale experiments can be identified as the stabilization of the banks by a vegetation induced bank strength as well as an increase in the hydraulic resistance.

Keywords: Riparian vegetation, hydraulic resistance, channel pattern, annular flume

Contents

Abstract 2
list of figures 5
list of tables 7
1. Introduction 9
Part I Literature review on meandering river, riparian vegetation and physical modelling 10
2. Literature review 11
2.1 Meandering river formation, flow and morphology 12
2.1.1 Meandering river morphology 15
2.1.2 Meander bend flow 15
2.1.3 Bar theory 17
2.1.4 Floods and overbank flow 20
2.2 Riparian vegetation 20
2.2.1 Engineering properties of riparian vegetation 25
2.2.2 Biotic factors 19
2.2.3 Abiotic processes 29
2.2.4 Biotic and abiotic factor importance 31
2.2.5 Patterns in riparian vegetation 32
2.3 Experimental scale self-formed river research 36
2.3.1 Previous experiments 36
2.3.2 Overbank flow and morphology 38
2.3.3 Scaled riparian vegetation 39
2.3.4 Scaled riparian vegetation patterns 42
3. Syntheses, research questions and hypotheses 43
3.1 Synthesis and research questions 43
3.2 Hypothesis 45
Part II Experimental setups and results 47
4. Methodology and methods 48
4.1 Methodology 48
4.2. Methods and materials 49
4.2.1 Alfalfa support experiments 49
4.2.2 Eurotank facility 50
4.2.3 Annular flume 53
4.2.4 Chillworth flume 55
4.2.5 Richardson and Carling (2006) velocity method 58
5. Results 60
5.1 Copper sulphate tolerance test 60
5.2 Eurotank experiments 61
5.2.1 Morphological development 61
5.2.2 Bank erosion and failure 68
5.2.3 Cut-offs 71
5.2.4 Hydrodynamics 73
5.2.5 Riparian vegetation cover development 78
5.2.6 Overview of the experimental meandering river development 80
5.3 Annular flume 81
5.3.1 Hydrodynamics 81
5.3.2 Morphological development 88
5.3.3 Riparian vegetation cover development 94
5.3.4 Overview of the annular flume development 95
5.4 Chilworth flume 96
5.4.1 Vegetation composition and density 96
5.4.2 Cross-sections, water levels and slopes 98
5.4.3 Flow, tracer dispersion and velocities 100
5.4.4 Hydraulic resistance 102
5.5 Baptist vegetation resistance modelling 104
5.5.1 Chilworth flume 104
5.5.2 Scale experiments 105

6. Discussion 106
6.1 Velocity measurement inaccuracy 106
6.2 Scale experiment flow and morphology 106
6.2.1 Experimental river morphology 106
6.2.3 Annular flume morphology 107
6.2.2 Channel bend flow 108
6.2.4 Transverse bed slope 108
6.2.5 Overbank flow and discharge division 109
6.3 Engineering effect scaling 111
6.3.1 Bank strength and failure 111
6.3.2 Hydraulic resistance 113
6.3.3 Sediment trapping 116
6.4 Biotic factor representation 116
6.4.1 Succession and rejuvenation 116
6.4.2 Development time scale 117
6.4.3 Large wooded debris 117
6.5 Vegetation patterns 117
6.6 Hierarchical control of the experimental meandering river development 119
6.7 Further research recommendations 119
7. Conclusions 120
8. Acknowledgements 121
9. Summary 122
10. List of symbols 124
11. References 126

List of figures

Figure 2.1 The hierarchal control order of riparian forest development
Figure 2.2 The different channel patterns of rivers.
Figure 2.3 The conceptual development of a meandering river bend
Figure 2.4 Cross-sectional view of a meandering river.
Figure 2.5 Cross-sectional view of the flow and shear stress vector in a meandering river.
Figure 2.6 Flow in an alternate bar and central bar channel.
Figure 2.7 Two types of flow form the channel to the floodplain.
Figure 2.8 Flow division between the channel and floodplain.
Figure 2.9 The direction of the flow in the channel and floodplain in a fixed bed flume study.
Figure 2.10 Flow velocity in a rough and non-rough channel floodplain system.
Figure 2.11 Two examples of riparian vegetation patterns along a meandering river bend.
Figure 2.12 Failure mechanisms of river banks.
Figure 2.13 The sum of the moments around the beam of failure determines the stability of the undercut bank.
Figure 2.14A Flow over submerged vegetation
Figure 2.14B Effective water depth schematization
Figure 2.15 The succession of riparian vegetation form a pioneer to a climax forested state
Figure 2.16 Relative importance of abiotic and biotic control of factors that affect vegetation development.
Figure 2.17 Cross-sectional view of the pointbar and the different abiotic vegetation disturbance and settling controlled zones.
Figure 2.18 River process control on vegetation development.
Figure 2.19 An impression of the different meandering river morphologic feature and the corresponding riparian vegetation cover.
Figure 2.20 Vegetation succession in relation to pointbar development.
Figure 2.21 Ridge and swale topography is visible in the riparian vegetation cover.
Figure 2.22 Abandoned channel vegetation development.
Figure 2.23 Vegetation pattern model output in relation to vegetation dispersal.
Figure 2.24 The decrease in the wetted area and deepening of the channels due to the change in channel pattern
Figure 2.25 The change in channel planform due to the introduction of alfalfa seeds.
Figure 2.26 Overbank morphology in the experiments of Braudrick et al. (2009).
Figure 2.27 Overbank morphology in the annular flume.
Figure 2.28 The cohesion values (kPa) and angles of internal friction (°) for alfalfa sprouts of different ages and in different density compositions.
Figure 2.29 Volume of eroded sediment over time for different vegetation covers of alfalfa.
Figure 2.30 Eroded sediment for different flood disturbance scenarios.
Figure 2.31 The length of alfalfa stems over time.
Figure 2.32A Alfalfa growth on the swales of the pointbar.
Figure 2.32B Bare sediment on newly formed inner bend accumulations.
Figure 4.1 The sequence of the experiments that are to be conducted in order to answer the main questions of this report.
Figure 4.2 An upstream looking image of the Eurotank setup.
Figure 4.3 The sediment feed and discharge during the experiment.
Figure 4.4 Sieving curve of the Eurotank and annular flume sediment.
Figure 4.5 Annular flume setup that allows controlled and constant over bank inundation levels and flow velocities.
Figure 4.6 The bare sediment filled flume. ***B*** *The recently seeded flume.* ***C*** *The seeded flume before the experiments with a 3.0 seeds/cm^2 density.*
Figure 4.7 The Chilworth flume. ***A*** *tree and litter composition* ***B*** *trees only composition*
Figure 4.8 Top down view of the Chilworth flume layout.
Figure 4.9 Overview of the ADZ model measurement locations (A) and resulting graphs (B).
Figure 4.10 RGB based tracer concentrations in the Eurotank facility.
Figure 4.11 Tracer dispersion in the meandering river experiment.
Figure 5.1 ***A*** *The number of sprouted alfalfa from an initial 50 added seeds for a range of copper sulphate concentrations* ***B*** *Alfalfa sprout length development over time as a result of different concentrations of copper sulphate additive.*
Figure 5.2 Reworked area in the alfalfa covered experimental river system and a control experiment.
Figure 5.3 The sinuosity of the vegetation covered floodplain river and a control experiment.

Figure 5.4 Meandering river cross-sections.
Figure 5.5 Transverse bed slope for the river initial stage, vegetation stage and a control experiment.
Figure 5.6 Surface elevation in the vegetation and a no-vegetation control experiment.
Figure 5.7 w/h ratios at different stages in the vegetation experiment and the control data.
Figure 5.8 Digital elevation maps and images of the meandering river development.
Figure 5.9 Erosion areas in the initial and vegetation stage meandering river.
Figure 5.10 A, B and C Outer bank failure in the meandering river.
Figure 5.11 Failed undercut meandering river vegetated channel margin.
Figure 5.12 Erosion rate of the scale meandering river bank over time.
Figure 5.13 Bend development of the vegetation stage experimental meandering river.
Figure 5.14 Wetted area of the non-vegetated control and vegetated river.
Figure 5.15 Flow over the un-vegetated and vegetated central bend inner bend.
Figure 5.16 Tracer plume passing for the pointbar location with a discharge of 1800l/h for a bare sediment and alfalfa covered floodplain.
Figure 5.17 Chézy and Darcy-Weisbach friction factor ranges for the meandering river floodplain.
Figure 5.18 Vegetation development overview in the meandering river
*Figure 5.19 **A** Burial of scale vegetation.*
*Figure 5.19 **B** Undisturbed pristine floodplain margins.*
Figure 5.20 Scale vegetation erosion features.
*Figure 5.21 **A** Secondary flow along the bed of the annular flume.*
*Figure 5.21 **B** The direction of the flow in the equilibrium no-vegetation annular flume.*
*Figure 5.22 **A** Low vegetation density vegetation cover region of influence from channel flow.**B** High vegetation density cover relative disturbance on the floodplain from channel flow.*
Figure 5.23 Overbank flow cells in the annular flume.
Figure 5.24 Tracer movement oscillations in the annular flume overbank.
*Figure 5.25 **A** Annular flume overbank Chézy values. **B** Annular flume overbank Darcy-Weisbach values.*
Figure 5.26 Retreat of the annular flume outer bank.
Figure 5.27 Bare sediment filled flume morphologic development.
*Figure 5.28 **A** The final morphology profile for a no-vegetation scenario.*
*Figure 5.28 **B** High vegetation density equilibrium profile.*
Figure 5.29 High vegetation density vegetation cover and channel development.
Figure 5.30 Morphologic development of the annular flume for a high vegetation density floodplain cover.
Figure 5.31 Erosion of the 1.5 seed/cm^2 vegetated outer bank.
Figure 5.32 Morphologic development of the channel bed for the light vegetation density scenario.
*Figure 5.33 **A** Annular flume bed after 15 minutes of flow.*
*Figure 5.33 **B** Equilibrium profile for the increased (3.5kHz) forcing run.*
Figure 5.34 Silica flour deposition along the channel margin.
Figure 5.35 Local erosion of the channel bed behind a debris sprout of alfalfa.
Figure 5.36 Annular flume low density high forcing vegetation pattern.
Figure 5.37 Overview of the undisturbed Chilworth flume vegetation cover.
Figure 5.38 The vegetation density at chest height in the flume.
Figure 5.39 The flume with the litter layer and bulk of the trees removed leaving the thickest trunks intact.
Figure 5.40 The water level mark in the flume for the different run conditions
Figure 5.41 Discharge based on cross-section and velocity plotted against the hydraulic radius.
Figure 5.42 The peak tracer velocity plotted against the tracer front velocity for the intact flume and the trees only scenario.
Figure 5.43 Fluorometer data of run T2 for the upstream r_2 (blue) and downstream r_4(red) locations.
Figure 5.44 Shear stress plotted against the Reynolds number.
Figure 5.45 Chézy and Darcy-weisbach friction factors for the Chilworth flume vegetation compostions.
Figure 9.46 The Chilworth experimental measurement based and model base roughness.
Figure 6.1 Comparion of the river Allier and the scale experimental river.
Figure 6.2 The transverse bed slopes in the scale experiments.
Figure 6.3 Bank erosion in the scale experiments expressed in width per hour.
Figure 6.4 The Baptist et al. (2006) mode output for the annular flume with a varying vegetation density.
Figure 6.5 Hierarchical control for the meandering river experiment.

List of tables

Table 4.1 Different copper sulphate test sample concentrations.
Table 4.2 Overview of the different densities of alfalfa used in the experiments and the required amount of seeds.
Table 4.3 Design conditions of the meandering river experiment
Table 4.4 Overview of the used discharges in the Eurotank facility.
Table 4.5 The annular flume disk velocity in the centre of the channel.
Table 4.6 Fixed annular flume parameters used in this report.
Table 4.7 Overview of the Chilworth runs and boundary conditions
Table 4.8 Dilutions used to calibrate the fluorometer used in the Chilworth experiments.
Table 5.1 Overview of the different stages in the meandering river development
Table 5.2 Overview of the meandering river velocities for different discharge and vegetation scenarios.
Table 5.3 Average channel velocities in the annular flume for a range of channel forcing's and overbank composition scenarios.
Table 5.4 Overview of the annular flume overbank velocities.
Table 5.5 Overview of the conducted runs and measured parameters in the Chilworth flume.
Table 5.6 Model input parameters for the specific flume environments.
Table 5.7 The scale experimental Reynolds number based roughness and the Baptist et al. (2006) model output.
Table 6.1 Roughness values in the experiments and literature.

1. Introduction

Meandering rivers are found in abundance on the Earth's surface. In a natural environment they interact with vegetation to shape entire landscapes. However meandering rivers have proven to be difficult to recreate in laboratory environments, until recently. In recent experiments the addition of scale vegetation to the flumes reduced the width/depth ratios of the channels. This proved crucial in forming a more meandering river planform. The same effect of vegetation on channel pattern occurred in the real world. The evolution of plants 250Ma. created and overall shift in channel pattern from braiding rivers to meandering (Gibling and Davies, 2012).

The dynamic interactions between riparian (from Latin riparius meaning *near the river*) vegetation and meandering river systems are not yet completely understood. They play a significant role in the evolution of both riparian vegetation and river systems (Eaton and Gilles, 2008, Osterkamp and Hupp 2010). The current state of knowledge on riparian vegetation and river interactions is based on work done in two separate fields. There is a contribution from a sedimentology, engineering and physical geography based field. The main focus of this field are the mechanics of flow and the morphology of rivers. Other work has been carried out from a more ecological and biological point of view. They regard riparian zones are highly biologically dynamic and diverse habitats (Gurnell and Petts, 2002).

The recent development of experimental scale meandering rivers (Van Dijk et al., 2012) may provide an excellent setup to combine the knowledge regarding rivers and riparian vegetation from both fields. The aim of this report is to investigate the influence of riparian vegetation patterns on meandering river morphology.

Part I. Literature review on meandering rivers, riparian vegetation and physical modelling

In order to identify the effects of riparian vegetation on meandering rivers a literature review is presented that provides background knowledge to the main subject. The first part of the review focusses on the main meandering river morphodynamics, channel bend and overbank flow mechanics. The second part of the review defines riparian vegetation and elaborates the various effects of riparian vegetation on the river. Furthermore the effects of the river environment on the riparian vegetation are explained and the resulting patterns in the vegetation cover are given. This is followed by a summarization of scale river experiments aimed at creating meandering rivers that serve as a basis for the design of the experiments used in this report.

2. Literature review

This literature report presents a theoretical background. It covers the basic theory of meander formation and the flow dynamics of meandering rivers. Riparian vegetation is explained in relation to the succession of vegetation and the effects on the river. Finally scale meandering river experiments are presented.

The processes in the dynamic river (chapter 2.1) and riparian vegetation systems (chapter 2.2) consist of multiple interactions between components of both systems. The hierarchy of the interlinked nature of riparian vegetation and river systems is visualized in figure 2.1 (Naiman et al., 1998). The basis of the system development is the geologic structure. The vegetation development is determined by both biotic (seed dispersal and succession) and abiotic or hydrologic (floods, drought and burial) factors) (Gurnell and Petts, 2002). The combined factors shape the riparian vegetation cover, which affects the river.

In figure 2.1 the Roman letter indices are used to describe the components of the system I,II,III and IV. The feedbacks between the components of riparian vegetation and meandering river systems are marked with the lower case letters *a* till *f*. In the rest of the literature review figure 2.1 is used as a basis for indicating which process is discussed. The geologic structure (I) is the meandering river it is disused in chapter 2.1. The effects of the hydrologic (II) regime are *a* (chapter 2.1.4) and *d* (chapter 2.2.3). The biotic characteristics (III) effects *b* (chapter 2.2.1), *c* (chapter 2.2.2) and *e* (chapter 2.2.3). These interactions together shape the riparian forest (IV) and create distinctive patterns (chapter 2.2.5. Finally scale meandering river experiments are presented in chapter 2.3 in terms of system development (chapter 2.3.1), overbank flow dynamics (chapter 2.3.2) and scaled riparian vegetation (chapter 2.3.3).

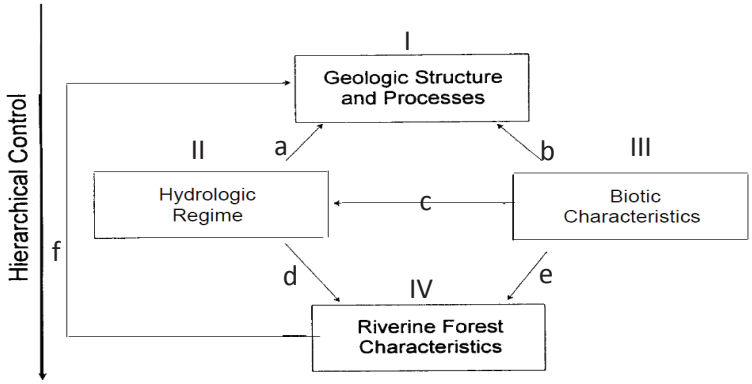

Figure 2.1. The hierarchal control order of riparian forest development (Naiman et al., 1998). The indices are added to this image.

2.1 Meandering river formation, flow and morphology

Rivers found at the earth's surface are shaped by the feedback between bars, channels, floodplain and vegetation. The ratio of floodplain formation and destruction determines the width of the river, which in turn determines the formation of bars and the channel pattern (Kleinhans, 2010). The resulting rivers can be divided into different classes, based on their planform and characteristics. Traditionally three classes were distinguished; braiding, meandering and straight (Leopold and Wolman 1957). A more recent classification ads a fourth type of river, sinous. Sinuous rivers have no lateral migration, unlike meandering rivers. In addition multi-channel or anabranched variants of each planform are found (Kleinhans, 2010). An overview of the river patterns is given in figure 2.2.

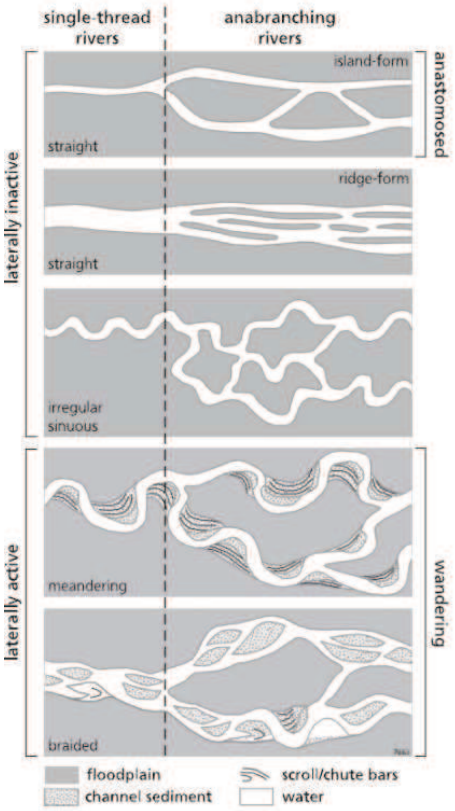

Figure 2.2. The different channel patterns of rivers. The main divisions are based on lateral activity and number of channels (Kleinhans and van den Berg, 2011).

Straight rivers occur in areas where the banks are relatively material. The strength of the banks prevents lateral migration. The anabrached straight river is known as anastomosing. The multiple channels of anastomosing rivers bifurcate upstream and converge again downstream. The channels display little lateral activity, due to the high bank strength. (Kleinhans and van den Berg, 2010).

The two important channel patterns related to physical scale river experiments are braided and meandering. Braided is often found for flow over non-cohesive beds. Without cohesion to stabilize the banks the river can widen itself by lateral erosion and form new channels (Tal et al. 2003). The braided systems consist of multiple active channels with multiple active bars in between them.

With added bank strength, either the result of cohesive fines or vegetation, the lateral expansion of rivers can be controlled and meandering rivers are able to form. In meandering rivers the locations of the bars are forced to the inner bends of the system (Kleinhans and van den berg, 2010). The main difference between a meandering and a sinuous channel is the erosion of the banks. In sinuous rivers no or very little erosion and thus lateral mobility of the channel is present. The focus of the literature report are meandering rivers.

Meandering rivers are a common form of natural river occurrence (Leopold and Wolman, 1957). They are characterised by the sinuous shape and lateral active behaviour. In the bends intricate secondary flow patterns develop that shape the morphology of the bend. Outside of the channel meandering rivers deposit fine sediment that forms overbank morphology. Furthermore they

balance the destruction and formation of floodplain deposits. This results in a relatively constant with depth ratio and prevents braiding of the river (Kleinhans and van den Berg, 2010).
The degree of meandering in a river is often expressed using the sinuosity. The sinuosity is calculated by taking the length of the channel and dividing it by the straight line distance in the direction of the valley. A lower sinuosity value means that the river is more straight. Higher sinuosity value tend to indicate a more curvy river.
The development of a meander bend can be expressed conceptually by plotting the rate of movement at the band apex against the r/w ratio. This results in a conceptual plot that distinguishes three different stages (figure 2.3) (Hooke, 1984). The initiation stage of the meander bend, is the onset of bend development. The growth period indicates the lateral expansion of the bend. The termination stage is the period that leads up to a bend cut-of. The occurrence of a cut-off will lead to a decrease in the sinuosity of the river. This can be a chute cut-off, in case of flow over the higher part of the active pointbar, or a neck cut-off. A neck cut-off occurs in high sinuosity systems where the upstream and downstream channel of a bend intersect (van Dijk et al., 2012).

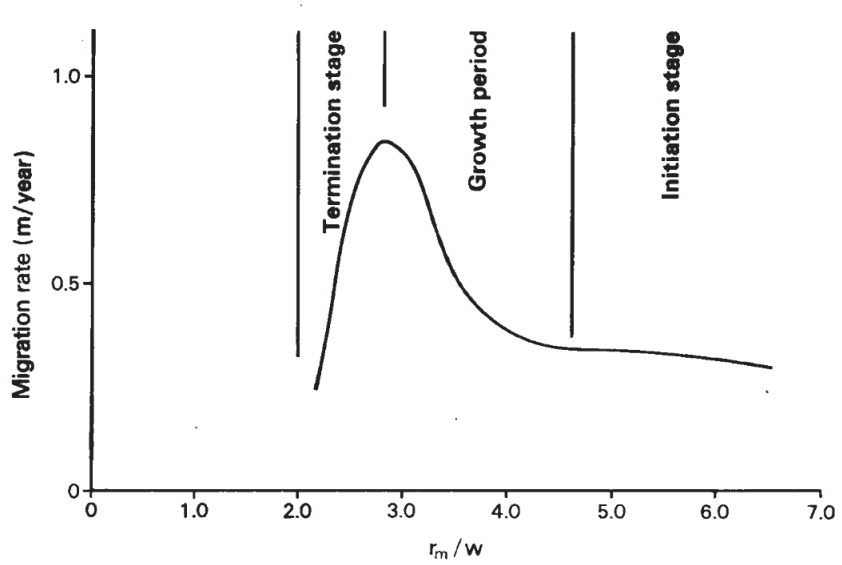

Figure 2.3. The conceptual development of a meandering river bend. Three different stages are indicated (Hooke, 1984)

2.1.1 Meandering river morphology

Meandering rivers can be subdivided into different distinctive morphological and sedimentological components. An overview of the different units is given in figure 2.4. The main characteristics of each morphological feature are given below.

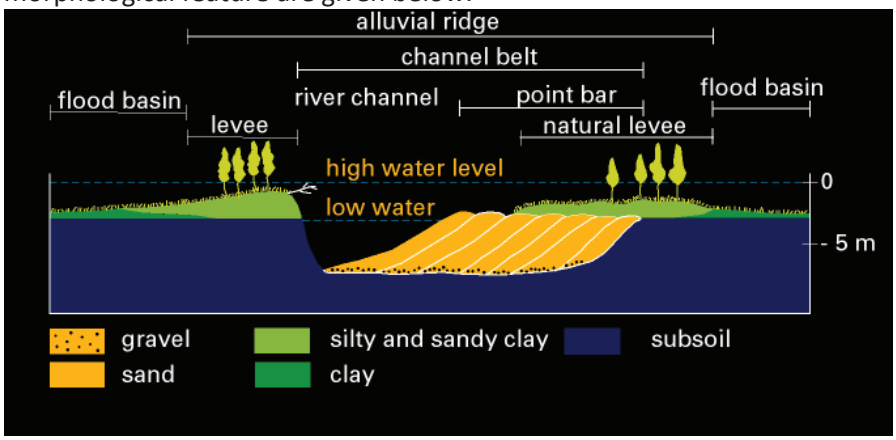

Figure 2.4. Cross-sectional view of a meandering river. Indicated in the figure are the different morphological units (Berendsen and Stouthamer, 2001).

Point bars

Within the main channel fixed bars are present on the inner bends of the channels. These bars are called scroll bars and accumulate into pointbar deposits (Kleinhans, 2010) The formation of scroll bars is driven by the secondary. Sediment is transported by the current towards the inner bend where it can accumulate. The sloping deposits often display a fining trend from the bottom to the top. This is due to the current that acts on the surface of the grains to transport them up the slope, but gravity acts on the volume to pull them down. This means larger particles, gravel, are deposited on the base of the channel and finer sediment is found higher up the slope.

The slope of the inner bar bend can be predicted by the transverse bed slope prediction equation (Talmon et al., 1995):

$$(1)\ \ tan\left(\frac{\delta z_p}{\delta y_p}\right) = f(\theta)\frac{2}{k^2}\left(1 - \frac{\sqrt{g}}{kC}\right)\frac{h}{r}$$

in which z_p is the pointbar height (m), y_p is the horizontal length (m), k is the Karman constant (0.4), C is the Chézy hydraulic resistance, h is the average water depth (m) and r the radius of the channel bend (m).

The transverse slope effect ($f(\vartheta)$) is:

$$(2)\ \ f(\theta) = 9\left(\frac{D_{50}}{h}\right)^{0.3}\sqrt{\theta}$$

where D_{50} is the median grain size (m), h is the average water depth (m) and Θ is the non-dimensional Shields parameter.

$$(3)\ \ \theta = \frac{\tau_t}{(\rho_s - \rho)D_{50}}$$

The total shear stress (τ_t) can be expressed as a function of the hydraulic radius and slope

$$(4)\ \ \tau_t = \rho g R S$$

The hydraulic resistance (C) is the Chézy value. That is calculated using the depth average flow velocity u (m/s), slope S (m/m) and the hydraulic radius R (m):

$$(5)\ \ C = \frac{u}{\sqrt{RS}}$$

where the hydraulic radius for a rectangular channel is:

$$(6)\ \ R = \frac{wh}{w + 2h}$$

The pointbar is not fixed in space, it moves in the outer bend direction due to erosion of the outer bend and accretion on the inner bend. The rate at which the bend migrates is determined by the strength of the outer bend and the accretion velocity of the inner bend. If these two are balanced, the meandering river is stable. Some numerical modelling has been performed on bend migration, but this considers only idealized representations of outer meander bend strength parameters. This is done for example in the work of Crosato (2007).

Levees and floodplain

Outside of the channel additional morphological features are present. On the margins of the channel levees are found. Levees are ribbon like, raised, wedge shaped features, aligned parallel and close to the channel. Their asymmetrical shape is the highest near the channel (Brierley et al. 1997). The levees form during floods out of proximal deposited suspended sediment (Cazanacli and Smith, 1998). There is a gradual fining in the levee when moving from the channel to the floodplain (Adams et al., 2004). Finer grained suspended sediment settles more distal and forms floodplain deposits. The exact boundary between both features is often poorly defined and can be indicated based on a local slope or grain size change (Adams et al. 2004). Multiple flood events of different magnitudes create interweaved grain sized layers of floodplain and levee deposits (Adams et al. 2004). The formation of floodplains is not only the result of vertical accretion, due to floodplain sedimentation, it also forms due lateral accretion of scroll bars. Additional features in meandering systems are crevasses. These are elongated sandy deposits, raised above the surrounding floodplain level. They can form as a result of a natural levee breach during a flood (Townsend, 2001).

2.1.2 Meander bend flow

The characteristic features that are the essence of meandering rivers are the bends. They are structures that induce complex helicoidal flow patterns. This secondary flow is generated because: "Faster near surface flow moves toward the outer bank because the centrifugal acceleration acting on it exceeds the centripetal acceleration due to super-elevation. The opposite is true for the slower-moving near-bed flow which therefore moves toward the inner bank" (Ferguson et al., 2003). The helicoidal flow in the river bend is illustrated in figure 2.5.

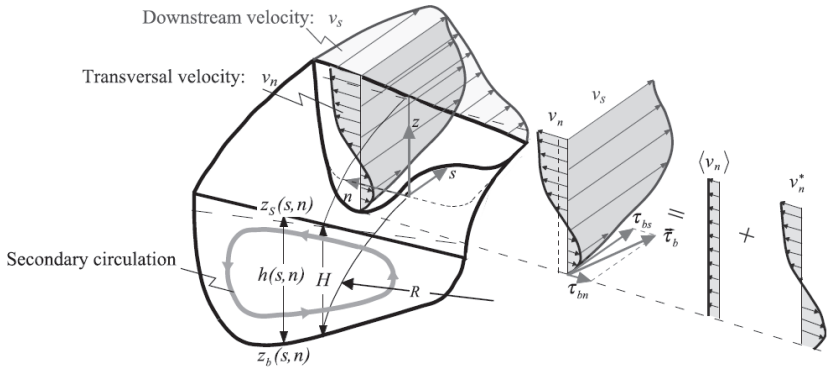

Figure 2.5. Cross-sectional view of the flow and shear stress vector in a meandering river bend (Blanckeart and de Vriend, 2003).

The shear stress distribution in a bend determines the direction of sediment transport. At the bottom of the bend the net shear stress is directed towards the inner bend. At the outer bend the shear stress is directed towards the outer bend and in the downstream direction (Blanckeart and de Vriend, 2003).

Different ratios of channel width and bend curvature might alter the secondary flow patterns in the river bend. This can result in flow separation, in sharp bends, which creates a zone of dead flow along the outer bend of natural rivers (Ferguson et al., 2003, Nanson, 2010). Furthermore the secondary flow is stronger for small width/depth (w/h) ratio channels (w/h<10). Even smaller ratios (w/h<8) can create a counter rotating secondary circulation cell that forms along the outer bend (Blanckaert and de Graf, 2001). The morphology of these sharp bends is characterised by bar pool formations along the outer bend and an overall increase in the cross-sectional area with a corresponding energy loss (Blanckaert, 2010). Finally the roughness and angle of the outer bank were found to in-or decrease the strength of the secondary current (Blanckaert et al., 2010).

2.1.3 Bar theory

The formation of a meandering river, from an initial straight river with a perturbation upstream, is given by bar theory. Although meandering rivers are abundantly present in natural environments, understanding the formation is relevant when considering the creation of meandering rivers in laboratory environments (van Dijk et al., 2010).

The initiation of meandering is based on the lateral shifting erosion due to the formation of alternate bars in the straight channel. The type of bars present in a channel can be predicted by the equations of Struiksma et al. (1985). Crosato and Mosselman (2009) expanded this theory, which is comprehensively summarized by Kleinhans and van den Berg (2010).

The formation of bars in a straight channel is predicted by using the interaction parameter (IP, equation 7). This parameter represents the balance between the adaptation lengths of water and of sediment.

The streamwise adaptation length for depth averaged transverse perturbations is λ_w. It indicates the distance in the downstream direction over which a perturbation is damped out. The adaptation length for perturbations in the cross-sectional river bed profile is indicated with λ_s.

$$(7)\quad IP = \frac{\lambda_s}{\lambda_w}$$

The λ_w is given by:

(8) $\lambda_w = \frac{h}{2C_f}$

The average depth is *h* (m), the average width *w* (m) and C_f is a dimensionless friction parameter:

(9) $C_f = \frac{g}{C^2}$

The adaptation length for perturbations in the cross-sectional river bed profile (λ_s) is given by:

(10) $\lambda_s = \frac{h}{\pi^2}\left(\frac{w}{h}\right)^2 f(\theta)$

The balance between the adaptation lengths of sediment and water in relation to the evolution of channel morphology can be explained by regarding a straight channel with an upstream perturbation. The perturbed flow enters the straight channel. Upon hitting the opposite bank the water level is raised and a spiral flow forms (chapter 2.1.2). This flow carries sediment to the opposite inner bend, where it is deposited and forms a bar. Since the equation is to a greater extent based on the w/h ratio this term tends to dominate the evolution of channels. Based on the w/h ratio of the channel several possible morphologic developments are possible. If the water adaptation length is longer than that of the sediment the system is damped. This means that in a narrow and deep channel (low w/h ratio) the amplitude of the bars reduces rapidly and a plane bed develops. This is called the overdamped state. Larger width depth ratios allow the bars to remain present in the channel and free alternate bars can form. If the water adaptation length is shorter than that of the sediment the system moves towards excitation. So for wider channels the formation of multiple bars in the channel is predicted. In central bar channels the banks are eroded evenly and the system moves towards braiding (Kleinhans, 2010).

In case of free alternate bar formation in the channel, with the channel in an under-damped state and of relatively narrow width, the bars in the river start to control the locations of erosion (Kleinhans et al., 2010). When regarding figure 2.6 it can be seen that for alternate bars the flow is forced towards the opposite side of the bar. If erosion of the opposite bank occurs the bank will gradually retreat. If this retreat is matched on the inner bend by sedimentation, an increasingly sinuous channel forms. Over time the locations of the free bars will become fixed to the inner channel bend locations and a meandering river could develop. An overview of explanations for the fixing of free bars is given by Kleinhans (2010). One of the mechanisms able to fix the bars is vegetation. This illustrates the potential influence of vegetation in river system development. However the free bars, in real rivers, are inundated almost continuously thereby limiting vegetation development on free bars and thus the fixing of the bars by vegetation.

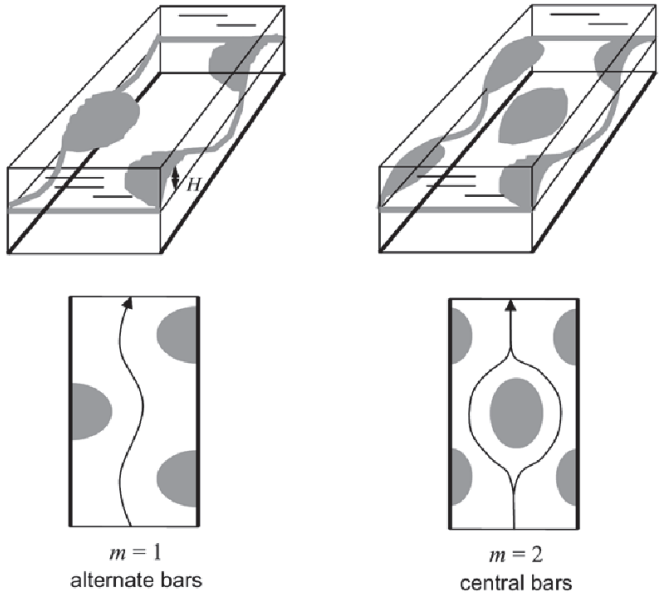

Figure 2.6. The flow and bar locations in a straight channel. The left shows fixed alternate bars and the right central bars (Crosato and Mosselman, 2009).

2.1.4 Floods and overbank flow

Floods are periods of increased discharge in a river that have the potential to inundate the surrounding floodplain area. The cause of a river flood varies based on the drainage basin and location. Possible causes are a sudden melt water pulse in spring and periods of severe or extended precipitation. The duration and extent of inundation are flood and drainage basins specific. The conveyance of flood water in a river is determined by the rivers sinuosity, channel width, floodplain width and the roughness of the channel and floodplain. The sinuosity of a meandering river, compared to a straight channel, can increase the travel time of a floodwave up to a factor 2.5 (Shiono et al., 1998).

The increase in water levels during floods has a strong effect on the sediment transport in rivers. This is due to the exponential scaling of sediment transport to the flow velocity and water depth. This makes floods the main driver of morphological change in the channel. When regarding the floodplains development floods are an essential requirement for sediment delivery and thus morphological change (Kleinhans, 2010). In addition floods are an important factor in vegetation pattern development, maintenance and destruction (chapter 2.2.3). Vegetation in turn affects the flood wave behaviour via the hydraulic resistance of the floodplain (chapter 2.2.1).

The flow from the channel to the floodplain can be classified as either advective or diffusive. Both mechanisms are found in real world environments. In case of advective transport a gradient in the water surface exists between the channel and the floodplain. This water surface slope gradient drives the flow from the channel onto the floodplain. The second mode of transport, diffusive, is found when the level of inundation in the channel and floodplain is equal. In this case the shear between the slow moving floodplain and faster moving channel flow creates turbulent diffusion that drives flow onto the floodplain (Adams et al. 2004). The two types of flow are illustrated in figure2.7.

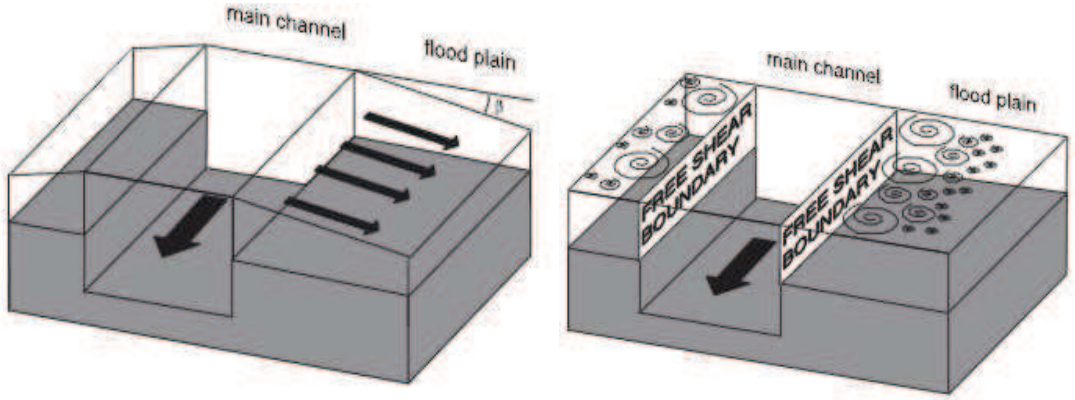

Figure 2.7 Two types of flow form the channel to the floodplain. The left picture shows advective flow driven by a water surface slope β. The right figure displays turbulent diffusion due to main channel and floodplain shear (Adams et al., 2004).

In case of inundation of the floodplains the flow is divided into a main channel flow and an overbank flow component (Shiono et al. ,1998, Adams et al., 2004). Due to inaccessible nature of floodplains during a floods, there is a lack of real world measurements (Stella et al., 2011) and flumes are used alternatively.

A straight concrete base flume study by Knight and Brown (2001) measured the division of the flow between the main channel and floodplain. This was done for a smooth (concrete) and rough (metal pins) scenario. The results are given in figure 2.8. When regarding the figure it can be seen that the larger fraction of the discharge is transported through the main channel for more rough conditions compared to the division for smooth condition. Furthermore the abrupt change in hydraulic radius, when the overbank area was flooded, resulted in an overall reduction of the systems Manning resistance coefficient.

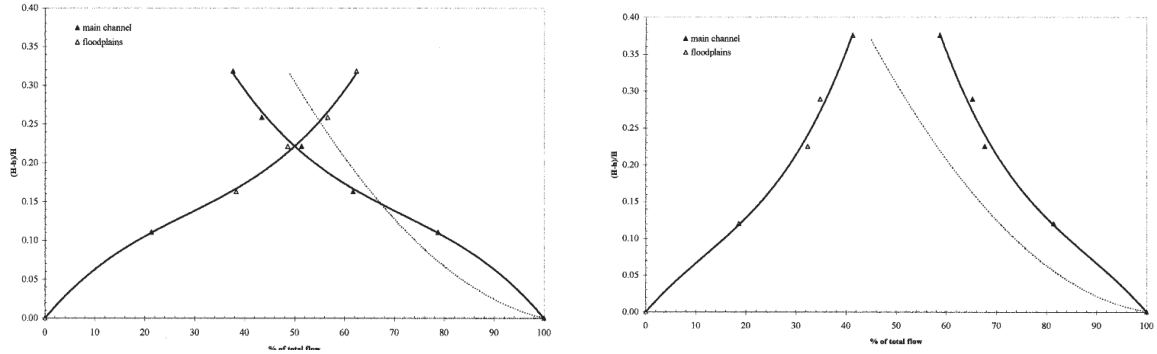

Figure 2.8 Flow division between the channel and floodplain (black line) and the percentage of the cross section that is occupied by the main channel (dotted line). The left figure is in of a smooth concrete base and the right is a rough floodplain (Knight and Brown, 2001).

Another fixed base meander planform and floodplain flume flow study conducted by Shiono et al. (1998) illustrated a large difference between direction of the channel and floodplain flow (figure 2.9). In addition the turbulence and shear between the main channel and floodplain were responsible for an overall loss of flow momentum.

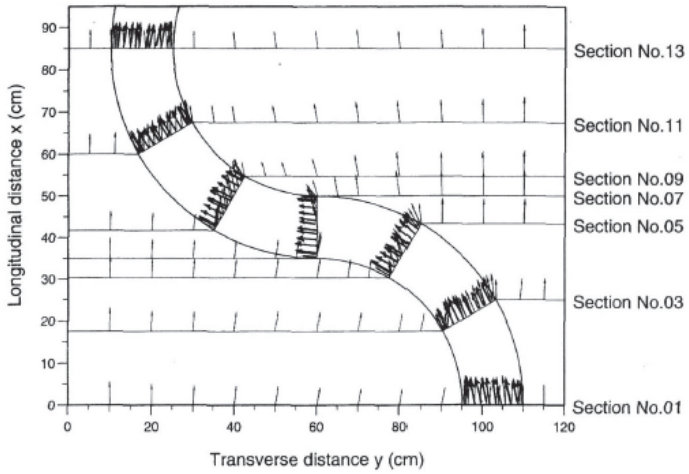

Figure 2.9. The direction of the flow in the channel and floodplain in a fixed bed flume study (Shiono et al. 1998).

A series of fixed based flume experiments with a simplified rough overbank, created by artificial grass and wooden poles, were conducted to investigate the vegetated floodplain and channel interactions (Mcbride et al., 2007). It was found that there is a general reduction in floodplain turbulence velocity for a vegetated floodplain. However the instantaneous shear around the vegetation was increased, so that sediment transport could potentially be amplified due to vegetation presence.

Jahra et al. (2010) performed a flume and modelling study aimed at describing the channel and floodplain flow for a rough vegetated floodplain. On one side of the flume a bare floodplain was created on the other side different rough conditions were implemented. The velocity decreased on the, increasingly vegetated, floodplains and increased in the main channel. Between the main channel and floodplain turbulent shear was present. The difference in velocity between the main channel and the floodplain for a completely vegetated overbank run can be seen in figure 2.10.

Straatsma and Baptist (2007) modelled the flow distribution in a vegetated floodplain environment. It was found that rougher conditions, on the vegetated floodplain sections, increased the velocity in the main channel. In case of less rough vegetated sections the flow velocities were higher on the floodplains and lower in the channel, compared to the more rough case. The difference in flow velocity between both roughness scenarios was between 0.1-0.2m/s. This has a significant effect on water level and sediment transport. The roughness as a result of vegetation is explained in more detail in chapter 2.2.1.

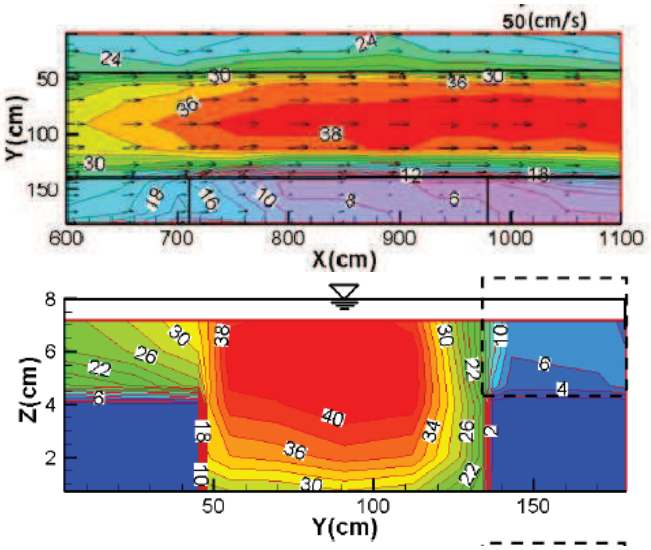

Figure 2.10. The top picture is a longitudinal view of the flume, the lower side is rough. The bottom a cross-section of the flume with the rough floodplain on the right. The colours and numbers indicate the velocity (m/s) (Jahra et al., 2010).

2.2 Riparian vegetation

The term riparian refers the biotic communities that are present on the margins of rivers, lakes, ponds and wetlands (Naiman et al., 1998) and thus vegetation along a river margin is known as riparian (figure 2.11). There is no uniform definition of riparian vegetation (Bendix and Hupp, 2000). The riparian zone definition, used in this report, states; " a biotic community living close to the river banks, which is sustained by and interacts with the stream to a great extent" (Perucca et al., 2006 after Hughes, 1997). The emphasis on the interactions is important, since other definitions lack this term. They simply state riparian vegetation is; "vegetation that inhabits the area between the active channel bank and the upper part of the active floodplain and terraces (Naiman et al., 1998)".
The type of vegetation, present along a specific river, depends partly on the location of the river. For every climatic region and continent has a different characteristic vegetation (Naiman et al., 1998). Over a longer timescale, riparian vegetation tends to reflect the climatic changes that occur in the local environment. For example a glacial to non-glacial period transition. The focus of this report are natural rivers in the current Western-European and North-American temperate climate regions.

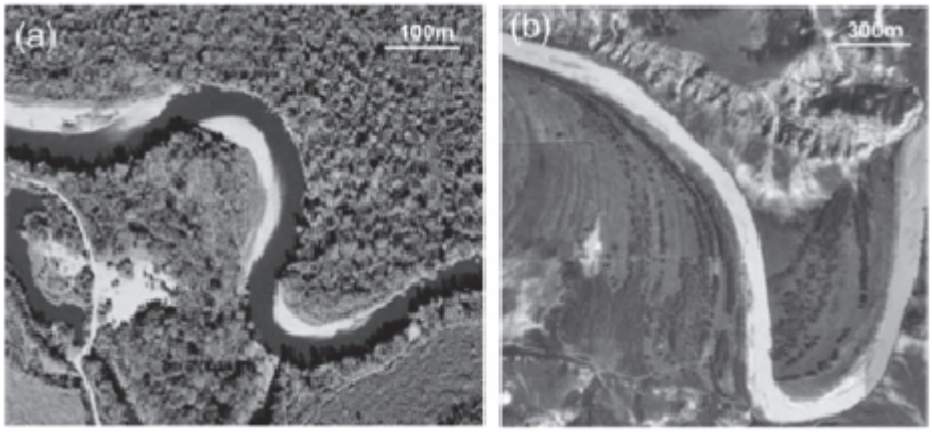

*Figure 2.11. Two examples of riparian vegetation along a meandering river bend that display a specific pattern. (**a**) Bogue Chitto river, Louisiana. The vegetation pattern consists of non-vegetated pointbars (**b**)Little Missouri river, North-Dakota. The pointbar ridges are preferentially occupied by vegetation (Perucca et al., 2006).*

2.2.1 Engineering properties of vegetation

The effects of vegetation (figure 2.1(b)) on rivers are sometimes referred to as passive (Perucca et al., 2007) or "engineering' properties (Gurnell and Petts, 2006) of vegetation. This is due to the potential effect of vegetation that resembles mechanic structures to control for example the erosion in a river. The engineering effects of vegetation are; added bank strength, an increase in the local roughness and the potential to trap sediment.

Bank strength

River banks can have a certain strength or ability to resist erosion. This can be due to a non-alluvial surrounding bedrock or other local features, such as an alluvial till or a thick layer of very cohesive material (Eaton and Gilles, 2008). In river banks, made of loose material, there is no natural added strength. The mechanical strength of loose sediment bank is initially determined by the sedimentary composition of the bank. So it is related to the strength of clay, sand and gravel to resist the gravitational pull on the bank. The qualities of sand and gravel are a large compressional strength, but a low cohesion or tensile strength (Micheli and Kirchner, 2002). When vegetation is added to a loose sediment river bank additional strength is provided via the roots of the plants. This is because the roots have a low compressional strength, but a high tensile strength. So the combination of roots and loose sediment makes a more resistant bank (Simon and Collison, 2002). The total strength of a river bank is determined by both mechanical and hydrological effects.
The hydrologic effects of vegetation are a reduction of the moisture content of a river bank. This is achieved by increasing the evapotranspiration from the soils as well as by intercepting a part of the

incoming precipitation (Gurnell and Gregory, 1994). These hydrologic processes tend to increase the shear strength (Simon and Collison, 2002).
The added strength due to vegetation growth increases over time, but for climax vegetation different effects are possibly present (Tal et al. 2003). For the presence of trees increases the weight of the section volume of the bank and increases the pore pressure locally. The increase in pore pressure is due to concentrating infiltration around the stem and roots of a tree (Simon and Collison, 2002).
An important remark to make is the relative effect of vegetated banks on the width of streams. The effect of vegetation on a river is larger for smaller streams. This is because in larger systems the discharge will eventually dominate the fluvial development of the river (Eaton and Millar, 2004).
The collapse of a bank occurs when the stress exerted on the bank exceeds the strength of the bank. The strength of a river bank can be expressed the relatively simple Mohr-Coulomb equation (eq.11):

$$(11)\ \tau_f = c' + (\sigma - \mu_w)tan\varphi'$$

In this equation τ_f is the shear stress at failure (kPa), c' is the effective cohesion (kPa), σ is the normal stress (kPa), μ_w is the pore water pressure (kPa) and φ' is the angle of internal friction in degrees (Simon and Collison, 2001).
The driving force of the failure is given by:

$$(12)\ \tau_f = Wsin\beta$$

In the equation W is the weight of the failure block and β the angle of the failure plain (°).
The effect of vegetation in relation to increased bank strength have been indicated by numerous researchers (Gran and Paola, 2001, Bertoldi et al., 2011). In order to accurately describe the added effect of roots a numerical expression is required. The root reinforcement is expressed with an increased soil strength term (c_r):

$$(13)\ c_r = T_r\left(\frac{A_r}{A}\right)(\cos\theta_d\, tan\varphi + sin\theta_s)$$

T_r is the tensile strength of roots (kPa), A_r/A the shear surface occupied by roots per unit area (root-area ratio) and Θ_d the shear distortion from vertical (degrees) (Simon and Collison, 2002). This method assumes the roots are perpendicular to the slip plane. Furthermore the equations consider the roots to fail at the same time. Finally the pulling out of roots during failure is not considered (Pollen and Simon, 2005). The slipping term of roots expresses the pullout force (F_p *in kPa*) as a function of the maximum tangential stress (τ' *in kPa*), the root length (L_r *in m*) and the root diameter (d_r *in m*):

$$(14)\ F_p = \frac{2\tau' L_r}{d_r}$$

The RipRoot model was developed in order to present a better representation of root reinforcement and bank failure. This model incorporates the effects of increased bank strength for older vegetation and the relation between bank height and effective vegetation reinforcement. This means that not all roots break on the same time. Furthermore it redistributes the total load over the intact roots at each model step (Pollen-Bankhead and Simon, 2009).
There are multiple erosional processes that erode the banks of rivers. In the bends of meandering rivers erosion tends to be the largest. This is due to the high shear stresses that occurs along the outer bank margin for normal river bends. This is important when regarding sediment entrainment. Mass failure is also prominent in the outer bend. It occurs as a result of the balance between the strength of the bank and gravity.
The failure of a river bank displays the same characteristics as mass failure events on hill slopes. The most common mass failure types are illustrated in figure 2.12 (Abernethy and Rutherford, 1998). The shallow slide occurs for steeps banks (>40°) that have undergone erosion at the base of the bank. Shallow slips are found in areas with a shallow (<30 cm) grass root permeated layer on top of stiff clay. The deep seated bank failures are found on less steep banks that are often covered by grasses.

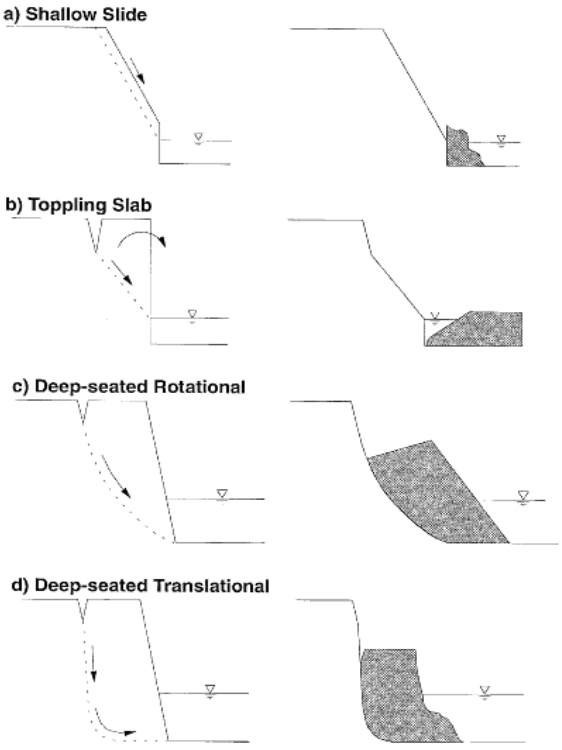

Fig. 2. Types of mass failures of Latrobe River banks.

Figure 2.12. Failure mechanisms of river banks (Abernethy and Rutherford, 1998).

In addition to the mass failures there are specific river related or hydrologic erosional processes. The entrainment of sediment from a bank is dependent on the protective qualities of the vegetation cover on the loose grains less on the mechanical strength delivered by the roots. In these situation the reduction of the flow by creating a degree of roughness can become more important (Abernethy and Rutherford, 1998). Vegetation tends to reduce the near-bank velocity and reduce the effective bank shear stress (Millar, 2000).

Toe erosion or undercutting, of the river bank, is the entrainment of sediment at the base of the bank. The results are an increased possibility of bank failure due to creating of an overhanging bank by the removal of the base of the bank. The centre of gravity of the overhanging river bank increases the tensile stress along the boundary of the overhang (figure 2.13). However the presence of vegetation roots is able to postpone the failure of the bank by increasing the tensile strength (Micheli and Kirchner, 2002). This means the bank needs to be undercut further before failure occurs. Large portions of failed bank have the potential to provide a sheltering effect to the sediment on the base of the banks (Micheli and Kirchner, 2002).

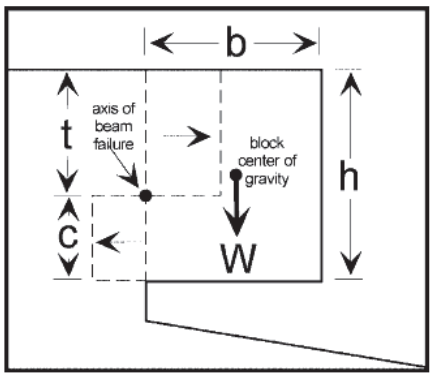

Figure 2.13. The sum of the moments around the beam of failure determines the stability of the undercut bank (Micheli and Kirchner, 2001).

Hydraulic resistance

The presence of vegetation poses a physical obstruction to the flow (figure 2.1(c)). The flow needs to move over or around the vegetation that increases the turbulence and thus creates a loss of energy. This can be regarded as an increase of the hydraulic resistance to the flow. The hydraulic roughness effects of vegetation become especially important during flood periods. The inundated vegetation roughness determines the water levels, flow velocities and sediment transport. These effects are mentioned by numerous authors and are described mostly qualitative (Gurnell and Petts 2002, Bertoldi et al., 2011).

When regarding vegetation and the resulting roughness in more detail, there are several factors present that are of importance in determining the degree of resistance. Examples are the turbulence around the stems (Baptist, 2003), the swaying and the flexibility of vegetation. Furthermore, when describing the effects of riparian vegetation to the hydraulic roughness, it should be taken into account that riparian vegetation is present in a range of growth stadia and compositions. Each local composition of plants has a different effect on the hydraulic roughness. A better and especially a quantitative grasp of the effects, applicable to a specific composition of vegetation species, is required in order to describe the roughness of vegetation. A series of equations were derived and tested by Baptist et al. (2006).

The hydraulic roughness influences the logarithmic velocity profile over the bed. This means that the effect on the velocity profile is key in accurately describing the effects of roughness (Stephen and Gutknecht 2002). The vertical velocity profile without added vegetation resistance is given by:

$$(15)\ u(z) = \frac{u_*}{k}\ln\left(\frac{z}{z_0}\right)$$

where u_* is defined as:

$$(16)\ u_* = \sqrt{\frac{\tau_t}{\rho}}$$

The total roughness of surfaces is expressed with the Nikuradse coefficient (k_s). This relates to the roughness height z_0 with $k_s/30$.Empirical relations such as D_{84} or $3D_{90} = k_s$ are often used to approximate the grain related Chézy roughness (*C'*). In case of laminar flow the formula is expanded by $ks + 3.3 * \frac{\nu}{u_*}$ instead of k_s. The Chézy roughness coefficient is given by:

$$(17)\ C = 18\log\left(\frac{12R}{k_s}\right)$$

Ferguson (2007) suggests the use of D_{84} in shallow gravel bed river environments. The roughness of the bed can be computed as:

$$(18)\ \left(\frac{8}{f}\right)^{0.5} = \frac{u}{u_*} = a_2 h/D_{84}$$

where a_2 is a number between 1-4. Alternatively a Reynolds number based roughness computation is available for wide open channels with laminar flow conditions (Yen, 2002):

$$(19)\ f = 24/Re$$

The different roughness coefficient can be related to each other by the following equation (Ferguson, 2007):

$$(20)\ C = \left(\frac{8g}{f}\right)^{1/2} = \left(\frac{g}{C_f}\right)^{1/2}$$

With sufficient levels of inundation relative to the local vegetation a complete submergence can occur. Four different zones can be distinguished when regarding flow velocity profiles over a fully submerged vegetated (Baptist et al., 2006). The zones are given in figure 2.14 A and B.

1. Flow influenced by the bed and vertical logarithmic boundary layer profile applies
2. Zone inside the vegetation, away from base and top, has a uniform flow velocity
3. Near the top of the vegetation there is a transitional profile between the uniform velocity in the vegetated section of the bed and a logarithmic velocity profile above it.
4. Logarithmic velocity profile, but with a zero displacement zone above the vegetation

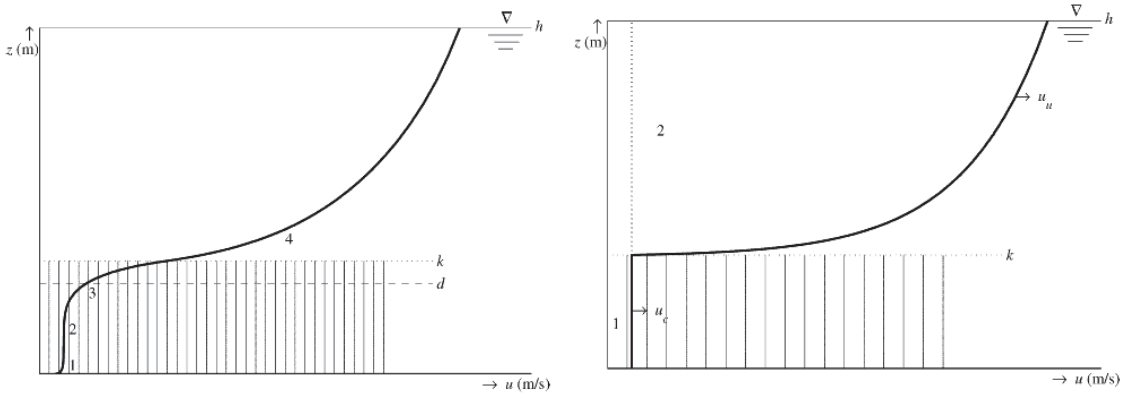

*Figure 2.14. **A** is the actual flow over submerged vegetation. **B** is the effective water depth schematization (Baptist et al., 2006)*

This representation can be simplified in order to use the method of effective water depth. This reduces the four zones to two (figure 2.14 B). These are; (1) a uniform flow velocity inside the vegetation and (2) a logarithmic velocity profile on top of the vegetation cover. The equation that describes the flow to trough the submerged vegetation u_c:

$$(21)\ u_c = \sqrt{\frac{1}{\frac{1}{C_b^2} + \frac{C_d m D h_v}{2g}}} + \frac{\sqrt{g}}{k} \ln\left(\frac{h}{h_v}\right)$$

Where m is the number of cylinders per m^2 of horizontal area, C_b is the Chézy bed roughness (eq. 17), C_D is the bulk drag coefficient and D is the cylinder diameter (m) and h_v is the vegetation height (m)
The logarithmic velocity profile above the submerged vegetation resembles is resembled by the natural logarithm and represents the standard profile description:

$$(22)\ u_u(z) = \frac{u_*}{k} \ln\left(\frac{z-k}{z_0}\right) + u_c$$

Larger vegetation, like trees and shrubs, is not likely to be completely submerged during floods. This means the above presented flow approximation is not valid. Instead a non-submerged approximation is required.
The total shear stress (τ_{ts}) in a non-submerged situation, of cylinders, is equal to the sum of the vegetation related (τ_v) drag and the bed shear stress (τ_b), where:

$$(23)\tau_{ts} = \tau_b + \tau_v$$

$$(24)\ \tau_b = \rho g \frac{u^2}{C_b^2}$$

$$(25)\ \tau_v = 0.5 \rho C_D\, m D h u^2$$

The uniform velocity through the non-submerged vegetation (u_{cb}) is:

$$(26)\ u_{cb} = \sqrt{\frac{1}{\frac{1}{C_b^2} + \frac{C_d m D h}{2g}}}$$

where the discharge (*q in m^2/s)* is given by:

$$(27)\ q = h u_{cb}$$

With lower Reynolds values the drag coefficient(C_d) is a function of the Reynolds number. This is given by the equation below for 0.2<Re<2000:

$$(28)\ C_d = \frac{21.12}{Re} + \frac{6.3}{Re} + 0.25$$

the Reynolds number range base C_d above the 2000 threshold is approximately constant, with a value of 1.5 (Järvelä, 2002).

The equations presented by Baptist (2006) are only valid when considering fixed cylindrical vegetation. It should be noted that in real environments the flexibility of stems allows bending, whereas stiff vegetation can sway. It was found that for flexible vegetation there is no additional increase in the equivalent roughness height due to the wavy motions (Stephan and Gutknecht, 2002). In case of a severe floodplain inundation there is the possibility of an increase in the roughness, due to the submergence of the tree canopy (Gurnell and Petts, 2002). In chapter 2.2.4 some of the fixed base flume work, related to the effects of floodplain vegetation and flow, were already presented. There have also been 1:1 scale experiments that investigated the effects of vegetation in relation to hydraulic resistance.

Järvelä (2002) implemented different compositions and densities of boxed, submerged, grassy cover with, non-submerged, willow branches in a flume and measured the Darcy-Weisbach friction factor (*f*) based on the energy loss in the flume. The friction factor decreased for increased flow velocities with a constant water level. With a doubled amount of leafy willow branches the overall friction in the flume doubled. The main contribution to the overall roughness, for the leafy willow run, was the leaves on the willow branches. In leafless vegetation runs, without a grassy cover, there was no change in the friction factor as a result of velocity. Instead the friction factor increased linearly with the water depth. So, the increases in friction were related to (1) the relative roughness addition of grasses compared to bare soil flume runs (2) the flow velocity increase for willow and grass runs (3) the flow depth for leafless vegetation on bare soil. Different combinations of willow and grass densities produced a significant amount of variance in the data.

Armanini et al (2005) tested the drag of, submerged, flexible willow branches in a flume. The drag resistance of the vegetation decreased with increased flow velocity. This is typical for flexible elements, because the higher flow velocities bend the vegetation. The bended vegetation reduces the exposed surface area to the flow and thus the drag.

Sediment trapping

The vegetation obstructs the flow and creates additional roughness (ch.2.2.1). This tends to reduce flow velocities and promote the settling of sediment (Gurnell and Petts 2002, Bertoldi et al 2011). This reduced velocity should increase the local sedimentation and amount of fines. Since the majority of riparian vegetation is situated on the banks and floodplain of meandering rivers the effects are most noticeable in the formation of overbank deposits (Hupp, 2000). When fines are deposited vegetation tends to increase the stability of fresh layers of fine sediment (Gurnell and Petts, 2006)

A measurement-based model study in the embanked floodplain of the Dutch river Waal correlated the development of vegetation to a reduction in local flow velocities and an increased trapping of sediment. This increased the local aggradation of the system and thus reduced the required timespan for the formation of floodplain and levees (Geerlings et al., 2008).

Apart from the flume experiment that were aimed at experimentally determining the roughness some were aimed at measuring sediment transport. Common sediment transport equation are not valid when regarding flow over vegetated surfaces (Baptist 2003). Therefore Baptist (2003) investigated the sediment transport over submerged vegetation. No bedform formation occurred under the vegetation cover compared to ripple formation in a non-vegetated sandy bed flume runs. With a setup specific, water level, vegetation composition and flow velocity an 80% decrease in the shear stress was measured. However the sediment transport did not reduce significantly, this was hypothesized to be due to the increased turbulence around the plant stems and the predominantly suspended sediment transport.

2.2.2 Biotic factors

The biotic factors (figure 2.1(III)) are the vegetation related properties that determine the development of the riparian vegetation cover (figure 2.1(e)). An overview of several important factors in the vegetation development is given below.

Succession and rejuvenation

Succession is the transition of a landscape unit to another. In case of vegetation succession is achieved by changing the composition or the species of vegetation in the landscape (Geerlings et al. 2006). Vegetation development is generally described as the transition from a pioneer state to a climax state, in this case a riparian woodland.

A classification of the different stages of riparian vegetation succession is established by Naiman et al. (1998). They determined that four stages could be identified in the succession of riparian environments. The four stage classification is given in figure 2.15.

1. Stand initiation stage. After a disturbance or depositional landform formation, pioneer plants start to colonize the area. This stage is the period between initial settling and full occupation of the area.
2. Stem exclusion stage. When the entire area is covered by vegetation the species with a competitive advantage, growth or spread rate, expand. This eliminates existing species and excludes other species from the colonizing the area. The height of the same species of plants tends to illustrate the age of the specimen.
3. Under story initiation stage. Under the canopy of existing trees shade tolerant species develop into a so called understory. These species can be the same as the stand initiation vegetation.
4. Old growth stage or climax vegetation. If large trees start to die, the vegetation enters this stage. The cleared space gives rise to new trees and other vegetation. This state is characterised by a great vertical and horizontal diversity in successional ages.

There is some local variation in composition of the climax vegetation. It is “greatly diverse” (Naiman et al., 1998) and “heterogeneous and species-rich” (Gurnell and Petts, 2002). However, when regarding the study of Geerlings et al. (2006), climax vegetation it is characterised by a low biodiversity.

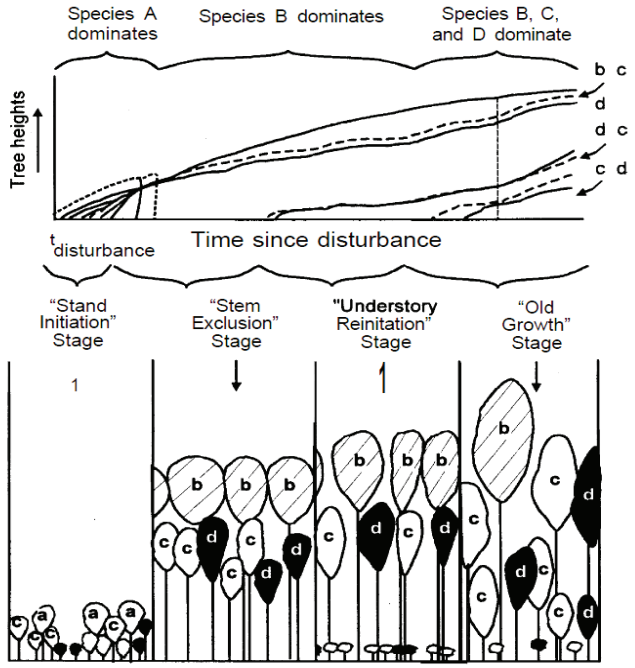

Figure 2.15. The succession of riparian vegetation form a pioneer to a climax forested state. The indexes in the vegetation a, b, c and d indicate different species (Naiman et al., 1998).

The succession of vegetation can be halted or terminated by a range of disturbances. Examples of these events are; fire, wind and fluvial processes (ch.2.2.3). In most cases the partial destruction of the vegetation cover can lead to rejuvenation. Rejuvenation is the renewed succession of the vegetation after a disturbance has taken place (Geerling et al. 2006). The factors controlling the vegetation distribution and development are explained in more detail below.

Distribution of seeds

The prime mechanism that is responsible for the distribution of vegetation in an area is the transport of seeds. Seed transport is species depended, for some species depend on the wind for transport whilst other require animals or fluvial transport.

The fluvial transport of seeds, hydrochory, is one of the most important dispersion mechanisms in riparian vegetation system (Gurnell and Petts, 2002). The timing of floods needs to be in phase with the seed availability in order to have a maximum seed distribution effect (Gurnell and Petts, 2002). Other important properties, concerning flood flow dispersion, are species dependent. These properties include the quantity of delivered seeds and the ability to be carried by the flow, the floating ability. (Gurnell and Petts, 2002). With larger floods wider dispersal of seeds can occur, due to an increased range of inundated locations (Gurnell and Petts, 2006).

After the transported seeds have been deposited the growth of vegetation is determined by (1) the suitability of an area for sustaining vegetation and (2) calm conditions that allow vegetation growth up to the time it takes to reach the reproductive age. Both are species specific requirements, this means the distribution in a system depends mainly on the tolerance range of a particular species (Hupp, 2000).

Timescales of riparian vegetation development

The period of time over which vegetation develops has been measured in the field. Three of such studies are summarized here to illustrate the time it takes for riparian vegetation to shift from a pioneer to a climax state. This is done for the river Allier (France) (Geerling et al., 2006) over a 40 year period, after a disturbance in the vegetation cover (Bertoldi et al. 2011) (Italy) and a bend cut-off (California)(Stella et al., 2011).

The age of the vegetation and different successional stages in the Allier, France, were studied based on aerial photographs taken between 1954 and 2000 (Geerling et al., 2006). The oldest vegetation along the river Allier was dated to 1954. The older vegetation consisted of forested areas, that were largely made up of poplar trees (*populus*). Areas younger than 15 years made up half of the riparian vegetation area, but supported only 10% of the forested area.

Bertoldi et al. (2011) studied the vegetation response along a braided river. It was found that a series of flood periods greatly reduced the vegetation cover, mainly *populus*, in the river. However they also measured a rapid recovery of the vegetation cover, from 15% to 40%, in time following 3 years.

The timescale of riparian vegetation development was examined for an abandoned channel of the Red Bluff river, California, by Stella et al. (2011). The oldest trees in the abandoned channel were dated to a period directly after the cut-off. The maximum age of species thus corresponded to the age of the cut-off, 40 years, and formed the climax vegetation in the area.

So the initiation of vegetation development is relatively instantaneous, when disturbances are removed from the systems. The transition from pioneer to climax vegetation can occur in a period of around 30 years based on these case studies.

Soil and sediment texture

In order for vegetation to grow the local sediment texture, soil depth, moisture and nutrient availability needs to be suitable enough to support a specific species (figure 2.1 (c)). The state of these factors is largely determined by abiotic factors (Perucca et al., 2006). The relative importance of biotic and abiotic factors on local soil composition and vegetation development was investigated after a channel abandonment (Stella et al., 2011). The conceptual figures are given below (figure 2.16).

The figures illustrate that the biotic factors do not start to play a dominant role until the system is left undisturbed for several years. This means that on the shorter timescale fluvial, abiotic, processes determine the local soil composition and thus vegetation development. Based on the figures it can be seen that the result of the abiotic dominance favours the development of pioneer species. This is because pioneer species can cope with the conditions of recently deposited sediment.

The characteristics of new deposits are a coarse texture sediment with little soil formation. The moisture retentive capacity of recently deposited sediment (sand) is poor, due to the low water

retentive capacity of sand. Over time the depth of the soil increases by soil formation. This results in an increase in the soil moisture retentive capacities and the ability to support more advanced species. The shift in sediment texture implies the accumulation of fines and thus floodplain formation in later stages of the channel abandonment. The advanced species mark a shift to a biotic (competition) dominated development. Finally it should be noted that internal processes of plants are also biotic (Stella et al. 2011). The discussion of these lies outside the scope of this report.

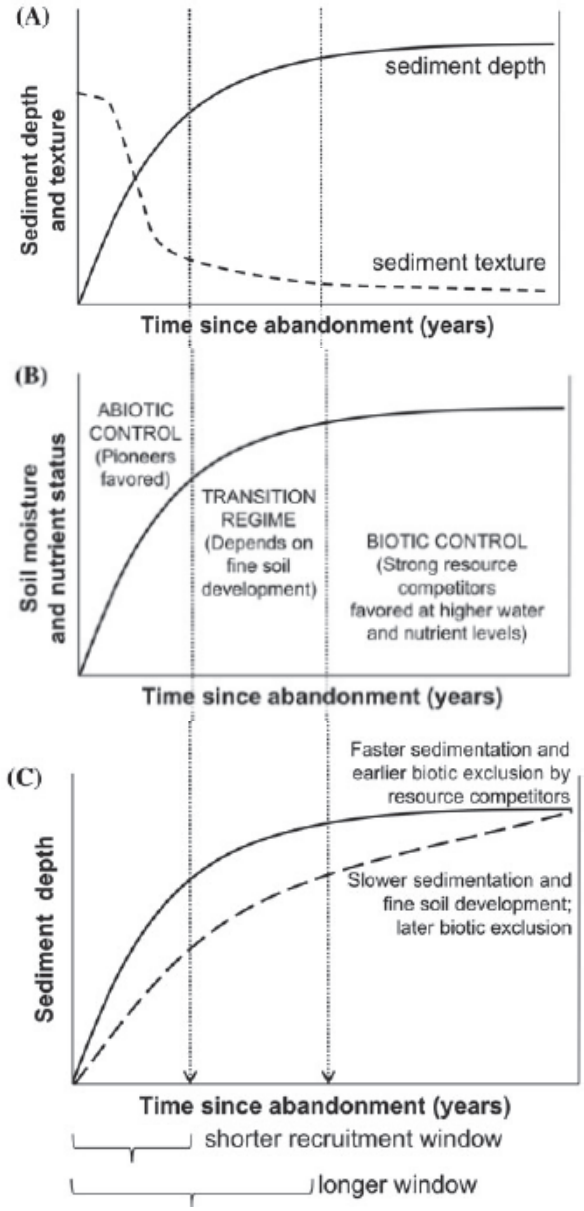

Figure 2.16. Relative importance of abiotic and biotic control of factors that affect vegetation development. On the horizontal axis is the time after abandonment and on the vertical is the relative importance of the corresponding factor (Stella et al., 2011).

Large wooded debris

Large woody debris (LWD) consists of fallen or uprooted trees and large braches. When introduced to the river the debris has the potential to affect several small scale processes. Trees that are uprooted during a flood event can be deposited in the channel and along the channel margins. Uprooting can occur by scouring around the base and pulling out by the drag force of the flow (Perona et al., 2012). When deposited the uprooted trees tend to orient themselves with the root base in the upstream direction (Edwards et al. 1999). In case of LWD deposition a sour zone is created around the debris

and a lee zone forms right behind the debris. In the lee of the LWD, sedimentation can take place and pioneer vegetation is able to grow (Edwards et al., 1999).
Often the fallen tree, in case of *Salix* or *Populus*, has the ability to re-grow. This could potentially start the succession cycle in the middle of the channel. This results in the rapid development of vegetation (Gurnell and Gregory, 1994, Edwards et al., 1999, Gurnell and Petts, 2006). In braided rivers the re-growth of LWD has led to a multiple stage succession of vegetation on bars. Thereby fixing the location of the bars. The same effect can be found on the pointbars of rivers if disturbances remain absent (Bendix and Hupp, 2000). The main control of the bar locations remains the river itself. For it requires several years for the vegetation to be able to withstand moderate floods, so longer periods of higher water levels reduce the vegetation on bar locations. (Edwards et al.,1999).

*2.2.3 Abiotic process*es

The abiotic processes are the effects of the river related processes on vegetation development, also known as the hydrologic control, and the engineering effects of the vegetation on the river (Gurnell and Petts, 2002). These two groups of abiotic factors are explained separately in this report. The engineering effects were discussed above (chapter 3.2). The main effect of floods as an abiotic factor is presented below. the relative importance of the biotic and abiotic effects is presented in chapter 2.2.4.

Floods

Floods (figure 2.1(II)) play a significant role in meandering river dynamics. They drive the morphological change in the channel (figure 2.1(a)) and on the floodplains (chapter 2.1.4). When regarding riparian vegetation dynamics floods have been recognised as an important disturbance factor as well as a vegetation growth related factor (figure 2.1(c, d)). For the river brings nutrients and moisture to the vegetation system (Perucca et al., 2006). In general it can be stated that; the duration and level of inundation (hydroperiod) controls the spatial extent of vegetation along a river reach (Bertoldi et al. 2011), affects the riparian vegetation patterns (Osterkamp and Hupp, 2010) and maintains the dynamics (Edwards et al. 1999).
The effects of floods can be divided into hydrological and geomorphological impacts. Hydrological impacts are the mechanical damage, the saturation of soil and the transport of seeds. Geomorphological effects alter the local substrate by erosion and deposition of sediment (Bendix and Hupp 2000).
The hydrological effects of floods vary. Periods of slightly increased discharge, small floods, occur with a high frequency. These flood pulses in the river, below bankfull discharge, are a vital tool to help maintain the heterogeneity in the riparian vegetation (van der Nat et al., 2003). This is done by uprooting immature vegetation (Perona et al., 2012).
The floodplain is only affected during larger less frequent, above bankfull, floods (van der Nat el al., 2003). They shape the overbank morphology (van der Nat et al., 2003) and can erode large amounts of floodplain sediment (Gurnell and Petts, 2006). This means they have the ability to uproot and transport large numbers of trees (Edwards et al. 1999), as well as distribute the seeds of the riparian vegetation (Gurnell and Petts, 2006).
The main reasons for vegetation destruction during the large floods are uprooting or physical destruction and the burial of vegetation on the banks of a river (Edwards et al. 1999, Bendix and Hupp, 2000). Prolonged periods of submergence, without uprooting, can result in a loss of vegetation by creating anoxic environments (Edwards et al. 1999). After a flood, drought is the main reason for the loss of pioneer vegetation (Gurnell and Petts, 2006). However locally vegetation and sedimentation can increase the water retentive properties (Gurnell and Petts, 2006, Stella et al., 2011).
The effects of floods on riparian vegetation development, from and ecological point of view are a combination of hydrological and geomorphological effects. The effects are: (1) the germination of plants in sediment deposited during floods, (2) the clearing of space for new species by the destruction of older vegetation, (3) the absence of floods after germination to allow the growth of vegetation, (4) the dispersal of seeds (Bendix and Hupp, 2000). A period of less disturbance after

germination is recognised as an important factor in vegetation growth. After germination the vulnerability of vegetation decreases with the plant growth (Gurnell and Petts, 2002).
The combined hydrological and geomorphological effects of floods strongly affect the settling of pioneer vegetation The effects have been combined into a schematic graph that illustrates the narrow zone in a river that allows, in this case, poplar seedlings to germinate (Bendix and Hupp, 2000). In the figure it is illustrated that there is only a narrow window that supports pioneer seedling settlement figure 2.17.

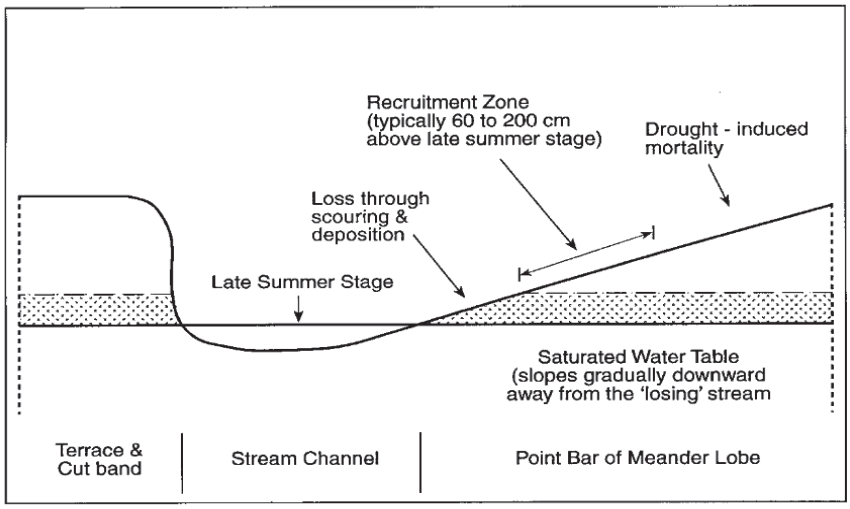

Figure 2.17. Cross-sectional view of the pointbar and the different abiotic vegetation disturbance and settling controlled zones (Bendix and Hupp, 2000).

2.2.4 Biotic and abiotic factor importance

Bornette et al. (2008) have developed a conceptual model, based on a large number of papers from an ecological point of view, that relates the hydrologic disturbances in a system to plant strategies. The model is given in figure 2.18. The *a-axis* represents the dominant process in the river, either erosion or sedimentation. The *b-axis* is the portion of the area that is submitted to erosion or deposition. The *c-axis* is the temporal scale of the flood disturbances. All scenarios lie on the curved surface spanned by the thick black line and the distal *b-axis*.

So for example at the distal part of the figure hydrologic disturbances are rare. This means biological interactions (biotic factors) are important. With an increased flood occurrence the biological interactions become less important (abiotic factor dominance). The vegetation development starts to depend on local refugia, sheltered areas, in a system. Based on the presence of erosion or deposition in the system these are either absent or present.

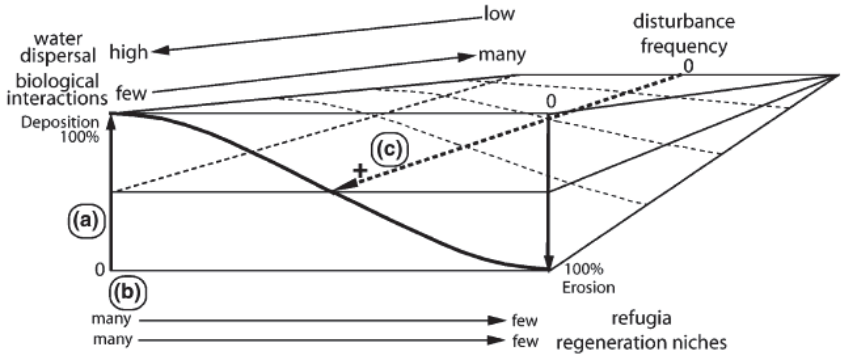

Figure 2.18. The a-axis is the dominant process in the river, The b-axis the frequency of the disturbance and the c-axis the temporal scale of flood disturbances (Bornette et al., 2008)

In present day environments the riparian vegetation is strongly affected by human influences. (Gurnell and Gregory, 1994). Although only the natural vegetation river interaction development is discussed in this report, human alterations in systems do allow for several studies related to vegetation changes and the effect on rivers. For both the man induced reduction in vegetation is found (Gurnell and Gregory, 1994) as well as the restoration of floodplain areas to more natural environments (Geerling et al., 2008).

2.2.5 Patterns in riparian vegetation

From the above presented riparian vegetation description it is clear that it serves an engineering role and control the river development. The hydrological processes of the river in turn affect the riparian vegetation development. The dependency of vegetation on soil suitability, water availability and river regime can create distinctive patterns in natural situations. These vegetation patterns (figure 2.1(IV)) will reflect the combined disturbances (Bertoldi et al. 2011).

Patterns in riparian vegetation occur in all river planforms environments. There have been several studies that focussed on vegetation in braided systems (Gurnell and Petts 2002, 2006). Vegetation patterns are also found in non-fluvial environments. An example of such a pattern is the banded vegetation present in the arid hill regions in Niger. The formation of banded vegetation patterns on hill slope is a function of the infiltration along the stems of vegetation and the generation of overland flow on bare sections of the hill (Thiery et al, 1995). An overview of the riparian vegetation species in relation to different morphological features (chapter 2.2.1) and the resulting patterns is given below. The different landforms and characteristic vegetation cover are visible in figure 2.19. The figure illustrates the problem with regarding the riparian vegetation systems from a pure ecological point of view. Although the figure is derived from a case study (Hupp and Osterkamp, 1985), the representation below does not distinguish several important morphological features on meandering river channel margins (figure 2.19). Since the figure is still used in recent publishing (Osterkamp and Hupp, 2010). It should be noted that this figure is a severe abstraction of reality and by no means a unifying illustration of river or riparian vegetation patterns in meandering rivers.

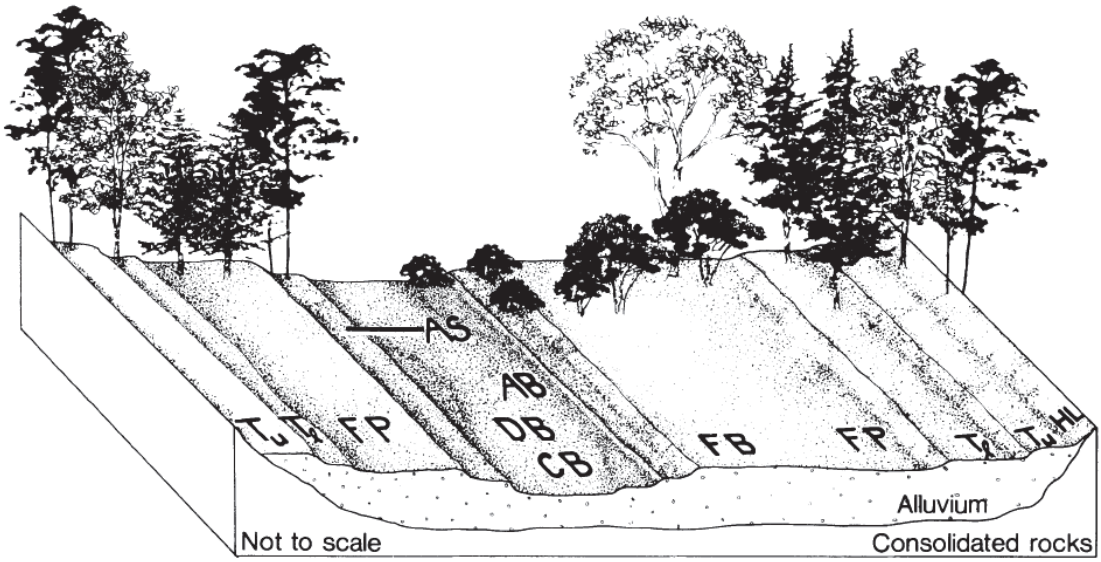

Figure 2.19. An impression of the different meandering river morphologic feature and the corresponding riparian vegetation cover (Hupp and Osterkamp, 1985). Cb= channel bed, DB= depositional barm AB=channel-shelf bank, AS= channel shelf, FB= floodplain bank, FP= floodplain, T_l=lower terrace, T_u= upper terrace and HL=hillslope.

Channel and Active pointbar

The channel of a perennial stream is inundated throughout the year. In case of the presence of gravel in the bed of the channel more advanced vascular plants are often not supported. So apart from some simple aquatic vegetation mostly algae are present, that feed on the high nutrient loads (Hupp and Rinaldi, 2007).

The depositional bar of the pointbar is largely devoid of vegetation, due to extended periods of inundation (40% of the time). In longer periods of low flow some herbaceous species as well as *salix* and *populus* seedlings can occupy this landform (Bendix and Hupp, 2000).

From the channel to the floodplain the succession of species (chapter 2.2.2) is often visible laterally. This is partly due to the flood disturbances decrease in that direction, this is illustrated in figure 2.20

(A). The pioneer vegetation settles on the new pointbar deposits. The older pointbar deposits were covered by vegetation in an earlier stage. This creates a lateral younger and less developed vegetation when moving from the older to the younger parts of the lower pointbars.

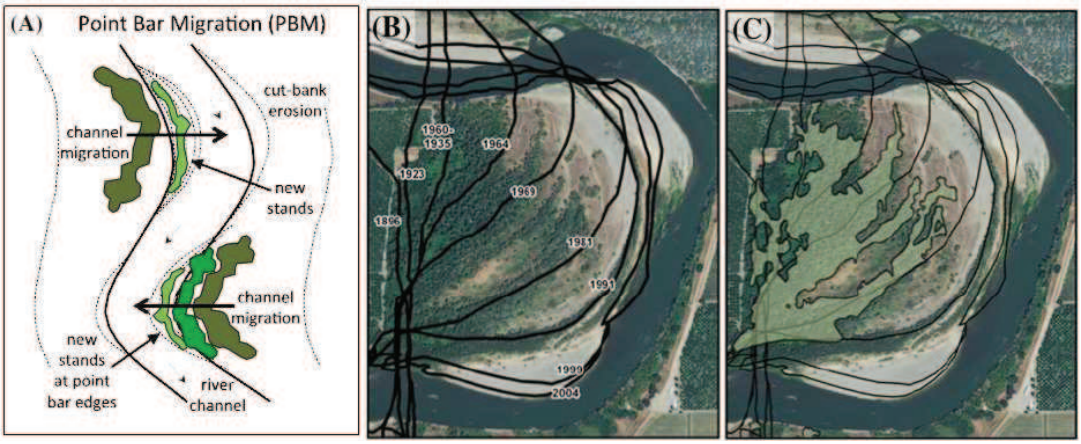

Figure 2.20. Vegetation succession in relation to stepwise pointbar development (Stella et al., 2011).

Channel margin

The higher parts of the pointbar or the banks of the channel are inundated roughly 10-25% of the time. This means dense populations of trees are found. Common species are *salix, alnus* and *populus* (Bendix and Hupp, 2000).The ridge and swale topography on the higher parts of the pointbar presents local highs and lows in an area. This means that there is a variation in the soil texture and water availability.

The swales tend to be coarser grained and are flooded more frequently and serve as an accumulation zone for flood debris (Hupp and Rinaldo, 2007). As a result the ridge and swale topography is often visible in the vegetation pattern in fluvial landscapes (Hupp, 2000, Perucca, 2006). An example of the ridge and swale topography, on the inner bend vegetation pattern is given by Nanson and Beach (1977). They found that the 0.5-1 m high ridges were preferentially occupied by pine. The lower swales lacked trees. The rows of pine trees are oriented in the direction of the swales, illustrated in figure 2.21. The ridge and swales could be dated by the age of the trees and linked the development of the pointbar.

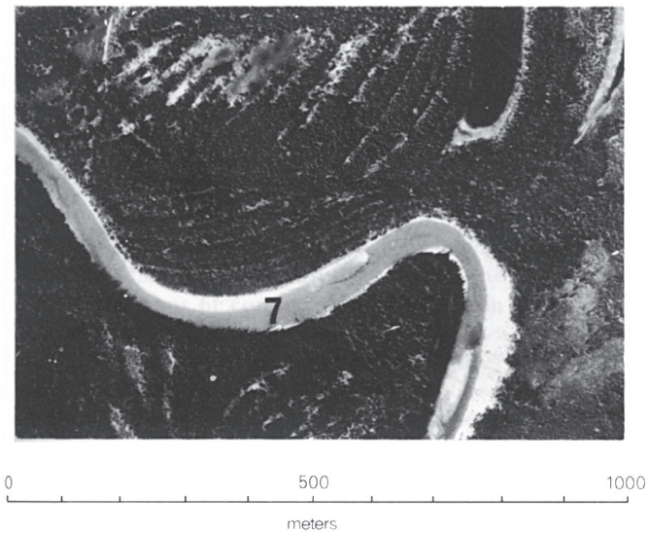

Figure 2.21. Ridge and swale topography is visible in the riparian vegetation cover of the Beatton river, Canada (Nanson and Beach, 1977).

Floodplain and terrace

The higher parts of the fluvial systems are disturbed less often. The lack of disturbance allows the succession of riparian vegetation to later stages. The 1-3 year flood recurrence allows forests that consist of *quercus, pinus betula and fraxinus* (Bendix and Hupp, 2000). So mature riparian forests are found on the floodplains, if no other limiting factors such as moisture availability are present.

The patterns in the riparian forest are not homogeneous. The variations in floodplain topography partly determine the patters via inundation depths, this means local features such as levees and crevasses can be related to vegetation patterns in the floodplain (Townsend, 2001). Furthermore Naiman et al. (1998) describes the soil found in fluvial areas as highly variable. There are spatial variations in texture and moisture content due to inundation of the active floodplain. The effect of this "mosaic" of soil causes a degree of vegetation heterogeneity, but does not dominate the overall vegetation pattern.

In some cases the vegetation patterns on the floodplain can be directly linked to seed dispersal by floods. Parallel bands of Salicaceae (Salix-family) were found along the floodplain of the Rhine at two distances from the river. The older vegetation was further away from the channel and the age coincided with a larger flood (van Splunder, 1998 cited by Gurnell and Petts, 2002). Since each species has its own seed characteristics complex patterns might occur due to floods of different magnitudes (Gurnell and Petts, 2002).

Abandoned channels

The remnant pieces of the active channels ad another degree of variance to the river landscape. They can be a local supply of water, in case of Oxbow lakes, and locally alter the vegetation cover (Perucca et al., 2006) This makes the channel as a whole stand out against the rest of the floodplain. The patterns due to more moisture availability are given in figures 2.22 E and F. Furthermore they serve as suitable locations for pioneer vegetation establishment. Since the abandonment of a channel occurs at a later phase than the formation of the surrounding area the vegetation tends to be younger. The difference in vegetation age or successional stage allows for the recognition of abandoned channels in river floodplains (Stella et al., 2011)

An example of an abandoned channel related vegetation pattern is given in figure 2.22 (D). The younger abandoned channels display less developed, lower, vegetation compared to the older vegetation of the abandoned channel margins. Within an abandoned channel patterns are also present. Due to the gradual silting up of an abandoned channel, the shallowest part starts the succession of vegetation (figure 2.22 (D)). This results in further developed vegetation at the inner bar location after a period of time.

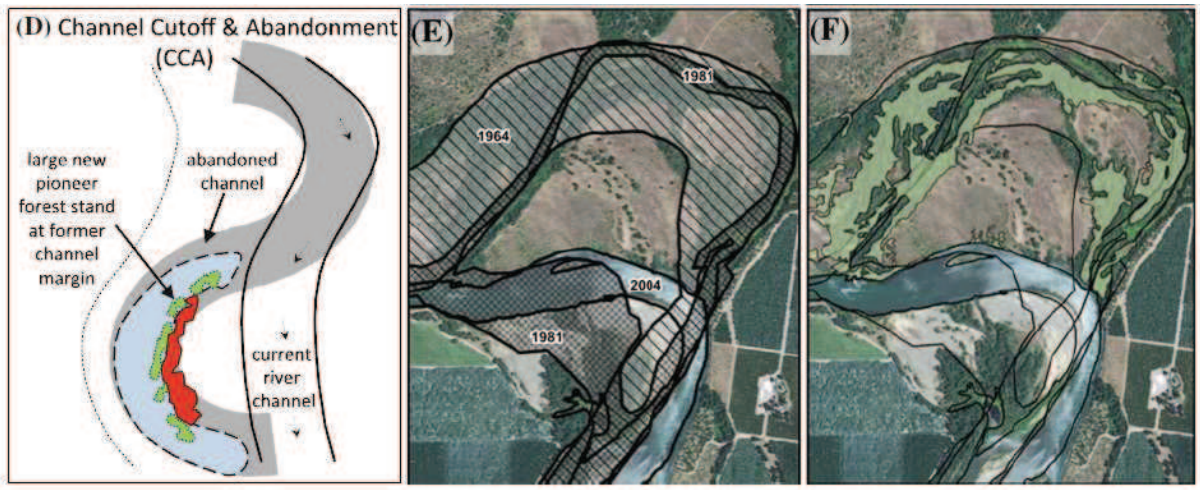

Figure 2.22 Abandoned channel vegetation development (Stella et al., 2011).

Vegetation pattern modelling

The development of riparian vegetation patterns in relation to meandering river dynamics have been modelled by Perucca et al. (2006). The parameters in the model related the timescales of vegetation development (T_v) to those of the river (T_r). The meandering river model is characterised by a continuous growth in bend amplitude and sinuosity.

In addition the decay of vegetation (T_{vd}) was related to the growth (T_{vg}). Furthermore a function was added that related vegetation growth to a specific region of the floodplain. The first scenario *A*, forces vegetation close to the river, thereby resembling the availability of water. The second function *B*, places vegetation at a larger distance from the river, as a result of flood disturbances. The last function *C*, allows vegetation growth at an intermediate distance from the channel, in order to simulate the result of moisture deficiency further away and flood disturbance nearby.

These three functions were implemented in the model and resulted in the plots of figure 2.23, with a T_v=T_r relation. This allows the formation of less vegetated patches of vegetation on the inner bend of the model river. The differences in the vegetation cover between the plots are due to the vegetation settlement functions *A*, *B* and *C*. In all model runs the primary control of the vegetation pattern is the river, but the secondary control on the vegetation pattern are the abiotic factors of flood disturbance and moisture availability.

It should be noted that the effects of vegetation on the meandering river were left out. A later study addressed the bank strength related effects and found a reduction in the meander amplitude growth (Perucca et al., 2007).

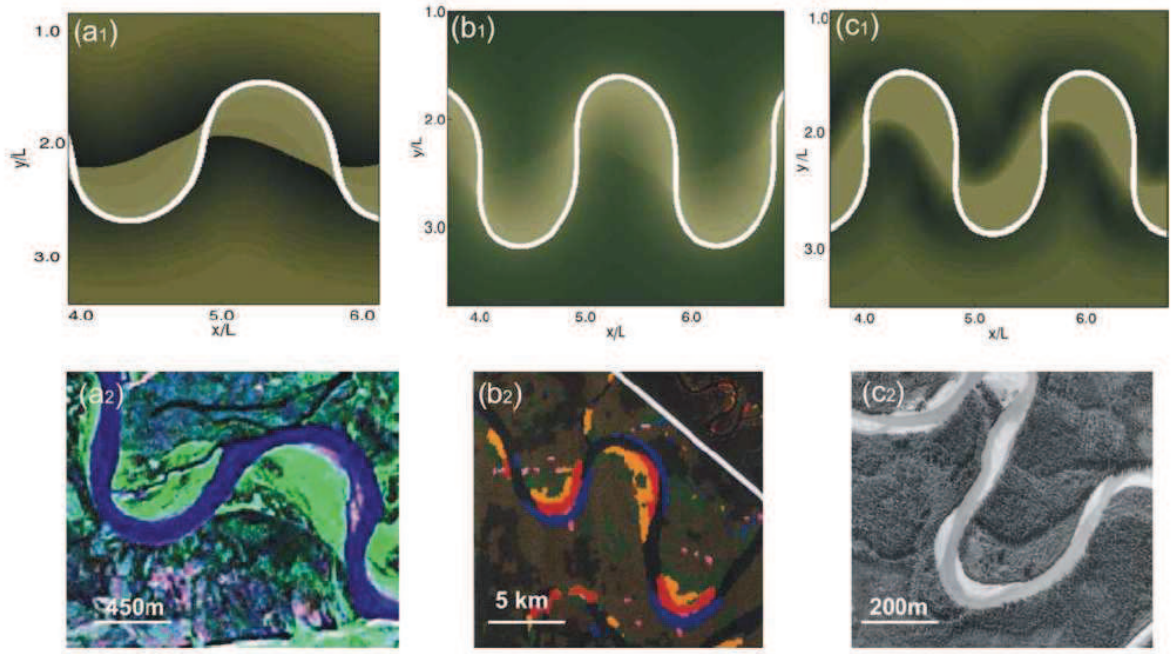

*Figure 2.23. In all model runs T_v=T_r. (**a$_1$**) at t=0.15 with vegetation function A. (**a$_2$**) Pelly river Canada. (**b$_1$**) at t= 0.2 with function B. (**b$_2$**) Ucayli river (Amazon) yellow is pioneer vegetation and green is young forest. (**c$_1$**) at t= 0.2 with function C. (**c$_2$**) Wood river Alaska. In all model results darker green indicates a higher vegetation density (Perucca et al., 2006).*

2.3. Experimental scale self-formed river research

Based on the above presented overview of meandering river and riparian vegetation dynamics it becomes apparent that the nature of these systems is intricate. The formation of a dynamic meandering channel proved to be complex. The majority of experiments carried out in the past resulted in braided systems. For unconstrained flow over a non-cohesive bed was found to be the main mode of instability and thus produced braided rivers (Grans and Paola, 2001). In more recent experiments, single thread sinuous (Tal and Paola, 2007) and truly meandering planform rivers were created (van Dijk, 2012).

In order to create more insights in the mechanisms that control these systems flume experiments will be used for this thesis. The main setup is an experimental flume meandering river. An overview of the research aimed at or related to experimental meandering rivers is given below.

2.3.1 Previous experiments

The change from braided to more meandering channels was achieved by adding a degree of additional bank strength to the flume sediment. Bank strength can be added in the form of either small scale vegetation, alfalfa (*Medicago sativa*) (Gran and Paola 2001) or mild cohesive material, silica flour (Peakal, 2007). Both measures slow the widening of the rivers and discourage channel cut-offs (Tal and Paola, 2010). A division in experimental setups can be made: those that use and investigate the behaviour of scale vegetation and the meandering river experiments. Finally a section is presented that describes the qualities of scale vegetation, mainly alfalfa, in light of biotic and abiotic factors.

Vegetation based floodplain formation in scale experiments

Initial research (Gran and Paola, 2001) was focussed at the effect of vegetation on a braided river. After the braided river had established itself alfalfa was seeded manually and homogeneous. The discharge was halved for the seed dispersal period in order to allow undisturbed vegetation growth. Several densities of vegetation were used in a range of experiments (0 to 9.2 seeds/cm^2) to increase the strength of the banks. The main results of the increased bank strength consisted of a decrease of the braiding intensity, increase in depth of the channel and an increase in the local transverse slope.

Tal and Paola (2007) performed experiments that started with a braided river in well sorted cohesionless sand. The flow regime of the river consisted of a two stage hydrograph with a low flow, no sediment transport, and a high flow stage, that reworked the channel morphology. To this river alfalfa seeds were distributed manually during the low flow stages (1 seed/cm^2). After 24 hours the vegetation had developed root systems and was 1 mm thick before the next flood. The increased bank strength focussed the flow into the main channel by reducing the width and preventing cut-offs. The main reason for the reduced occurrence in cut-offs is the increased threshold for cut-off initiation as a result of the larger transverse gradient that can be maintained by the increased bank strength (Tal and Paola, 2010)

The added vegetation led to a decrease in the wetted area and an increase in the depth of the channel (figure 2.24). The channel pattern changed from braiding to a sinuous single channel (figure 2.25). The single channel shifted between wandering and irregular sinuous. A dynamic balance between vegetation destruction, at the outer bends during floods, and establishment, at pointbars during low flow condition, was present.

So vegetation slowed bank erosion. This resulted in an equal rate of outer bank erosion and inner bend deposition. Important to note is that they claim varying the discharge is key to allow the feedbacks between plants and the flow. Low stage flow enables the growth and settlement of seeds on bare surfaces whilst high flow stages transport sediment (Tal and Paola, 2010).

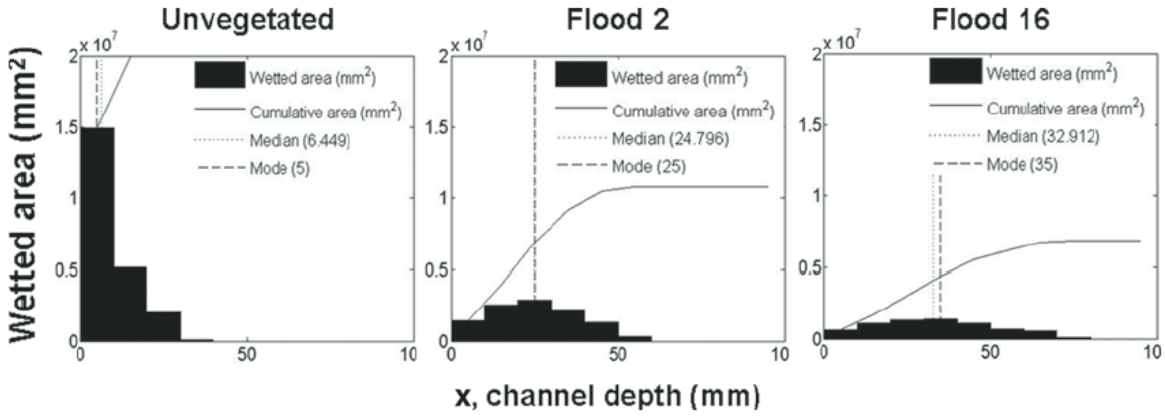

Figure 2.24 The decrease in the wetted area and deepening of the channels due to the change in channel pattern (Tal and Paola, 2007).

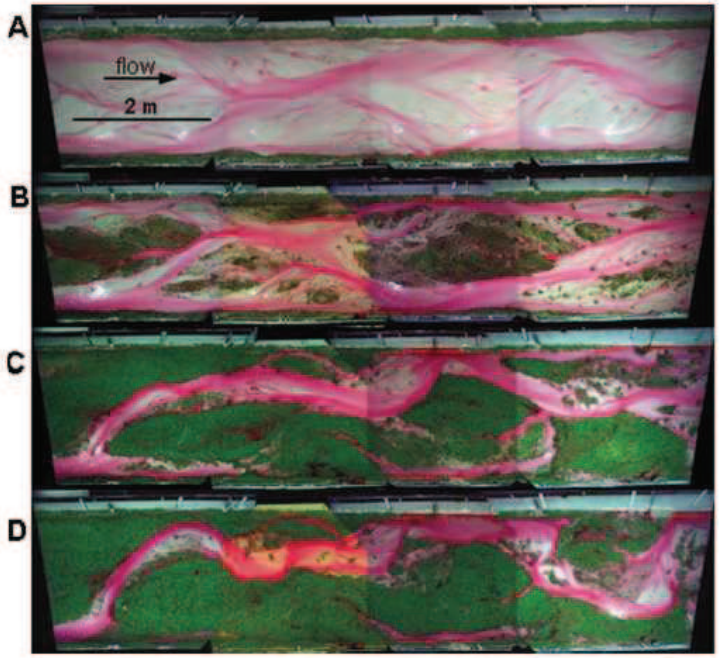

Figure 2.25. The change in channel planform due to the introduction of alfalfa seeds. (A) initial state (B) 6 flood cycles (C) 18 flood cycles (D)23 flood cycles balanced state where outer bank erosion and floodplain formation are balanced (Tal and Paola, 2007).

Braudrick et al. (2009) produced a lateral migrating meandering channel with repeated cut-offs. This was achieved by an increased bank strength by using, manually distributed, alfalfa sprouts. Furthermore the blocking of troughs (chutes) on the pointbar by suspended sediment deposition. After a cut-off occurred the lightweight sediment blocked the old channel. The blocking of early chute formation and abandoned channels prevents the formation of multiple channels and thus the transition to braiding. Instead of silica flour a lightweight plastic was used to represent the fines.

The introduction of alfalfa, to a poorly sorted sediment bed, resulted in narrower and deeper channel system. In case of a high densities alfalfa cover the lateral movement of the river halted, thereby creating a low dynamic anastomosing system with occasional sharp bends (Van de Lageweg et al., 2010).

Van Breemen (2011) observed reduced lateral erosion for a vegetated compared to a bare sediment meandering river. Furthermore the width of the channel was largely depended on the growth duration of alfalfa sprouts.

Perona et al. (2012) focussed on the ecomorphological aspects of small scale vegetation. They investigated the erosion timescale of pioneer small scale vegetation (*Avena Sativa L.*) in relation to

hydrologic disturbances. They homogeneously seeded a flat sand filled flume with a low density cover (0.23 seeds/cm^2) and added a low and a high flow disturbance to the system. If floods occurred to rapid after seeding, so in the early stages of plant development, uprooting occurred. With an increased period of time the floods did not affect the vegetation.

Silica based floodplain formation in scale experiments

The experiment carried out by Peakal et al. (2007) used the addition of fine material to add a degree of cohesion to the channel banks. This fine material was silica flour or crushed quartz (98% SiO_2). Silica flour is white and has a D_{50} in the range of 1-20 µm. It is affected by capillary and weak van der Waals forces. These forces scale appropriately to represent the cohesion introduced by vegetation and clay in real systems.

The experiment was carried out with a constant discharge. The channel morphology dynamically changed over time in a way that is characteristic for meandering rivers. At the upstream end of the initial straight channel a meander bend formed. The inner bends displayed scroll bar formation and a ridge and swale topography. Over time the meander migrated by inner bend accretion and outer bend erosion. Silica flour deposition accumulation took place on the higher parts of the bars and prevented the occurrence of chute cut-offs early in the bend development. Eventually chute cut-offs occurred and the remnant channels were filled with silica flour. This prevented the change to a braiding system.

Kleinhans et al. (2010) and van Dijk et al. (2010) were able to form a gravel bed meandering river with one active channel and chute cut-offs. This was done by adding 20% silica flour to a relatively poor sorted sediment. The poorly sorted sediment resulted in hydraulic rough conditions (Re*> 11.63). This proved crucial in maintaining sediment transport in the river. The added silica flour in the experiment was deposited on the floodplains lows, thereby filling up the swales. At the downstream section of the bend, past the apex, a fraction of the water moved onto the floodplain and created overbank splays of silica. Furthermore the inflow was angled at 30° to create an initial perturbation. Without the incorporation of silica flour a moderately braided pattern formed. An improvement of the angled inflow is a moving upstream boundary. This presented the river with an continued upstream perturbation that migrated downstream and resembled a more realistic upstream boundary for meandering rivers (van Dijk et al., 2012). The implementation of an upstream mobile boundary in the vegetation experiment conducted for this report could prove to be a key feature in maintaining bend development and morphologic change in the river.

2.3.2 Overbank flow and morphology

Floodplain flow

The majority of floodplain flow related research has been carried out in fixed flume setups (chapter 2.1.4). The scale experiment floods were never deliberately set above bankfull levels. This resulted in marginal inundation level overbank flow. On the vegetated floodplains of Gran and Paola (2001), for example, the flow was laminar instead of turbulent like in real world circumstances. The laminar flow creates a larger zone of interference for the alfalfa stems than is found in real vegetated turbulent floodplains.

Overbank morphology

In the experiments of Braudrick et al. (2009) overbank morphology developed. With a constant bankfull discharge some of the water flowing out of the channel carried the fine lightweight suspended sediment out of the channel and onto the floodplain. There vegetation trapped the fine sediment and created overbank deposits (figure 2.26).

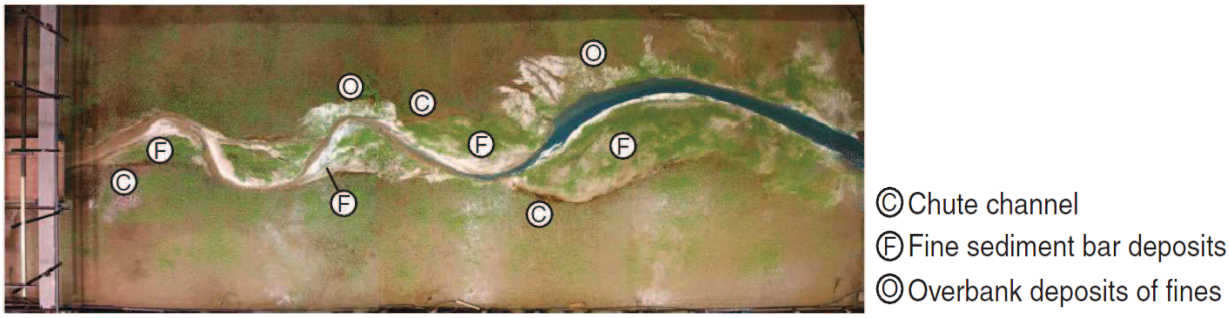

Figure 2.26. Overbank morphology in the experiments of Braudrick et al. (2009).

An experimental annular flume setup, specifically designed to investigate overbank deposition in scale experiments, illustrated that fine suspended sediment, silica flour, is able to form overbank deposits. Additionally it was shown that there is a balance between the location of deposition, proximal or distal, in relation to flow conditions. The settling of suspended sediment carried out of the channel is determined by a delicate balance between water height, flow strength and settling velocity (figure 2.27). It is hypothesized that fluctuating water levels might prove key in controlling the overbank flow driven sediment transport and settling of fines (Teske, 2011).

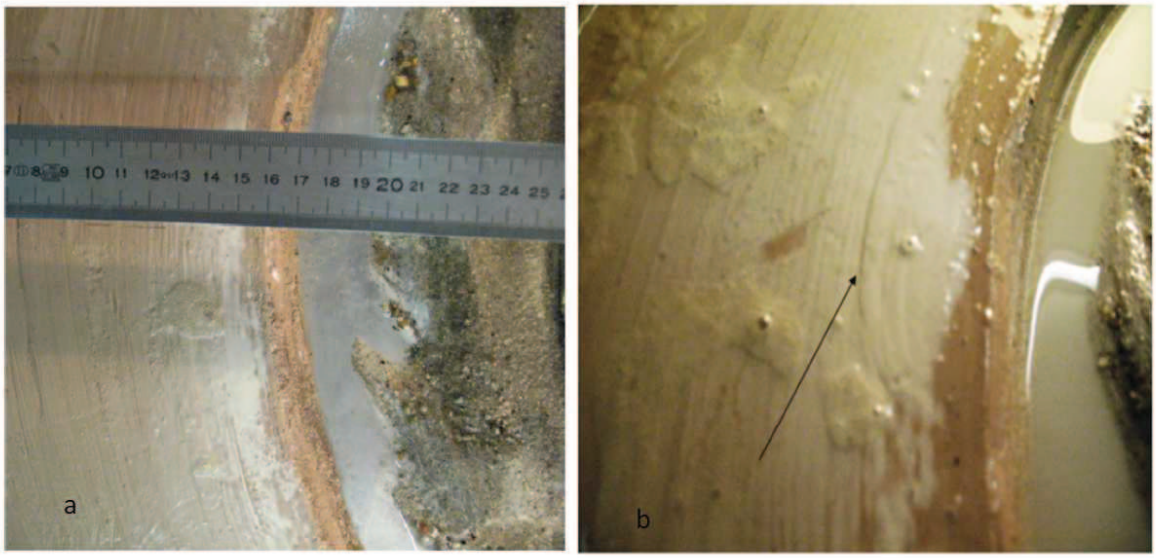

Figure 2.27. Overbank morphology in the annular flume. (a) displays proximal silica flour deposition for a floodplain inundation of 0.2 mm and 0.2 m/s of channel flow. (b) raised proximal silica flour deposition and distal deposition for 1 mm of floodplain inundation and 0.2 m/s channel flow (Teske, 2011).

2.3.3 Scaled riparian vegetation

The majority of the conducted experiments used alfalfa seeds for the scale vegetation. Although some research has looked into other species (Van de Lageweg et al. 2010) alfalfa proved the most suitable for scale experiments, due to appropriate scaling and easy germination.

A single alfalfa sprout roughly scales as a tree with a solitary trunk and high branches. A 1 mm alfalfa stem thickness is comparable with 80 mm trunk thickness of real vegetation (Gran and Paola, 2001).

The representation of the different abiotic, biotic and engineering properties of the recent, vegetation based, scale experiments is given below. Finally some of the riparian vegetation pattern related results are presented.

Engineering properties of scale vegetation

In experiments conducted with the addition of silica flour two different failure mechanisms were observed. The first was bank toppling and the second toe erosion. The presence of toe erosion is the result of the larger angle of friction that can be attained by the silica and sand mixture (van Dijk et al., 2010).

The alfalfa bank strength properties have been investigated by Van de Lageweg et al. (2010). Alfalfa mainly contributes to mechanical reinforcement of the river banks. A second effect of vegetation is an increased binding of the sediment. This is caused by organic material accumulation on the sand grains (Tal and Paola, 2010). The cohesion value and angle of internal friction are presented in figure 2.28. No general trend in the cohesion values as a result of larger densities of vegetation and an increased growth period were detected. The angles of internal friction were lower for more densely vegetated banks (Van de Lageweg et al., 2010).
In addition scaled erosion tests, known as Friedkin experiments (Van de Lageweg, 2009, Van Breemen, 2011), have been carried out. The Friedkin experiments marked a clear reduction in the eroded volume of sand for a seed density of 2.2 seeds/cm^2 and higher (figure 2.29). At a lower density (0.5 seeds/cm^2) there was an increase in the erosion of the bank around the stems of alfalfa. Another factor that contributes to the stability of the banks, by cohesion, is the capillary rise of groundwater. The effect of this is dependent on the size and distribution of sediment (Kleinhans et al., 2010).

Vegetation density (seeds/cm^2)	Growth duration (days)		
	0	3	5
0	1.7 ± 0.8		
0.5		5.0 ± 4.1	-0.1 ± 2.2
1.0		6.5 ± 2.7	5.1 ± 3.9
2.2		5.7 ± 2.1	9.0 ± 1.1
4.4		7.0 ± 2.9	8.8 ± 4.3

Vegetation density (seeds/cm^2)	Growth duration (days)		
	0	3	5
0	41.0 ± 1.7		
0.5		43.2 ± 7.4	48.0 ± 4.2
1.0		36.8 ± 5.0	38.8 ± 7.4
2.2		35.4 ± 3.9	30.2 ± 2.2
4.4		37.1 ± 5.5	35.9 ± 8.0

Figure 2.28 The cohesion values (kPa) and angles of internal friction (°) for alfalfa sprouts of different ages and in different density compositions (Van de Lageweg et al., 2010).

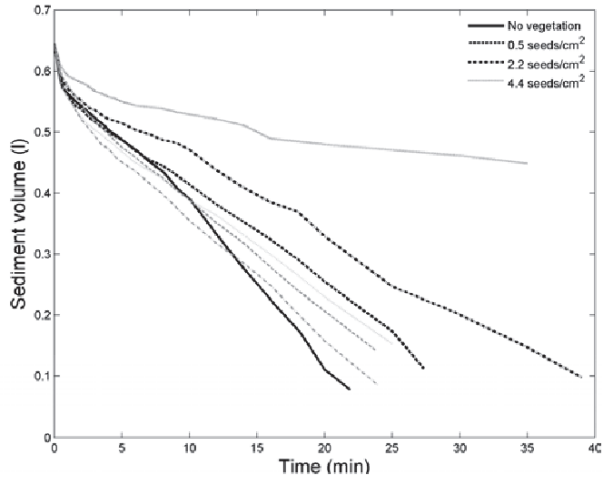

Figure 2.29. Volume of eroded sediment over time for different vegetation covers of alfalfa (Van de Lageweg et al., 2010).

The qualitative effects of vegetation on the roughness of the floodplain and the corresponding reduction in overbank flow velocities are mentioned by Gran and Paola (2001) and Braudrick et al. (2009). There is no numerical description found of the added roughness effect of scale vegetation in self-formed meandering river flume experiments. However there has been some research that was conducted in conventional flumes as well as some fixed bed meandering flumes (chapter 2.2.4).
The sediment trapping ability of riparian vegetation in scale channel pattern experiments has received little attention. There is only one reference to this effect. According to Braudrick et al. (2009) the sedimentation of fine lightweight sediment on pointbar lows is increased by the trapping effect of vegetation according. In the experiments of Perona et al. (2012) the uprooted vegetation accumulated together. This induced severe erosion of the bed locally. In general they found that the vegetation cover resulted in a reduction of the eroded sediment. The degree of the reduction was larger for a higher flood flow disturbance (figure 2.30).

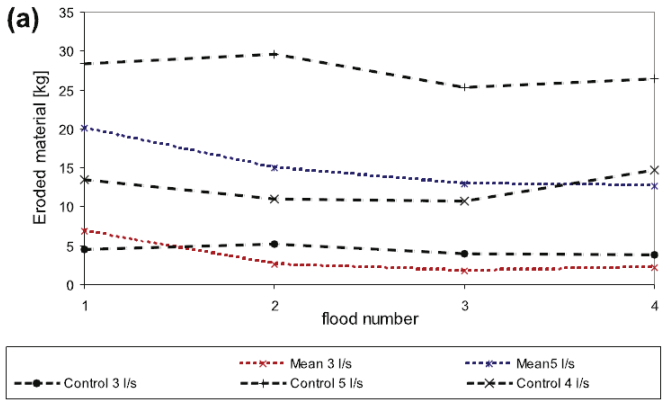

Figure 2.30. Eroded sediment for different flood disturbance scenarios (Perona et al., 2012).

Biotic process representation

In natural systems succession is an important process in real riparian vegetation (chapter 2.2.2). However in scale experiments the use of only one vegetation species, alfalfa, eliminates the biodiversity and succession found in real systems. When a single time of distribution is considered the second phase in the successional sequence (figure 2.15) is the only successional state that is represented in the flume. This means that there is a dominant species of roughly the same age that starts to grow around the same time.

The incorporation of multiple seed distribution phases in experiments is a way to increase the successional stages in scale rivers. For the younger seedling tend to be smaller. This means the increase in vegetation height could be used to implement succession in scale systems. The main limitation in applying this is the rapid growth of alfalfa. So after a short period of 6 days no vertical differentiation can be made in the vegetation pattern over time .

The dispersal methods of alfalfa in flume experiments is performed by using two different methods. The first method used is the manual seeding of scale vegetation (Braudrick, 2009, Tal and Paola 2007). This method ensures a homogeneous vegetation cover and allows a controlled density to be used. This method should be comparable to the seed distribution by wind and water of willows and cottonwood (Gran and Paola, 2001).

The second method is a more natural distribution by the flow (van Breemen, 2011). The discharge of the river is increased whilst seeds are introduced. After a fixed amount of time, the water levels are lowered again and the flow is turned off to allow the vegetation to grow.

The alfalfa used in the majority of the scale vegetation experiments germinates after 24 hours with root and stem development (Tal and Paola, 2007). It will reach a height of approximately 30 mm and a thickness of 1 mm in a 10-14 day period (Gran and Paola, 2001) and continue to be present in experiment that lasted up to 120 days (Tal and Paola, 2010). The growth of alfalfa is given in figure 2.31.

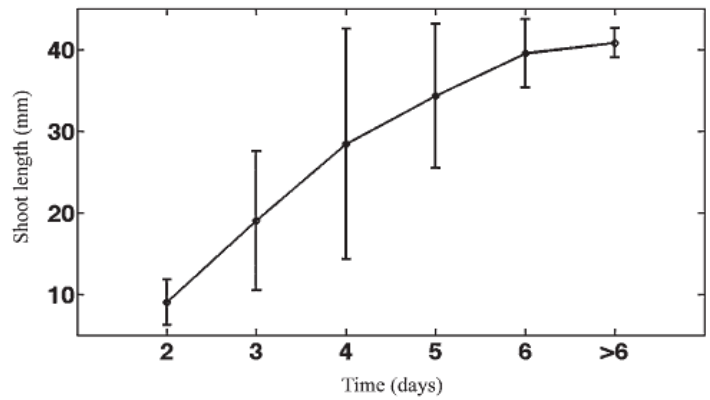

Figure 2.31. The length of alfalfa stems over time. The initial growth is rapid and levels over time. After four weeks plants tend to deteriorate (Tal and Paola, 2010).

Abiotic process representation

Flood stages have been implemented in the scale experiments. They proved to provide a window for vegetation growth and settlement on bare surfaces during low flow (Tal and Paola, 2010). The floods in river experiments lacked the potential to uproot vegetation on the floodplains, but outer bend erosion proved to be able to erode the vegetated outer banks (Tal and Paola, 2007, van Breemen, 2011). The root depth in relation to flood disturbance was crucial in controlling vegetation uprooting in flat flume experiments. For longer root systems could withstand floods whereas less developed vegetation was removed (Perona et al., 2012).

Based on the research conducted by Van de Lageweg et al. (2010) and Van Breemen (2011) it was found that alfalfa has a reasonable tolerance rate to acidity and it does not require any light to germinate. Sandy soils are suitable for sustaining alfalfa growth. This makes the species suitable for laboratory conditions.

2.3.4 Scaled riparian vegetation patterns

Since the focus of the majority of the vegetation related experiments aimed at creating meandering river no attention had been paid to the patterns that are present in the vegetation cover. Furthermore, the distribution of seeds in the flumes was largely performed manually. This essentially eliminates the presence of patterns by flood driven seed dispersal. Based on previous experiments the only recognisable pattern is the bare sediment on the accumulated active part of the pointbar (Bendix and Hupp, 2000). It can be seen in the experiments of Tal and Paola (2007) (figure 2.32 B).

The flood based seed dispersal allows for more vegetation pattern formation. This is due to the settling of alfalfa seeds on the low (swales) of the pointbar (Van Breemen, 2011). This allows the distinction of several phases of seed distribution and scroll bar accumulation (figure 2.32 A). No detailed look into the experimental pattern was carried out.

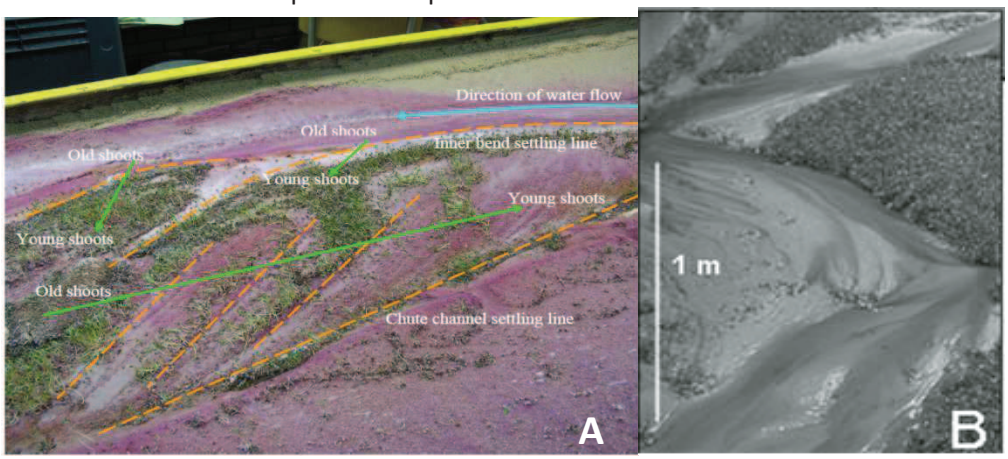

*Figure 2.32. **A** Alfalfa growth on the swales of the pointbar (van Breemen, 2011). **B** Bare sediment on newly formed inner bend accumulations (Tal and Paola, 2007).*

3. Synthesis, research questions and hypothesis

In this section a synthesis of the literature review in chapter 2 is presented. The knowledge of meandering river dynamics in relation to riparian vegetation cover development is combined with the recently development self-formed meandering rivers. This results in a set of sub questions that are aimed at investigating specific effects of riparian vegetation on meandering rivers.

3.1 Synthesis and research questions

Meandering rivers are sinuous channels that are created by the feedback between bars, flow, outer bend erosion and inner bend accretion. The processes that determine the general flow behaviour of meandering have been studied in real rivers and flumes and are relatively well understood. In natural environments the meandering river reaches are often vegetated.

The presence of riparian vegetation exerts a poorly understood degree of influence on the meandering river. The vegetation along the channel margin provides additional mechanical and hydrological reinforcement of the river banks (Simon and Collison, 2002). This has the potential to control the erosion and accretion of the bends and thus the river width (Kleinhans, 2010). The rougher vegetated floodplains focus the overbank flow into the main channel (Jahra et al., 2010) and trap increased amounts of sediment (Geerlings et al., 2008).

The succession of the riparian vegetation and the formation of vegetation patterns has been studied mainly from an ecological point of view (Naiman et al., 1998). The riparian vegetation evolution is strongly linked to the hydrologic control of the river. Floods control the dispersal of seeds, moisture availability and determine the local soil texture composition (Perona et al. 2012). Floods also destroy vegetation by physical destruction, burial and an anoxic environment during inundation of the floodplain (Bendix and Hupp, 2000).

The interplay of all the above described processes form patterns in the riparian vegetation cover and affects the meandering river dynamics. Although some modelling studies have attempted to increase the understanding of riparian vegetation patterns and river system dynamics (figure 2.1(f)), there remains a lack of a detailed comprehension of ecomorphologic processes (Osterkamp and Hupp, 2010).

Recently researches have succeeded in creating self-formed truly meandering rivers in a laboratory environment (van Dijk et al. 2012). This has been achieved by increasing the bank strength and controlling the formation of chute cut-offs, by adding slightly cohesive sediment (van Dijk et al., 2012). Alternatively small scale riparian vegetation was used to add bank strength, which resulted in a sinuous channel with meandering characteristics (Tal and Paola, 2007, Braudrick et al., 2009).

The meandering scale river research so far has been focussed on creating a meandering river in laboratory environments. The success of creating meandering rivers provides a suitable setup to investigate the interactions between riparian vegetation and meandering rivers. It poses a potentially powerful tool to untangle their interconnectivity and investigate this chicken and egg question.

Recent research has investigated the general effects of riparian vegetation on the planform of laboratory rivers. Detailed aspects of the ecosystem engineering effects of scale vegetation on experimental meandering rivers, as well as the interactions between riparian vegetation patterns and channel dynamics, remain unanswered.

Unlike the effects of vegetation on bank strength (Lageweg et al., 2010, van Breemen, 2011), no quantative look into the other engineering effects of scale vegetation has been carried out. So far roughness, due to the presence of vegetation in scale experiments, has been mentioned qualitatively by Gran and Paola (2001) and Braudrick et al. (2009). Furthermore the roughness of real vegetation is investigated in schematized flume (Järvelä, 2002) and modelling studies (Straatsma and Baptist, 2007). In order to comprehend the system behaviour as a result of vegetation induced hydraulic resistance, a quantative expression of roughness is required. The first question (1) is:

- *What is the added roughness by scale and real riparian vegetation in floodplain flow?*

The distribution of discharge between the floodplain and the overbank area during floods has been studied in fixed base flumes (Jahra et al., 2010). The fixed based experiments illustrated a reduced overbank flow and an increased fraction of the discharge through the channel, as a result of vegetation roughness. In those setups there is no feedback between the flood water division and the morphologic development of the channel. The second question (2) is:

- *What is the distribution of discharge over the floodplain and channel in a vegetated compared to a non-vegetated flood regime situation?*

The effects of scale vegetation on controlling the experimental channel planform has been recognised. A vegetation induced increased bank strength, reduced the width of a braided system and created a more meandering river by increasing bank strength and controlling chute cut-offs (Tal and Paola, 2007). Without vegetation meandering rivers have been created by using the strength of silica flour (van Dijk et al., 2010). The introduction of scaled vegetation to an already meandering river has not been studied before. Therefore the next question (3) is:

- *What is the effect of a riparian vegetation cover on an experimental meandering river pattern?*

In addition the effects of vegetation on meandering river bend mobility and erosional mechanics, as well as the impact of eroded alfalfa on the river, have not been studied. The next two questions (4,5) are:

- *How does riparian vegetation affect the inner bend accretion and outer band erosion?*
- *What is the role of the eroded outer bend vegetation on the channel?*

The last hydraulic resistance related effect of vegetation is the trapping of suspended sediment. This has been mentioned by Braudrick et al. (2009) to be present in a scale river and by Geerling et al. (2008) in real rivers. However no controlled research has been carried out of this effect in scale experiments. The question (6) is:

- *How does the, literature suggested, riparian vegetation sediment trapping effect influence the formation of overbank morphology?*

Finally, in the recent series of channel pattern flume experiments no work has been performed that registered and evaluated the changes in the vegetation cover patterns in relation to meandering river dynamics or biotic and abiotic processes. The final question (7) is:

- *What is the effect of a scale meandering river on riparian vegetation pattern development?*

3.2 Hypotheses

Based on the literature review in the first section of this report hypotheses can be formulated to provide preliminary answers to the questions. The hypotheses will be tested in a series of flume experiments. The experimental approach and setups are explained in more detail in chapter 4.

Hypothesis 1

The hydraulic resistance of riparian vegetation has been shown to be dependent on a wide range of factors. These are; density, species composition, seasonal timing, floodplain inundation depth and flow velocity (Järvelä, 2002, Armanini et al., 2005). In earlier studies a general trend of increased roughness for flow through more dense vegetated areas has been shown in modelling studies (Straatsma and Baptist, 2007) and flume experiments (Järvelä, 2002). Therefore it is likely that the addition of vegetation on the floodplains results in an overall increased hydraulic resistance.

Hypothesis 2

The influence of vegetation on the discharge division will most likely manifest itself through the added resistance on the floodplain. This reduces the flow velocities through the vegetation and results in a larger fraction of the discharge through the channel. For similar results were found in a compound channel floodplain study (Jahra et al., 2010).

In contrast to the compound study a loose sediment based meandering river is used in the experiments conducted for this report. This means the distribution of discharge is likely to determine the sediment mobility during floods and the morphological development of the river. Similar to the braided river experiments by Gran and Paola (2001) the added alfalfa could focus the flow and deepen the experimental meandering river channel. This could further increase the portion of the flood discharge in the channel.

Hypothesis 3

By introducing scale vegetation to a meandering river there is an increase of the bank strength of the experimental channel (Van de Lageweg, 2010, Van Breemen, 2011). The increased bank strength will most likely control the lateral mobility of the meandering experimental channel. This could either reduce the overall sinuosity of the system or allow a larger transverse gradient, at which chute cut-offs occur. If the last is the case it should increase the sinuosity of the river.

Hypothesis 4

The stronger vegetated outer banks will be more resistant to erosion of the banks by the flow (Eaton and Millar, 2004, Pollen and Simon, 2005). The inner bend accretion in turn will be forced by the created space in the outer bend of the scale meandering river. Furthermore the potentially reduced lateral activity could decrease the overall sediment supply and thus the accretion velocity of the inner bend.

Since the outer bend is stronger and kept together by roots, when vegetated, the failure and erosional mechanics could potentially differ for a vegetated compared to non-vegetated bank. The erosion of sediment by entrainment of the flow is potentially reduced as a result of the roots (Abernethy and Rutherford, 1998). The added vegetation also increases the overall strength to allow more severe undercutting processes than in a non-vegetated river (Micheli and Kirchner, 2002).

Hypothesis 5

The uprooted sprouts that enter the channel are likely to accumulate on the highest part of the banks, as was found by Van Breemen (2011). The local sprout accumulation has a potential to create a downstream sheltering effect, which could prevent erosion or induce sedimentation (Edwards et al., 1999). Alternatively the aggregates of scale vegetation debris could create local scouring of the river bed, similar to the experiments of Perona et al. (2012)

Hypothesis 6

The formation of overbank morphology could be increased due to the presence of vegetation on the floodplain by a vegetation induced reduced flow velocity. The sediment trapping effect of vegetation is most likely density-dependent. In low densities the turbulence around the stems could counteract with the settling of fines by re-suspending the fines. For this effect is found in real environments (Baptist, 2003) and in less dense scale vegetation environments (Van de Lageweg et al., 2009). Higher vegetation densities could increase settling by reducing flow velocities. Alternatively high densities could block the flow onto the floodplain and thus restrict sediment transport.

Hypothesis 7

After vegetation is manually and homogeneously introduced to the meandering river it becomes possible to determine the influence of the river on the homogeneous scale vegetation cover. The changes in the homogeneous vegetation cover are expected to be the result of the removal of existing vegetation by erosion, similar to the flat flume experiments of Perona et al. (2012). The erosion and sedimentation processes drive the change in riparian vegetation pattern. The interplay of river development and existing vegetation cover could allow the formation of some of the patterns described by Perucca et al. (2006).

With multiple phases of flood stage flow driven seed dispersal more intricate patterns could form. Some of the expected patterns are the formation of parallel band of vegetation on the floodplain, as described by (Gurnell and Petts, 2002) for a real system. Alternatively seed deposition on the higher scroll bar could be linked to multiple phases of accretion (Stella et al. 2011) or ridge and swale topography (Nanson and Beach, 1977). Finally In case of chute cut-offs more intricate vegetation patterns could arise (Stella et al., 2011).

Part II. Experimental setups and results

In the second part of the report the methodology of the conducted experiments is given. This is followed by a detailed description of different flumes and the way the flumes are used to investigate the main question. Furthermore the results of the different flume experiments are presented. The growth experiments are presented first, which are followed by the scale meandering river development. Detailed aspects of the experimental river, the overbank flow and outer bank erosion, are elaborated in the controlled annular flume environment. In order to present a degree of scaling to the scale experimental vegetation hydraulic resistance a series of measurements in a full scale natural vegetation covered flume are presented. Finally the results are and the conclusions are presented.

4. Methodology, methods and materials

4.1 Methodology

Setup of the experiments

Three different setups are used to answer the main questions. The main focus is the effect of riparian vegetation in a meandering river environment. This will be investigated in a self-formed meandering river flume experiment. A scale vegetation cover will be added to a bare sediment meandering single thread channel in the Eurotank flume (chapter 4.2.2). In addition a bare sediment control experimental river will serve as a control experiment in order to isolate the effects of vegetation. A constant discharge will be used with brief above bankfull discharges to inundate the floodplain and allow a comparison between the floodplain related flow effects of a bare sediment and vegetated river. Due to the morphologic feedbacks in the experimental river a second scale experimental setup will be used to isolate the scale vegetation induced hydraulic resistance effect and serve as a frame of reference for vegetation dynamics and pattern related effects (figure 4.1).

The annular flume setup (Teske, 2011) will create a consistent channel and overbank flow (chapter 4.2.3). This allows a rapid succession of pilots that link the vegetation density to the erosion of the outer banks and floodplain velocity. In addition the annular flume will create an environment where silica flour creates morphologic features (Teske, 2011).

The way alfalfa affects the hydraulic resistance will be compared with the series of 1:1 scale flume measurements of real vegetation. The hydraulic resistance of western European riparian vegetation will be determined in an overgrown abandoned outdoor flume at the University of Southampton (UK) (chapter 4.2.4). In contrast to the idealized vegetation used in other experiments (Järvelä, 2002) the UK location has a naturally formed cover of grass, shrubs and trees. This is similar to the vegetation cover found in real riparian forested floodplains after human disturbance and allows a better representation of the vegetation induced hydraulic resistance. A schematic structure of the hypothesis that will be answered with a specific experimental setup is given in figure 4.1.

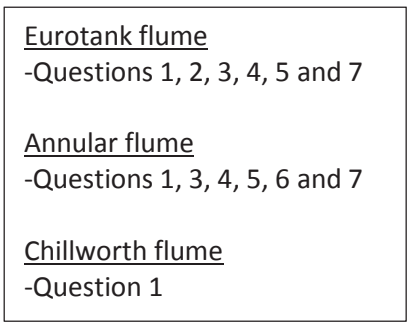

Figure 4.1. The sequence of the experiments that are to be conducted in order to answer the main questions of this report.

Scaled riparian vegetation cover

The scale vegetation in the flume experiments will consist of a homogeneous vegetation cover. A homogenous cover, seeded once, essentially eliminates all the potential effects of the river on the formation of scale riparian vegetation patterns. The second benefit of using a homogenous cover of evenly aged vegetation is the absence of successional differences. Furthermore when seeds are distributed only once the density will not change over time. If the experiments are carried out within four weeks no deterioration of the alfalfa sprouts is present and the vegetation effect is constant. This means that all of the changes in initial bare sediment meandering river, after introducing the vegetation cover, are due to the vegetation cover.

Furthermore intricate riparian vegetation patterns are most likely to be absent in a homogeneous cover environment. Some of the erosion driven changes in vegetation patterns in the uniform cover establishment could potentially be linked to literature described patterns in riparian vegetation cover and related to an erosion driven river forcing on vegetation patterns.

The density at which vegetation needs to be spread can be determined quickly with the annular flume setup. The key is to find a vegetation density range that provides bank strength to non-cohesive sand, but does not eliminate lateral mobility of the channel. The range of vegetation density is based on past research (Van de Lagweg, 2010, Van Breemen, 2011).
With a controlled vegetation cover density the roughness can be determined from the water depth and flow velocity of the overbank flow. Since the stems are the only parts of the alfalfa that are submerged the Baptist et al. (2006) equations, for fixed tube vegetation, could be determined for the alfalfa cover as a first estimate of the roughness.

4.2 Methods and materials

This research project is aimed at investigating the effects of riparian vegetation on a meandering river. In this chapter an overview of several flumes and data collection methods, that were used for conducting the research, are given. In addition a small support experiment is given, aimed at investigating the tolerance of alfalfa (*Medicago sativa*) to an anti-fungi additive

4.2.1 Alfalfa support experiments

Copper sulphate tolerance

In a recent series of flume experiments the alfalfa lifespan was strongly reduced by a type of fungi (*fusarium* wilt). Furthermore, the fungi prevented the sprouting of newly seeded alfalfa in later stages of the experiments. In order to prevent the fungi from developing in the experiments copper sulphate ($CuSO_4 \cdot 5H_2O$) was recommended (Temmerman, personal communication, 2011). A test was developed to determine the tolerance of alfalfa in relation to sprouting and growth over time.
The tolerance to alfalfa was tested by setting up growth experiment for a range of copper sulphate concentration. For this experiment five identical, pre-washed, containers were filled with the same sediment as used in the annular flume experiments. To these samples a fixed amount of alfalfa seeds were added (50) and watered once with a 100ml of copper sulphate solution. The copper sulphate dilutions were made by diluting a 1 g/100 ml solution. An overview of the added concentrations is given in the table 4.1 below.
The vegetation was left to grow undisturbed, apart from daily watering (without copper sulphate), at room temperature (22°C) and equal ambient lighting conditions for all samples. The alfalfa growth was monitored by taking daily photographs of each sample container. In addition the number of alive sprouts was counted and the length of the stems was measured with a ruler.

Sample number	Added concentration (mg/100ml)
0	0
1	0.001
2	0.010
3	0.100
4	1.000

Table 4.1. Different copper sulphate test sample concentrations. Sample number zero serves as a control experiment.

Alfalfa seed distribution density determination

The alfalfa that was introduced in het flume experiments and setups was added in different densities, a low 1.5 seed/cm^2 and a high 3.0 seed/cm^2 density. Since the amount of sprouted alfalfa differs, based on the local flume environment, the density is related to the number of seeds per square cm (seeds/cm^2). For this research the suggested quantity of seeds by van Breemen (2011) was recalibrated. This was done by counting the amount of seeds in a single gram and extrapolating for larger areas and densities. The results differed from the Van Breemen (2011) densities. A higher amount of seeds was required to achieve the prescribed seed/cm^2 density. An overview of the different densities and corresponding seed quantities is given in table 4.2. The alfalfa seeds were

distributed manually in all experiments at these predetermined densities. They were left to grow without disturbances for 6 days with a daily watering regime.

Alfalfa density (seed/cm^2)	Surface area (cm^2)	Seed quantity (g)	Van Breemen (2011) seed quantity (g)
1	150	0.27	0.10
3	150	0.81	0.30

Table 4.2. Overview of the different densities of alfalfa used in the experiments and the required amount of seeds compared to the Van Breemen (2011) suggested quantities based on sample extrapolation.

4.2.2 Eurotank facility

The Eurotank facility is located at TNO at the Uithof in Utrecht. It houses a 6 m wide by 11 m long flume with a 10 cm thick bed of poorly sorted sand (figure 4.2). The flume was used to create a self-formed meandering river. The width of the flume system was reduced to 3 m in order to support two river experiments. The first experiments was used to evaluate the effects of alfalfa and the second served as a control. The overall setup of the flume is based on previous experiments (Van Breemen, 2011, Van Dijk et al., 2012).

Experimental conditions

The river was designed to represent a bed load gravel bed river. The flow was sub-critical (Fr<1) and fully turbulent in the channel (Re>500). In order to ensure sediment transport the shear stress was higher than the critical shear stress ($\theta > \theta_{cr}$). The layout of the flume consisted of an upstream boundary, with a controllable discharge volume, that entered the flume through a laterally mobile inlet. In addition sediment was fed to the system at the inlet. At the downstream end a weir was present where the flow entered a wide basin where the water was collected and re-circulated through the flume.

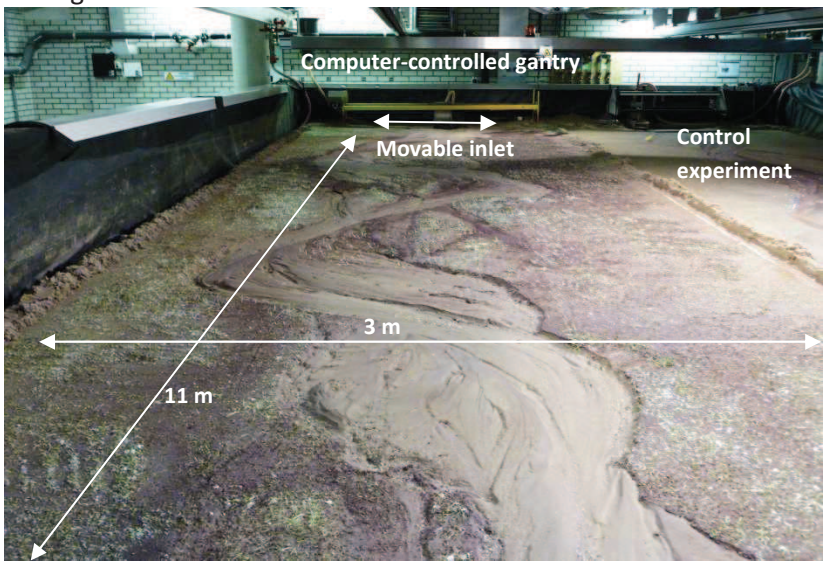

Figure 4.2. An upstream looking image of the Eurotank setup. The computer controlled gantry serves as the base of the laser scanner and cameras (van Dijk et al., 2012).

The approach taken to create a self-formed meandering river consisted of flattening the sediment bed at a fixed slope. In the flatbed a straight 15 cm wide 1 cm deep channel was carved. The initial channel was smaller than the required channel dimensions. This corresponded to river in the under-damped regime (Van Dijk et al., 2012). The upstream disturbance was maintained by moving the upstream boundary sideways. The upstream inlet was moved at a rate of 10 mm/hr with an amplitude of 30 cm (Van Dijk et al. 2012). The inlet was set a half a channel width offset, this means the inlet was focussed at the floodplain and the half of the channel.

Parameter	Value
Initial channel width (m)	0.15
Initial channel depth (m)	0.01
Slope (m/m)	0.01
Reynolds number	>2000
Froude number	<1
Shields mobility (θ)	$\theta > \theta_{cr}$

Table 4.3 Design conditions of the meandering river experiment Eurotank facility (Van Dijk et al., 2012).

Discharge and sediment feed regimes

A number of discharge scenarios were used during the run. The initial meandering river was formed with a 1800 l/h discharge. A brief flood discharge was used for overbank velocity measurements. The same two discharges were used in the initial stages of the vegetated river. Due to lack of lateral mobility in the river the constant discharge was increased from 1800 to 2250 l/h. After seeding of vegetation a very low discharge was used to water the flume. The duration of the watering interval was 4x15 minutes per day for the 6 day growth period. An overview of the different discharges is given in table 4.4. The discharges and sediment feed used throughout the vegetation meandering river experiment is listed in figure 4.3. The initial sediment feed and discharge values were used for the control experiment.

Flow scenario	Discharge (l/h)	Duration (min)
Alfalfa watering	600	15
Constant discharge	1800	-
High discharge flood regime	2500	5
Vegetated constant discharge	1800	-
Vegetated constant high	2250	-
Vegetated flood regime	2500	5

Table 4.4 Overview of the used discharges in the Eurotank facility.

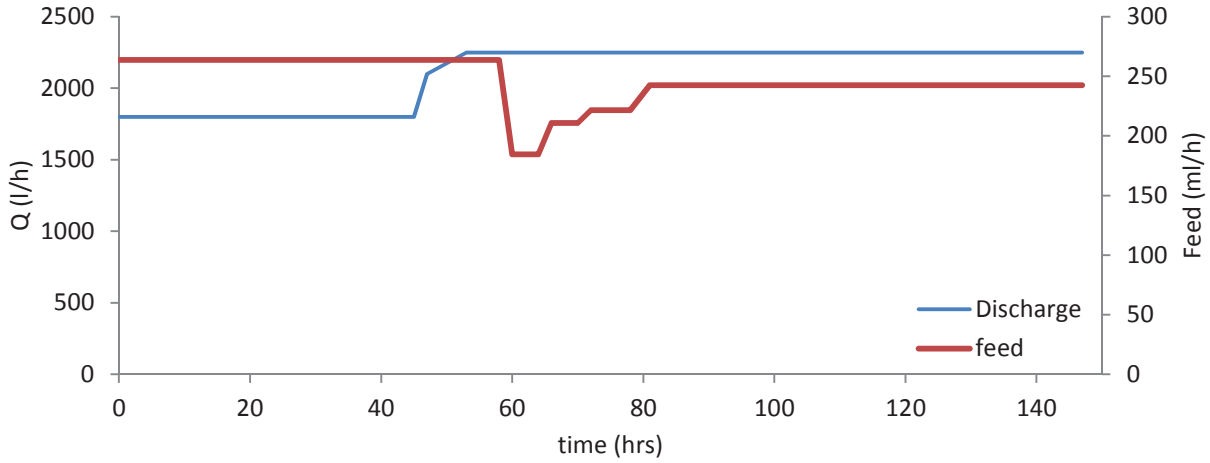

Figure 4.3 The sediment feed and discharge during the experiment.

Materials

A poorly sorted river sand was used to ensure hydraulic rough condition (Kleinhans, 2010). A slightly different river sand was used in the Eurotank flume compared to the annular flume and alfalfa growth experimental setups. The Eurotank sediment sieve curve is given in figure 4.4. It has a D_{50} of 700 µm and a D_{90} of 2000 µm. At the upstream boundary of the flume sediment was fed at an initial rate of 240ml/h. The feeder sediment was identical to the bed sediment, apart from a removed larger than 2 mm fraction in order to prevent damage to the feeder.

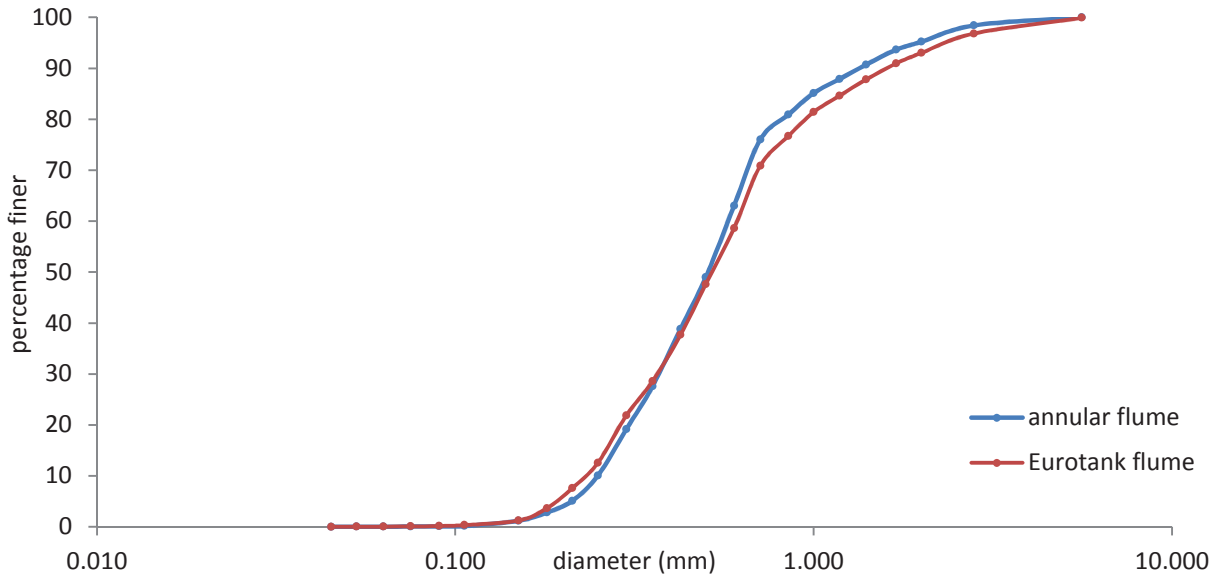

Figure 4.4 Sieving curve of the Eurotank and annular flume sediment.

After the meandering river had sufficiently developed itself alfalfa seeds were distributed. The distribution of seeds was done by dispersing fixed quantities over a 1x1m surface area in order to achieve a 1.5 seed/cm^2 cover. At the upstream inlet the flume was left un-vegetated to allow the lateral shift of the inlet. At the time of seed dispersal the flow was reduced to 600 l/h in order to prevent seeds from settling in the channel. After seeding a low flow stage was implemented twice a day to water the vegetation

In order to prevent fungi from affecting the vegetation, copper sulphate was added to the re-circulating water in the basin at the downstream end of the flume. The volume of the downstream basin was 0.25 m*0.65 m*6 m= 0.975 m^3. This meant a total of 9 mg of copper sulphate was added based on a series of alfalfa growth tests determined in chapter 5.1.

Data collection

The flume is fitted with an automatic laser scanner and cameras (0.25 mm/pixel) that captured the complete dry flume at selected intervals of time. The laser scanner output was used to create a digital elevation model (DEM) of the flume morphology with a resolution of 2 mm. The collected images were stitched together to form RGB-images of the flume at the laser scan intervals. Furthermore single detail series of photographs were made at specific flume locations during the run. Flow velocities were measured by taking multiple photographs of a section of the flume, with a fixed 0.6 second interval, whilst releasing a contrasting fluorescent tracer. The velocity measurement method is an image based adaptation of the Richardson and Carling (2006) (chapter 4.2.5).

Data reduction

The digital elevation models of the flume where used to determine the inner bank transverse bedslope, sinuosity, bend curvature and bend migration. The sinuosity was determined by manually marking the main river channel on the DEM grid. The distance between the data points was used to compute the along river length of the system via the Pythagoras equation. The curvature of the bends was determined by manually marking the main channel direction along a bend. This was converted to a maximum curvature value and location by an automated curve fit script.

The rates of erosion, expressed as width per hour (w/hr), were based on the erosion between two consecutive DEM time steps. This means 2-4 hour intervals were considered. The erosion of the bend was determined on the maximum curvature location in the system for each time step. Finally several cross-sections were made at the bend apex locations that provided the local width, depth and transverse bed slope steepness.

4.2.3 Annular flume

The term annular refers to a circular continuous flume channel. Often this type of flume is used in experiments aimed at recreating the environment of turbidity currents. These environments require a high velocity flow in an infinite length of channel. In annular flumes the flow is generated without the use of pumps. Instead a circular plate on the water surface is the driver of the flow. The base of the flume is rotated in the opposite direction. The opposite directed drivers of the flume flow counteract the secondary flow that would otherwise form in the continuously bended channel (Sumner et al,. 2008). The setup constructed by Teske (2011) only drives the top of the water surface in a single direction. It was found that this creates a secondary current in the channel, which makes the setup especially suitable for river (morphodynamic) related research.

The annular setup, that is used for this research project (figure 4.5), consists of a 0.8 m wide metal basin that can be filled with either clay or sand. In the clay or sand a continuous circular channel is created with a fixed 0.20 m radius by using a channel template. The unique feature of this annular flume is a floodplain area on either side of the channel. The outer bank, 15 cm wide, floodplain allows overbank flow and morphologic development. In the centre of the setup a rotating metal shaft is present. On top of the shaft a removable large disk is fitted. The disk supports up to 12 paddles that drive the flow in the 11.4 cm wide 1.2 cm deep initial channel (figure 4.5). The flow velocity in the channel and the inundation depth of the floodplain can be controlled. The range for channel flow velocity lies between 0.05 and 0.5 m/s and the floodplain inundation depth is variable between 0-1.5 cm. The forcing of the flow is the disk or paddle velocity at the centre channel radius (table 4.5) (Teske, 2011). The water level in the flume can be increased and lowered gradually to simulate the passing of a flood wave.

Forcing condition	Paddle velocity (m/s)
1	0.25
2	0.29
3	0.41
4	0.63

Table 4.5. The annular flume paddle velocity in the centre of the flume channel.

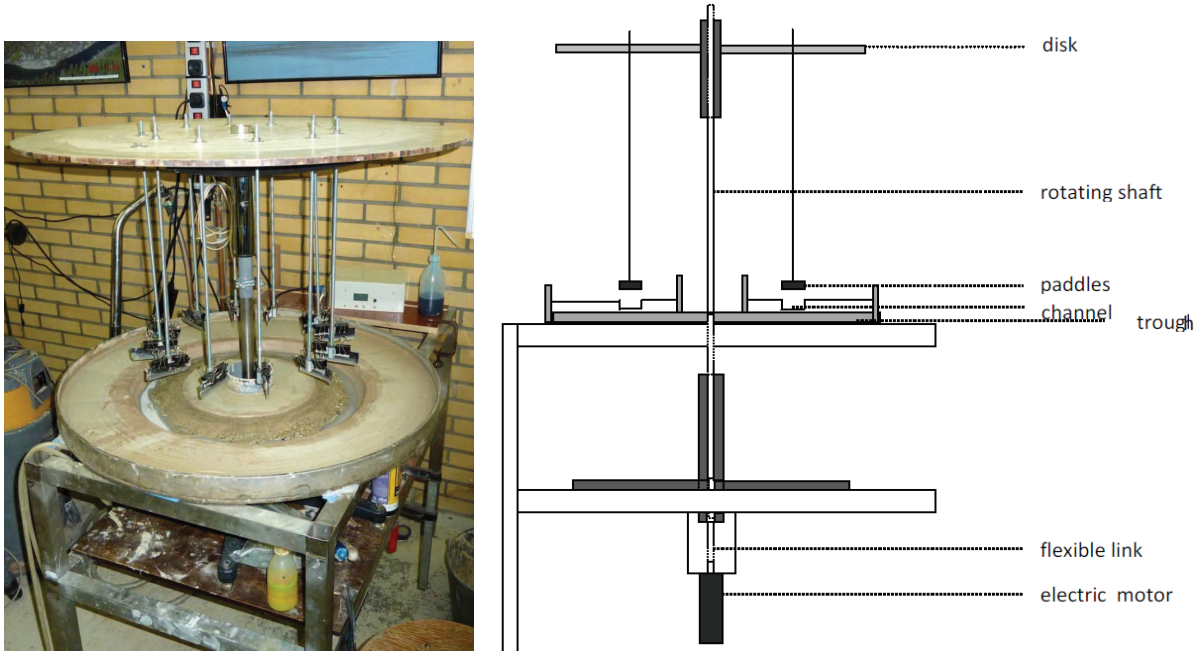

Figure 4.5. Annular flume setup that allows controlled and constant over bank inundation levels and flow velocities (Teske, 2011).

Experimental conditions

Multiple experiments were conducted for this research that had the same initial conditions, listed in table 4.6. The flow in the channel was sub-critical (Fr<1) and fully turbulent (Re>500) in order to

prevent hydraulic smooth conditions a poorly sorted river sand was used (Kleinhans, 2010). For each experimental environment, the no-vegetation and vegetation covered floodplain, the same flow forcing's and floodplain inundation depth scenarios were used. The floodplain inundation levels consisted of a low 2 mm and a larger 4 mm water level. The water depth on the floodplain was measured when the flume was stationary. The flow velocities in the flume were kept constant for a specific run.

Parameter	Value
Bend radius *(m)*	0.20
Initial channel width *(m)*	0.114
Initial channel depth *(m)*	0.0012
Slope *(m/m)*	0

Table 4.6 Fixed annular flume parameters used in this report.

Materials

The sediment on the bed of the flume and the floodplain was the same poorly sorted river sand, with: a D_{10} of 250 µm, D_{50} 480 µm and D_{90} 1350 µm (figure 4.4). In addition silica flour, ground quartz 98% SiO_2, was added as 20 volumetric percentage of the channel bed during runs. The added silica (M6) had a D_{50} of 30 µm.

The first runs with the flume were performed with a sand filled flume. These experiments formed the reference measurements against which the vegetated experiments could be compared. The sand filled flume is given in figure 4.6 A. In later runs vegetation was introduced to the flume. It was seeded manually at a two different densities (1.5 and 3 seed/cm^2).

Before seed distribution the channel was covered by a wooden ring to prevent seeds from sprouting in the channel. The ring was weighted down to prevent it from floating when adding water to the system (figure 4.6 B). After seed dispersal the alfalfa was left to grow undisturbed for 6 days, during this period the vegetation was watered daily. The resulting vegetation seed density of 3 seeds/cm^2 on the inner and outer bend floodplain is given in figure 4.6 C.

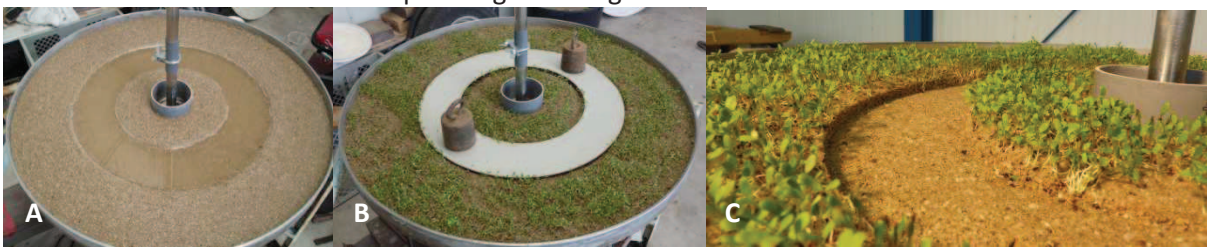

*Figure 4.6**A**. The bare sediment filled flume. **B** The recently seeded flume. **C** The seeded flume before the experiments with a 3.0 seeds/cm^2 density.*

Data collection

The flow velocities in the channel were previously calibrated for a clay channel (Teske, 2011). However the use of sand and vegetation made it necessary to re-determine the velocities. The channel velocities were measured by timing tracer dispersion in the channel, using film. Film was also used to determine the outer bank erosion. This meant a camera needed was suspended directly above the channel margin and floodplain area. In order to quantify the erosion rate a ruler was placed perpendicular to the channel in the camera view. The same setup was used to take a series of consecutive images, with a fixed 0.6 second interval, of tracer movement on the flume floodplain. Instead of a ruler perpendicular to the channel a parallel ruler was used to create a frame of reference for the measurements. The resulting data was analysed by adapting the Richardson and Carling (2006) method, this is described in more detail in chapter 4.2.5. Finally, cross-sectional profiles of the bed development were made after regular intervals of continuous flow by measuring down from a horizontal reference plane with digital callipers.

4.2.4 Chilworth flume

The Chilworth flume is located at the University of Southampton (UK). It consists of a fixed concrete base trapezoidal channel that is 1.5 m wide and 51 m long. The slope of the flume is fixed at 0.00 5m/m. Approximately 20 years ago the flume was taken out of use and left with a 0.5 m sand layer in it. Over time the flume became naturally vegetated and now hosts a wide selection of vegetation that consists of shrubs and trees. The vegetated flume, used for the experiments in this report, and an empty non-vegetated flume are shown in figure 4.7. A schematic representation of the flume is given in figure 4.8.

Figure 4.7 ***A*** *The vegetated flume looking in the downstream direction. The basis of the vegetated flume is visible on the right side of the picture. Photographs was taken in the downstream direction.* ***B*** *The cleared out flume. The image is taken in the upstream direction.*

At the upstream end of the flume multiple reservoirs are present that are linked by a several valves. The reservoir water needs to be pumped to a smaller holding reservoir in order to run the flume. Three large pumps are present to regulate the water level in the small reservoir. From the smaller holding tank water can be led into the flume by controlling a valve or weir at the upstream inlet. At the downstream end of the flume a variable weir is present, where the water flowed into a reservoir. A net was fixed (2.5cm mesh size) to ensure no leaves were transported into the reservoir tanks. The downstream reservoir is linked to the upstream reservoir by a large 0.6 m diameter concrete pipe in order to recirculate the water in the flume.

At multiple locations bridges were present that allowed measurements along the width of the channel. The measurement locations r_2,r_3 and r_4 are indicated in figure 4.8. At the measurement locations rulers were placed in order to determine the water level gradient in the flume.

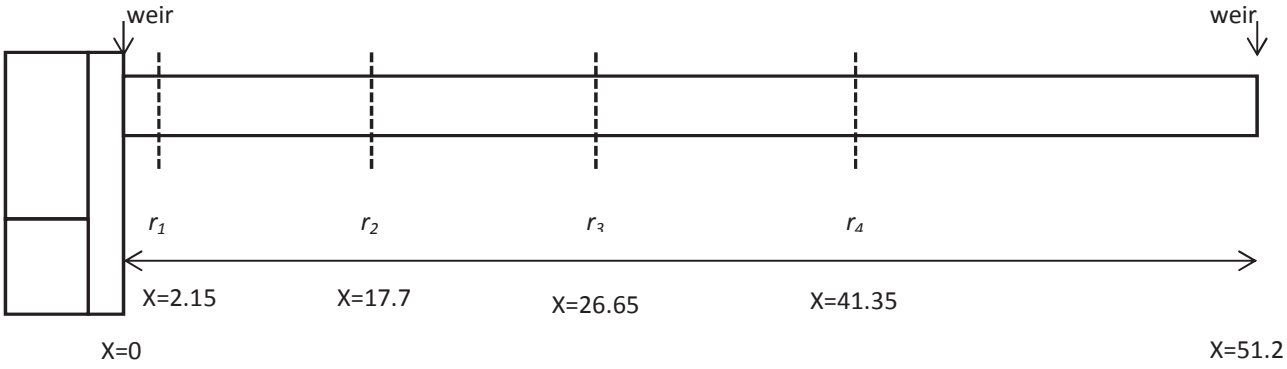

Figure 4.8. Top down view of the flume layout with the different reservoirs upstream. The up- and downstream weirs and measurement locations are indicated. The flow is from left to right.

Experimental conditions

The flow through the vegetation was investigated for a range of flow stages and three different vegetation compositions. The first vegetation composition was an unaffected vegetation cover (figure 4.7) and is referred to as the tree and litter layer flume composition. The second composition condition the flume consisted of just the stems of the larger vegetation and a removed litter layer (figure 4.7 B). It is referred to as the trees only flume environment. The final composition was an empty flume, with the stems cut at the base. The main control of the flow conditions in the flume were the upstream and downstream weirs (figure 4.8). The flow in the system is expressed in terms of openings of the upstream weir (24 rotation maximum) and downstream weir level (lowered or raised). An overview of the different runs with the corresponding vegetation composition and boundary conditions is listed in table 4.7.

Run (T)	Vegetation composition	Upstream weir opening (turns)	Downstream weir state
1	Trees + litter	3	Down
2	Trees + litter	4	Down
3	Trees + litter	8	Up
4	Trees + litter	24	Up
5	Trees + litter	24	Up
6	trees + litter	12	Up
7	Trees + litter	8	Up
8	Trees	3	Down
9	Trees	3	Up
10	Trees	4	Up
11	Trees	8	Up
12	Trees	24	Up
13	Empty	8	Up
14	Empty	24	Up
15	Empty	4	Up
16	Empty	3	Up

Table 4.7 Overview of the conducted runs and weir boundary conditions.

Data collection

An overview of the flume was made by taking overlapping photographs at an oblique angle of approximately 45 degrees and perpendicular to the flume every 2 m to map the vegetation cover. Furthermore a series of images taken at chest height with a contrasting background were used to estimate the vegetation density at every 2 m along the flume length by Matlab based RGB analysis.

For all runs the water levels were determined at multiple locations (r) in the flume (4.8) by reading of gauge staffs. In order to prevent bias in the water level measurements the same person read the gauge staffs. Furthermore cross-sections were measured at the water level measurement locations along the flume

The velocities in the flume were measured using the Richardson and Carling (2006) tracer dispersal method. The measurements were made by manual (30 second interval) sampling of the flume water at an upstream (r_2) and downstream location (r_4). Before the tracer was released the flume was left to run for 15 minutes in order to attain an equilibrium in the water level.

Fluorometer calibration

The velocity measurements in the flume, made by discrete sampling, were analysed with the Turner 10-AU fluorometer. The machine was calibrated by using consecutive dilutions of a Rhodamine WT standard solution containing 20% active ingredient. The dilutions are given in table 4.8. These dilutions served as reference sample to set up the fluorometer. The final step of the conventional calibration procedure is to subtract a background sample from the measurement site. This step was left out for the calibration of the fluorometer in the conducted experiments. No exact concentration

measure was necessary in the used velocity method. Only a relative tracer response of the fluorometer was required in order to compare the upstream and downstream measurements.

Dilution	Dilution of initial sample	Pp (unit)
Standard	0	10000ppt
1	100	100ppt
2	10000	100ppm
3	10000000	100ppb

Table 4.8 Dilutions used to calibrate the fluorometer used in the Chilworth experiments.

4.2.5 Richardson and Carling (2006) velocity measurement method

In the Chilworth experiments a time series of dye concentration was measured at two locations in order to determine the overall flow and the proportion of dead zones for the listed flume scenarios. This methods was also adapted to be used in the scale experiments conducted for this report. This is the aggregated dead zone (ADZ) method of Richardson and Carling (2006). The method uses traceable solute concentration measurement at an upstream and downstream location (figure 4.9). Based on the differences in the tracer curves at the upstream and downstream location details are obtained of the flow, including the velocity. The symbols of equations 29-33 are illustrated in figure 4.9.

The ADZ residence time or mixing time *T* is given by:

$$(29)\ T = t - \tau$$

The study reach advective time delay, used to compute the velocity without taking dead zones into account, is given by:

$$(30)\ \tau = \tau_d - \tau_u$$

The reach mean travel time, used for the velocity with dead zones, is given by:

$$(31)\ t = t_d - t_u$$

The momentum based velocity (U_m) is given by:

$$(32)\ U_m = \frac{L}{t}$$

In this equation L is the reach length (*m*). the advective time delay velocity, represents the channel velocity with an ADZ volume of zero, it can be calculated by using τ.

This momentum or advective time delay based velocity measurement can be used to compute the overall roughness by implementing it into the Darcy-Weisbach, Chézy or Mannings equation. The dispersive property of the reach (D_f) is given by:

$$(33)\ D_f = \frac{T}{t}$$

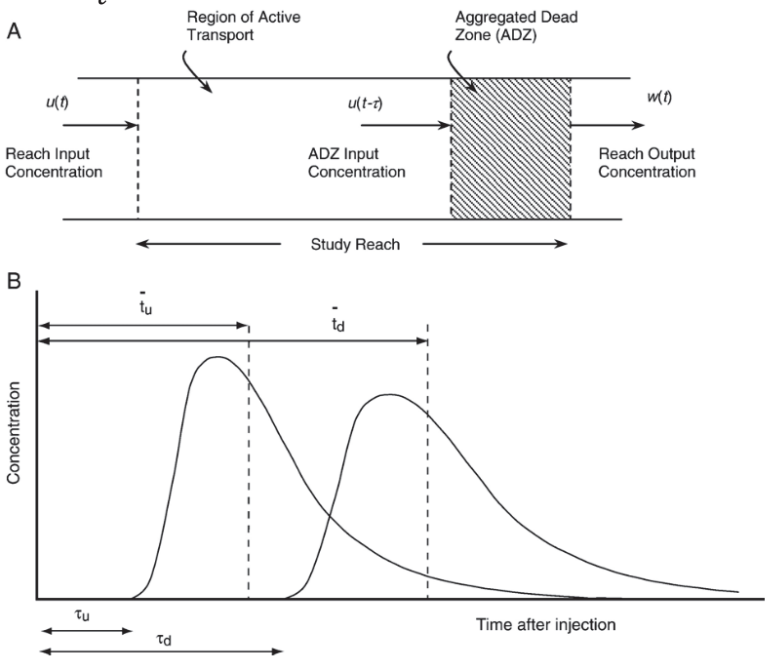

Figure 4.9. Overview of the ADZ model measurement locations (A) and resulting graphs (B) (Richardson and Carling, 2006).

Application to scale experiments

This method was applied in the flume experiments by taking a series of photographs of fluorescent tracer dispersion in a flume. The interval between two consecutive images was fixed at 0.6 seconds. The distance over which the tracer was monitored was flume setup specific. It was calibrated by including a ruler in the image. In order to determine the concentration of tracer form an image the Matlab image toolbox was used. This allows a RGB-band based extraction from the image. As the

tracer moves past a fixed point in the image the relative contribution of one of the RGB-bands increases, the specific band depends on the colour tracer used. A comparison of the relative tracer peak at both the upstream and downstream part of the image figure 4.10 yields the same response as given in figure 4.9.

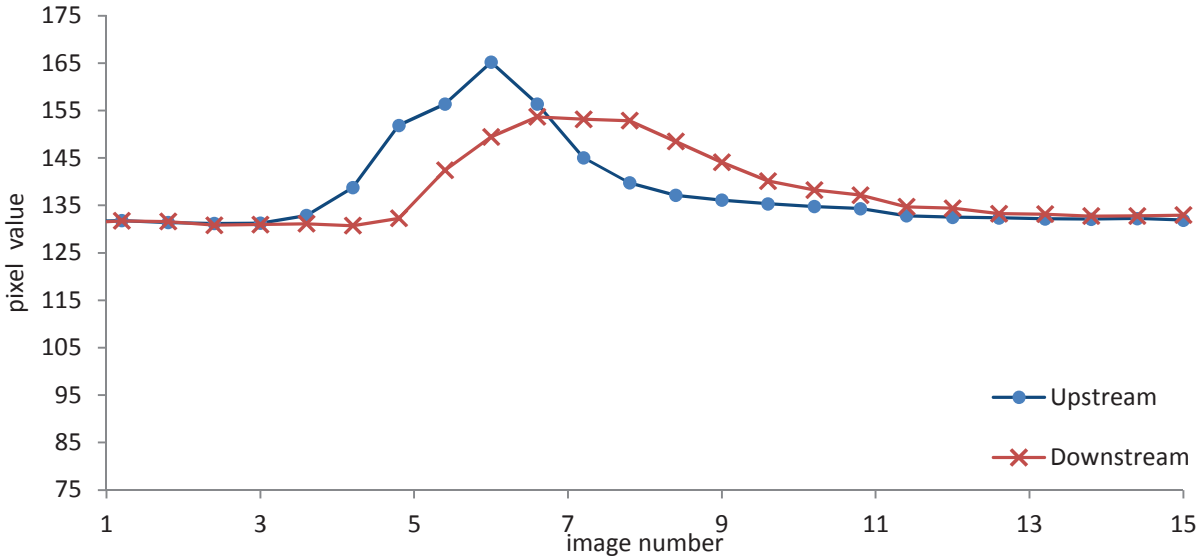

Figure 4.10. RGB based tracer concentrations in the Eurotank facility.

An adaptation of this method is applied to the overbank flow. This methods uses just two consecutive images. The tracer front is identified using a RGB conversion and threshold. The two threshold images yield a Boolean field with true values for the distance covered by the tracer in the timespan between the images. The distance can be determined by calibrating the pixel in the image to a real distance and applying Pythagoras rule. An example of such an image conversion is given in figure 4.11C and the original two images are given in figure 4.11 A and C.

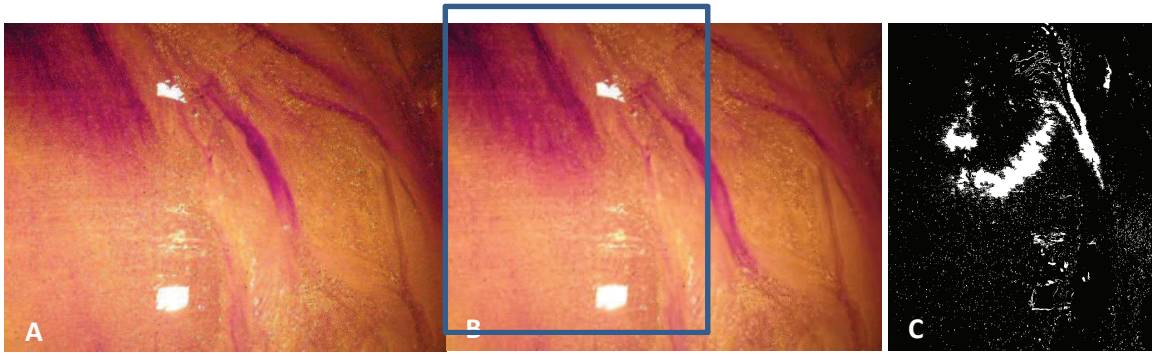

*Figure 4.11.**A** and **B** Tracer dispersion with a 0.6 second difference in time. The (**C**) image is indicated by the blue rectangle. **C** The white areas indicate the tracer displacement between the two consecutive (**A** and **B**) thresholded time lapse. The flow is from top to bottom.*

5. Results

A detailed overview is given of the results of the conducted experiments. First the smaller tests are presented that were aimed at creating and sustaining an alfalfa vegetation cover. Secondly, the Eurotank facility self-formed meandering river experiments are presented. This experiment serves as the main setup to investigate the effect of riparian vegetation on a dynamic meandering river system morphology. This is followed by the annular flume findings that present a more controlled environment to investigate the hydraulic resistance of scale vegetation. Furthermore the behaviour of sediment and vegetation in this setup serves as a basic frame of reference to some of the vegetation related interactions between river flow and vegetation in the meandering river. Finally real size natural vegetation flume experimental results are given from the Chilworth measurements. The found natural vegetation hydraulic resistance presents a frame of reference to the alfalfa as a scale riparian vegetation cover.

5.1 Copper sulphate tolerance test

The tolerance of alfalfa to copper sulphate was investigated in an attempt to prevent fungi (*Fusarium wilt*) from affecting the vegetation seeded in the flume setups. The influence of a range of copper sulphate concentrations on the development of 50 alfalfa seeds, as well as a control run, are given in figure 5.1 A.

When comparing the different copper sulphate concentrations to the control sample a reduction in the number of sprouted alfalfa seeds can be observed. In the control run and 0.01 mg/l samples little variation is present. However, based on the graphs presented below, a severe reduction in the number of sprouted alfalfa is present from concentrations of 0.1 mg/l onward. In addition the length of the alfalfa stems, that did sprout in the copper sulphate samples, was greatly reduced compared to the control and 0.01 mg/l units.

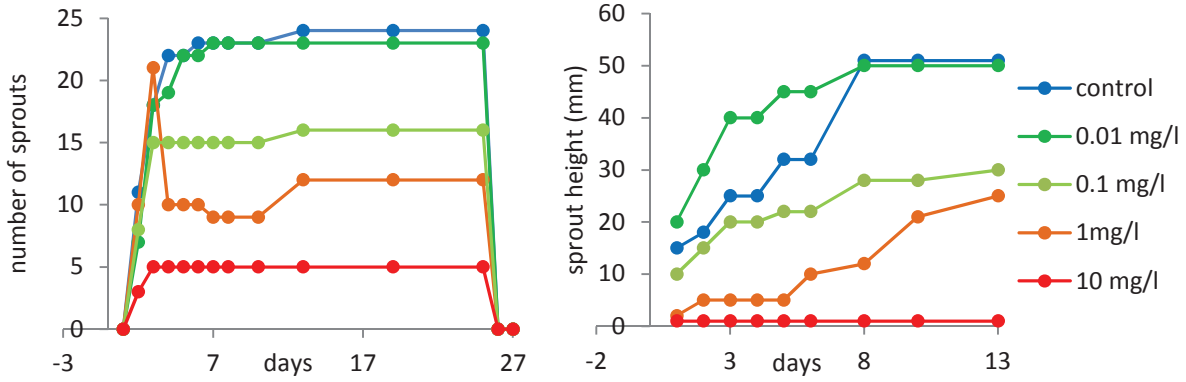

*Figure 5.1.**A** The number of sprouted alfalfa from an initial 50 added seeds for a range of copper sulphate concentrations. The numbers in the legend indicate the added concentration in mg/l. **B** Alfalfa sprout length development over time as a result of different concentrations of copper sulphate additive. The numbers in the legend indicate the added concentration in mg/l.*

The same trend can be observed when regarding the maximum length of the sprouts over the growth period (figure 5.1 B). The lowest concentrations and the control experiment show a rapid growth of the sprouts. The 0.1 mg/l response is lower than the lesser concentration and the control. The control response in turn is lower than the 0.01 mg/l growth trend. For the sample with the largest copper sulphate concentration no alfalfa growth could be detected. The second largest concentration had a delayed onset of the growth compared to the other samples (figure 5.2 B).

5.2. Eurotank experiments

The experiments conducted in the Eurotank investigated the effects of a scale riparian vegetation cover on a self-formed meandering river. In turn the effects of the meandering river on the homogeneous vegetation cover were investigated. In this chapter the morphologic development of the river is presented. This is followed by a more detailed analysis bank erosion and failure. The cut-off mechanisms are presented in chapter 5.2.3 and the hydraulics in 5.2.4. Finally the role of alfalfa as debris and the evolution of vegetation pattern is given.

5.2.1 Morphological development

The experiment in the Eurotank facility lasted for 150 hours of flow over an eight week period. The river development over time can be divided into three stages. The first is the formation of a self-formed meandering (figure 5.8 A,B) river from an initial straight channel, referred to as the initial stage. The changes after the addition of vegetation is the vegetation stage (figure 5.8 C, D). The final stage are the changes after reseeding the flume at 89 hours (figure 5.8 E). An overview of the different stages in relation to the river flow time and discharge is given in table 5.1.

Stage	Time (hrs.)	Discharge (l/h)
Initial	0	1800
Low discharge vegetation	30	1800
Vegetation	50	2250
Final	89	2250

Table 5.1. Overview of the different stages in the meandering river development.

Initial stage

The river development in the initial stage started with erosion in the section of the river close to the inlet, due to the offset. Downstream of the initial (1 m) erosion zone sedimentation occurred that build out a bar. After 3 hours a river bend started to form, as a result of the upstream perturbation. The initial upstream bend angled the flow towards the straight downstream channel side. This initiated the erosion of the bank and the development of a second bend. The lateral movement of the inlet maintained the upstream perturbation and after 13 hours several small amplitude bends formed (figure 5.8 A). These bends build out in the floodplain direction and were not cut-off. This marked a steady increase in the sinuosity (figure 5.3). Figure 5.8 B displays the final step in the initial stage development.

Vegetation stage

The second stage, referred to as the vegetation stage, considers the changes after adding a homogeneous (1.5 seed/cm^2) vegetation cover to the flume (30 hours). The development of the river in the vegetation stage was characterised by: a reduction in bend w/h ratio, steeper outer bank and transverse bed slopes, sharper and more asymmetric bends.

In the first 3 hours of the vegetation stage river, the no-vegetation planform remained visible (figure 5.8 C). The downstream bend (figure 5.8 C(III))c hanged to a more asymmetric and sharp bend. Upstream in the system, the central bend (figure 5.8 C(II)), had expanded in the floodplain direction. The most upstream bend (figure 5.8 C(I)) was characterised by an initial state chute cut-off that remained active due to the vegetation.

In the first 10 hours of the vegetation state the lateral migration reduced, with the maintained constant (1800 l/h) discharge. This can be seen in the reduction of the reworked flume area. The reworking halted at the moment of vegetation introduction. A control experiment did not displays a gradual increase in the reworked area over time (figure 5.2). In this period a reddish soil like material developed on the vegetated floodplain. It was present in the majority of the flume overbank throughout the experiment.

At the 45 hour mark the discharge was gradually increased to 2250 l/h at 54 hours (figure 9.27). This led to a continuation of outer bend erosion and river development. The bend development up to this point had increased the river sinuosity (figure 5.3). The vegetated river sinuosity, when compared to a non-vegetated control river, displays an absence of sinuosity reductions in the 0-70 hour period. In the control river sinuosity fluctuations were present, as a result of alternating between phases of pointbar formation and chute cut-offs.

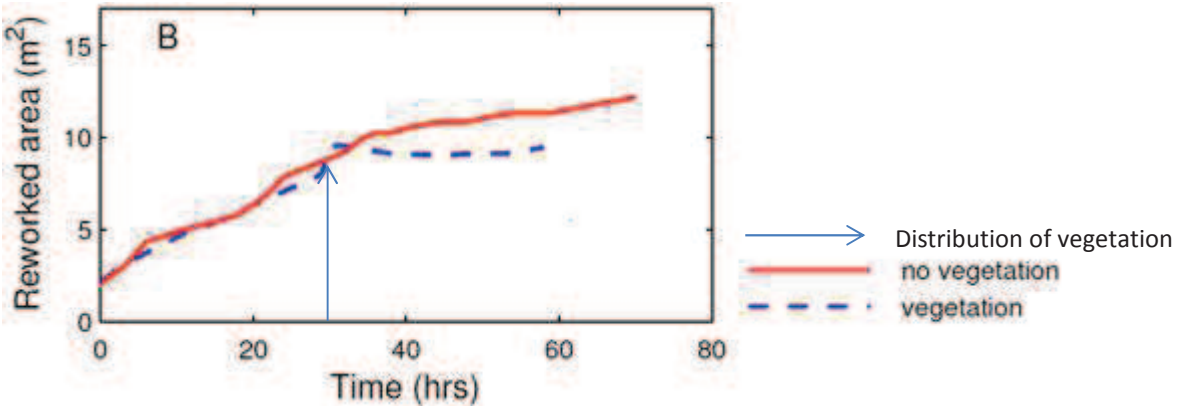

Figure 5.2. Reworked area in the alfalfa covered system and a control experiment. The blue arrow indicates the moment of vegetation dispersal.

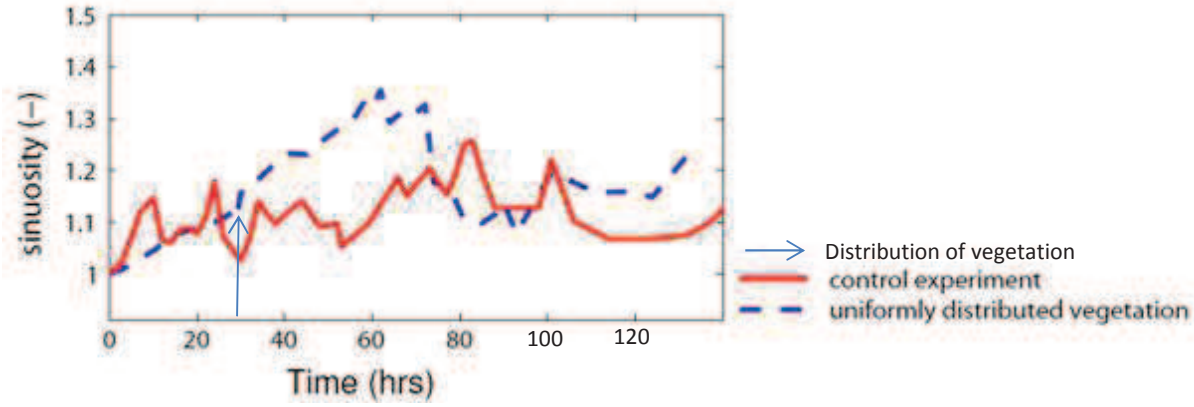

Figure 5.3. The sinuosity of the vegetation covered floodplain river and a control experiment. The blue arrow indicates the moment of vegetation dispersal.

Apart from the overall increase in sinuosity the central bend had undergone several changes compared to the initial state. This can be observed by comparing two cross-sectional profiles. The profiles are given for the no-vegetation system at 29 hours (figure 5.4 A) and the vegetated river development at 41 hours (figure 5.4 B). In the initial stage river the height of the inner bend scroll bar accumulation was below the initial floodplain level. In the vegetation stage system the scroll bars were higher, reaching the original undisturbed floodplain level. When regarding the outer bend bank, it can be observed that in the vegetation stage a more steep side slope was. Furthermore, the inner bend scroll bar slope, transverse bed slope, is noticeably steeper in the vegetation covered system. The changes in the bend morphology were present in the sorting patterns. Although in both stages the coarser sediment was found along the outer bend margin the higher vegetated stage scrolls consisted of finer grains than the lower initial stage pointbars.

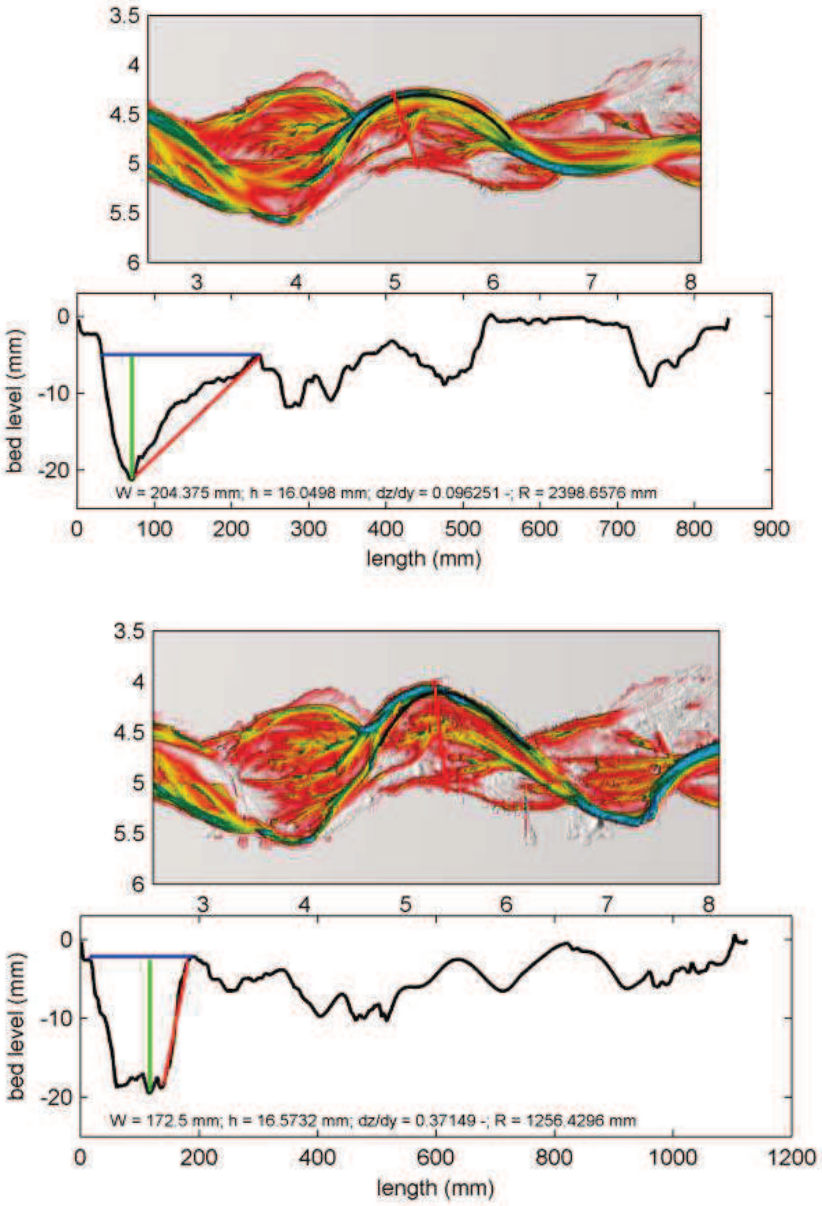

Figure 5.4. ***A*** *Cross-section in the initial stage river at 29 hours.* ***B*** *Cross-section in the vegetation stage river at 41 hours.*

The detailed change in transverse bed slope, during the experiments, is given in figure 5.5. The control experiment without vegetation is plotted as well. The control experiment and the initial stage system display a low (0.027-0.18) slope over a wide range of r/w ratios (6.5-23.9). The vegetation covered system slope values (0.1-0.48) lie above those of the non-vegetation system and are found in a more narrow band of r/w ratios (1.1-8.2). The steeper transverse bed slope indicates a change in the secondary current that moved the grains up the scroll bar and gravity moving the grains down the slope.

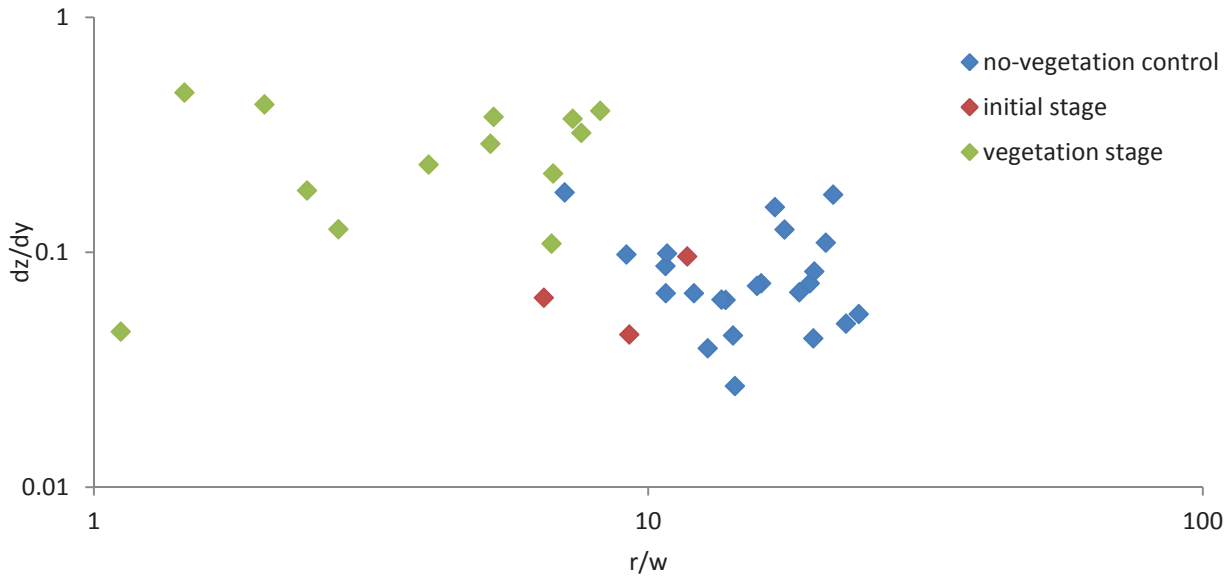

Figure 5.5. Transverse bed slope at the apex for the river initial stage, vegetation stage and a control experiment.

At 56 hours (figure 5.8 D) the downstream end of the river had formed new bends that displayed the same asymmetric shape as the figure 5.8 C(III) bend. These downstream bends were formed by the angled flow from the sharp downstream bend at 33 hours. After the first new sharp bend had developed, a second and progressively third sharp bend formed due to an angled flow of the upstream bend.

In the upstream section of the river, the sediment feed was equal to the initial stage feed rate. This equal feed created a splay over the first river bend (figure 5.8 D). This splay filled up the low areas in the pointbar (figure 5.8D). When regarding the equilibrium sediment feed volume of the river without vegetation (263 ml/hr) and the equilibrium feed right after the formation of the splay (184 ml/hr) a 80 ml/hr (30%) reduction in sediment transport was present.

The central system bend displayed a clear asymmetry. The asymmetric development was coupled to a change in the scroll bar accumulation locations in the flume (figure 5.8 D). Instead of the central bend scroll bar accumulation, that were found in the initial stage, the bars accumulated downstream of the bend apex. In addition the outer bend was less wide and deeper than in the earlier development stage.

The change in the overall depth of the river is illustrated in figures 5.6 A and B. The fraction of the flume belonging to a certain surface elevation is given. This was done using the DEM-data and surface elevation based standard deviation and mean values. The blue dotted line (figure 5.6 A) indicates that the vegetation scenario has a larger tail in the low surface elevation range. This means that the vegetated river, compared to the control experiment, had an increased local depth (bends). This is also given in figure 5.6 B, where the incorporation of vegetation results in a lower z_5 value. The second effect of vegetation on the overall flume is an increase in the overall surface elevation. This can be seen as the increase in z_{50} and z_{95} after the vegetation dispersal (figure 5.6 B).

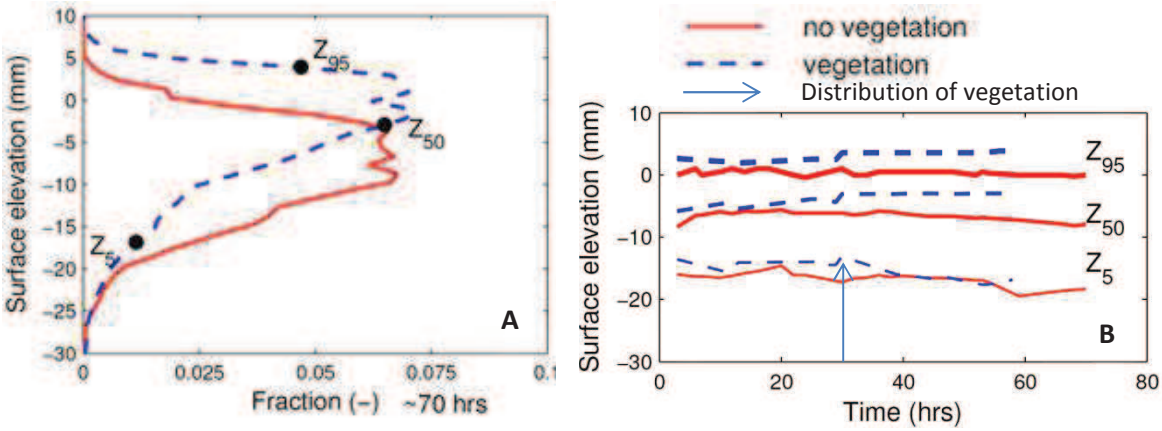

*Figure 5.6. **A** Surface elevation in the vegetation and the no-vegetation control experiment. **B** surface elevation in the flume over the first 70 hour periods.*

Apart from the deeper outer bank scour the width of the bends reduced. These developments led to a change in the w/h ratios of the central river systsem bend (figure 5.7). The control experiment and initial stage vary between w/h ratios of 10-20. The vegetation stage low discharge shows the reduction in the w/h ratio after 30 hours. The higher discharge vegetation state bend w/h ratio reduces even further, to a minimum of 4.5, before increasing again.

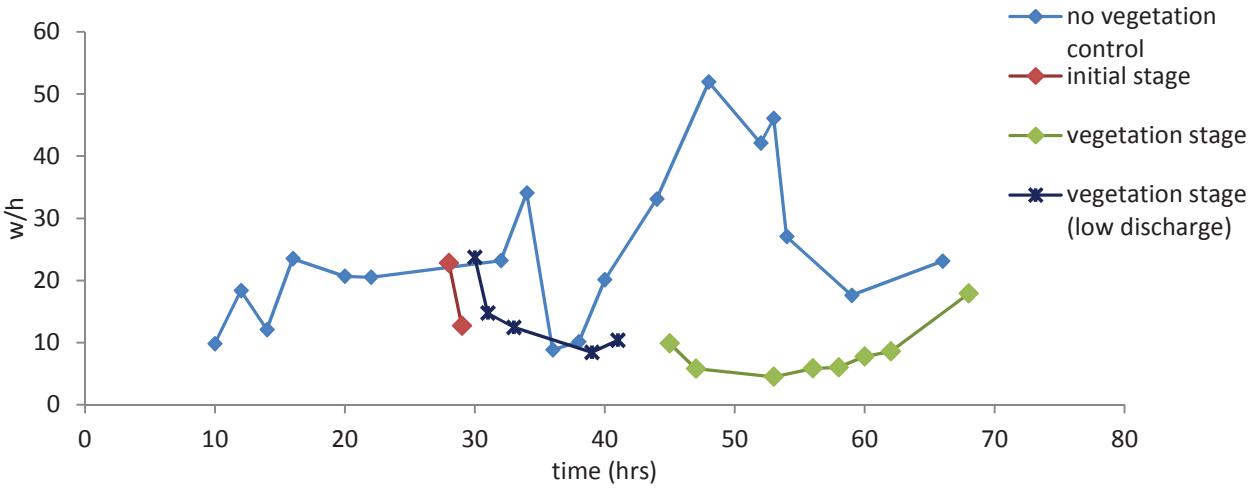

Figure 5.7. w/h ratios at different stages in the vegetation experiment and the control data.

At 70 hours (figure 5.8 E) the sharp bends, that had developed in the downstream end of the system, had pointbars accumulations without vegetation. These newly formed deposits were cut-off over the pointbar, this led to small sinuosity fluctuations (figure 5.3). It also meant that the downstream vegetated floodplain was left undisturbed in the remainder of the experiment. The pointbars of the cut-off bends were below the original floodplain level. In the upstream part of the river the development was different.

In the central bend severe sediment accumulation occurred on the upstream side (figure 5.8E). This led to increased water levels upstream of the sediment bar in the channel. The increased water levels caused a larger flow over the floodplain, in the direct downstream direction. The floodplain flow incised by headcuts in the upstream direction. Eventually the headcuts reached the channel creating a straight channel (78 hours). This resulted in forced cut-offs downstream, which marked the decrease in the system sinuosity (figure 5.3).

Final stage

The third and final stage covers the morphologic development after reseeding of the flume (89 hours) with the same 1.5 seed/cm^2 density after the above described cut-off at 78 hours. The upstream meander bend started to become more sharp and migrated towards the edge of the flume, where it remained during the rest of the experiment. The new channel, incised in the floodplain, developed into several short lived sharp meander bends. These newly formed bends displayed the same sharp bend characteristics as the earlier stage system bends. It took approximately up to 134 hours for the river to start forming more stable and longer amplitude meander bends, similar to the initial stage river (figure 5.8F). These bends were present up to the end of the experiment. The final stage in the river development is not taken into account in the below presented data that covers the detailed vegetation state system development.

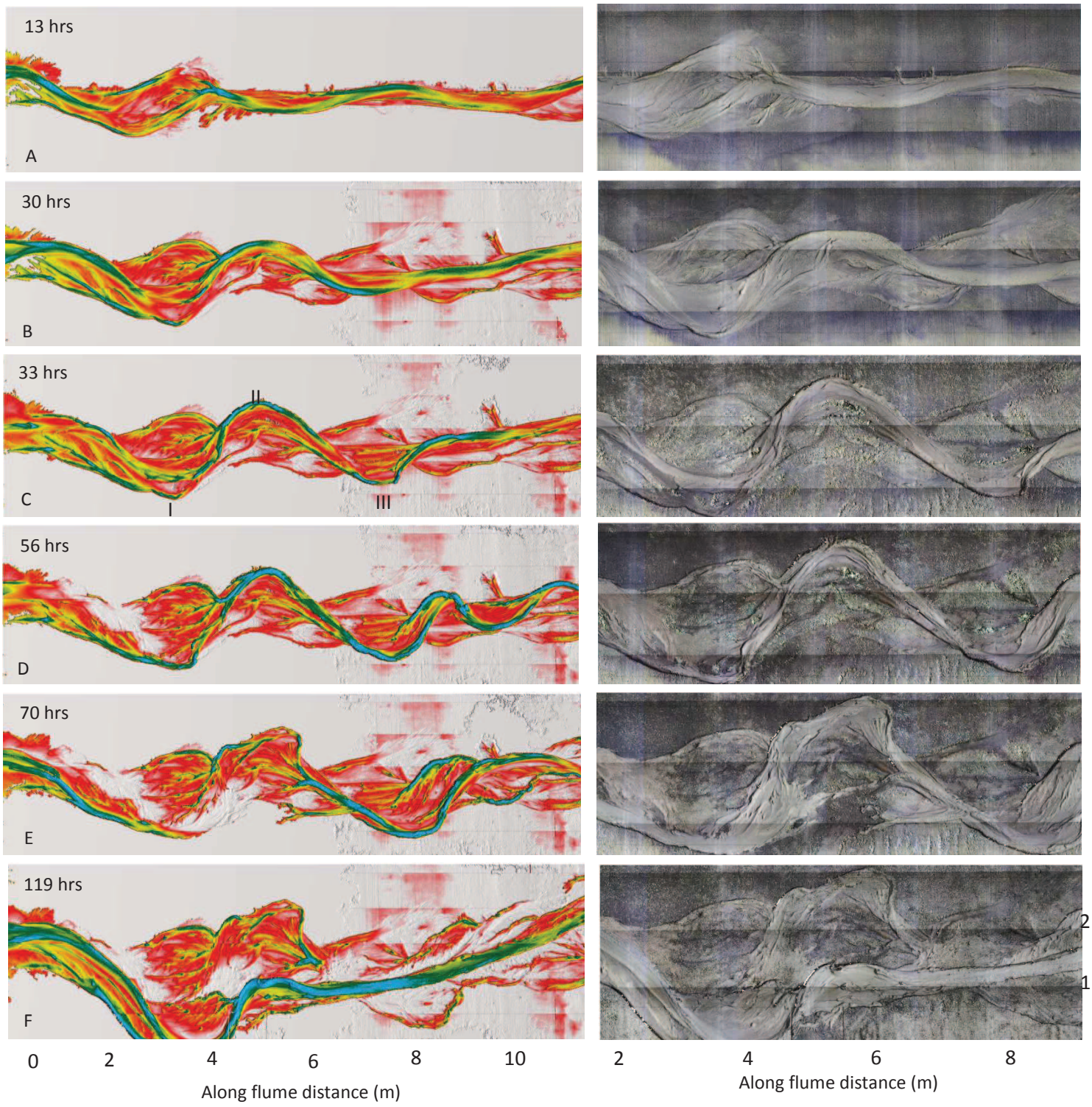

Figures 5.8. The development of the self-formed meandering river. The corresponding time steps are given in the top left of the DEM. The flow is from left to right. The height scale is given in the bar at the bottom

5.2.2 Bank erosion and failure

The detailed development of the bends, that drove the overall morphological change, is presented. The bend erosion and failure mechanics are given for the initial and vegetation stage systems. This is followed by the erosion rates in the initial and vegetation stage.

Bend erosion

The rate and locations of outer bank erosion in the flume were monitored using images taken at regular intervals. The resulting bank erosion, for the central bend location of figures 5.4, in the initial state river is given in the figure 5.9 A and C. The vegetation state is given in figure 5.9 C and D. The flow time, on which the images are based, is equal (55 minutes) as is the discharge (1800 l/h). A comparison of the initial river with vegetation state shows that the erosion was more local and focussed at the centre section of the bend in the vegetation environment. The initial river had a more spread out erosion of the outer bend. Furthermore the alfalfa covered floodplain erosional process is less gradual than in the initial state system. This is visible as the more abrupt transition from blue to red in figure 5.9B. Over time the discharge of 1800l/h proved insufficient to erode the vegetated banks and no lateral movement occurred. The increase in discharge led to a renewed and on-going erosion in the system. The local focus character of the vegetated floodplain erosion remained the same.

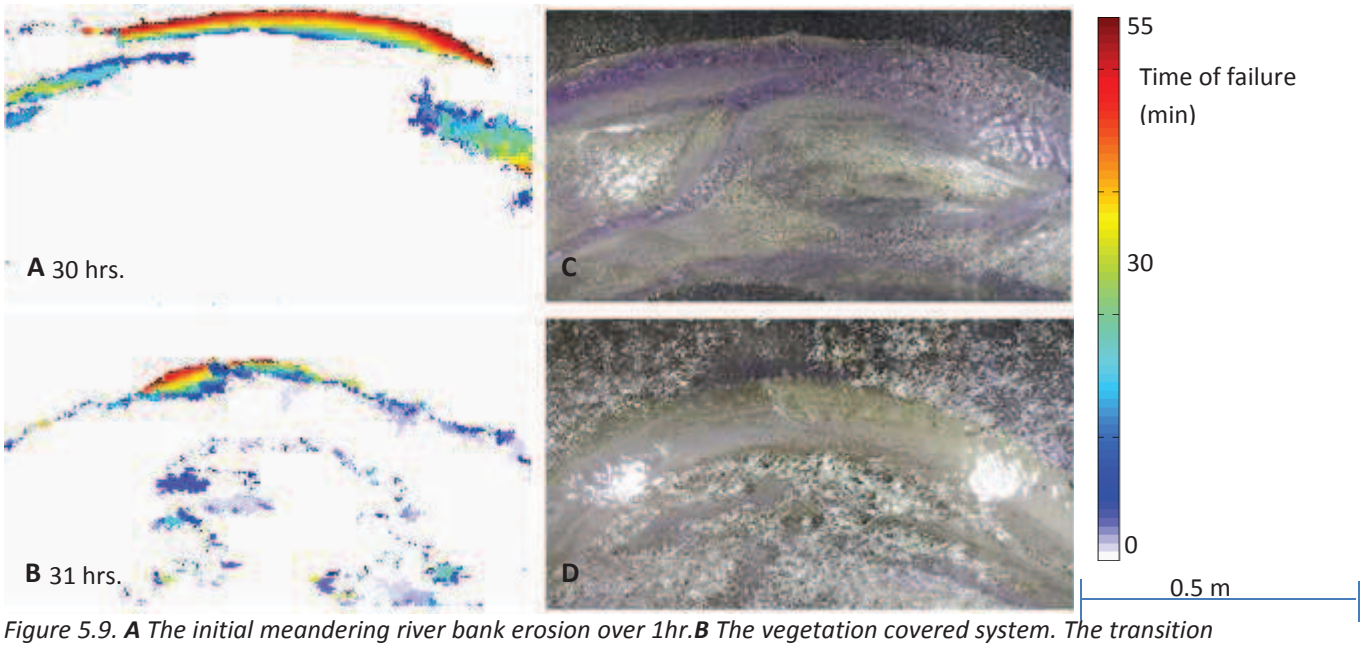

*Figure 5.9. **A** The initial meandering river bank erosion over 1hr.**B** The vegetation covered system. The transition from blue to red indicates the time of erosion. **C** and **D** are the corresponding images.*

Bank failure mechanisms

The main mechanism of bank failure in the initial meandering river was either entrainment of the fine sediment by the flow or mass wasting of larger grains. Once moved the larger grains ended up at the base of the outer bank. Over time the grains were transported as bedload in the downstream direction by the flow. The occasionally present largest clast fraction (>10 mm) of the sediment bed remained in place once eroded from the outer bend. There was a difference in the failure of a non-vegetated bank compared to a vegetated bank in the meandering river.

The failure mechanics in the vegetation state were identical for both the low (1800 l/h) and higher (2250 l/h) discharge scenarios. The outer bends started to fail after the channel had deepened and became steeper along the outer bend margin. The failure mechanics of the steeper vegetated bank was an instantaneous failure of larger fractions of the floodplain (figure 5.11). A time-lapse of the outer bank has been used to create figure 5.10, that display the step wise erosion.

The highlighted section in A is about to fail. In B (30 seconds later) the failed section of the bank is present at the base of the failed bank. The failed section is made up of aggregates of alfalfa and sand bound together by the reddish soil like material. Over time, approximately 30-50 minutes of flow, these clumps, were broken down into smaller aggregates. The aggregates moved as bedload in the downstream direction. Some smaller sections of failed outer bank material tended to travel onto the next downstream pointbar. The same failure of the banks was observed in later stages of the vegetation cover, where in some regions, vegetation was absent, but the reddish soil material was still present.

The timing of erosion at a specific location in the bend for both the initial and vegetation state river environments, was coupled to the development of scroll bars. When a single scroll started to migrate along the inner bend in the downstream direction, the outer bend responded by retreating. The exact mechanisms and timing of this apparently coupled system laid outside the scope of this research.

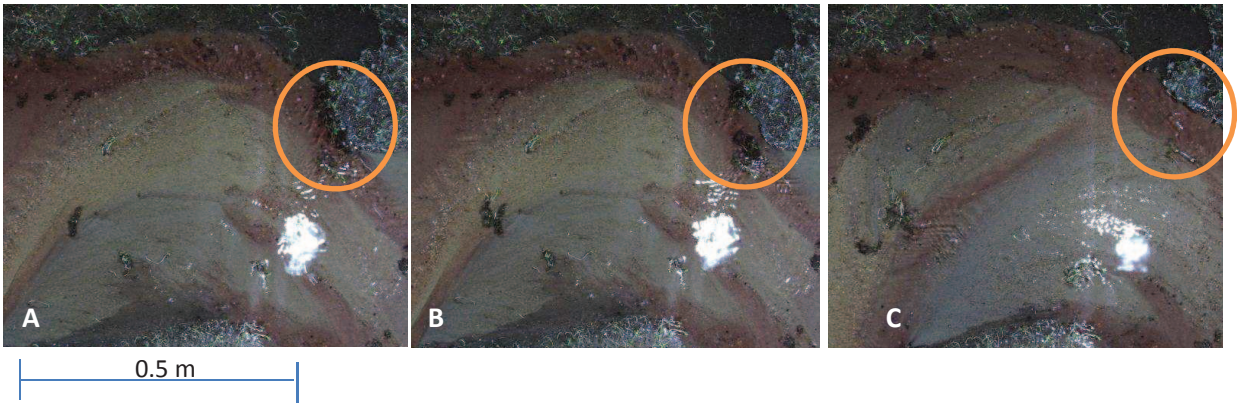

*Figure 5.10.**A** Section of the outer bend about to fail, **B** failed section on the bed of the channel 45 seconds later. and **C** the failed bank material has been moved by the flow after 40 minutes.*

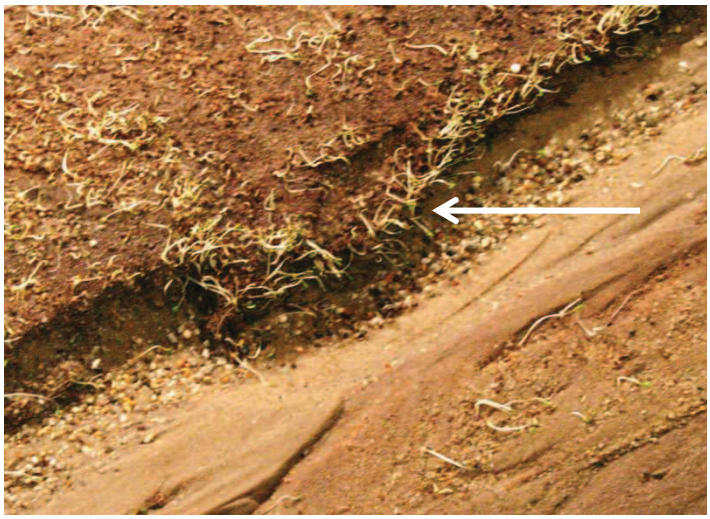

Figure 5.11. Large bank failure section in the flume along the outer bank of a developing bend. The failure is indicated by the white arrow.

Erosion rates

The erosion rate of the vegetated meandering river and the control experiment are fiven in figure 5.12. The r/w ratio of the vegetated river is lower than that of the bare sediment system. The corresponding erosion rates vary over a smaller range of w/hr than the bare sediment floodplain scenarios. The control system data has a large outlier with a 0.5 w/hr erosion rate. This is a time step taken in the first few hours of the experiment. The reduction in the r/w system as a result of continued erosion is visible when comparing the 1800 l/h with the 2250 l/h stages of the vegetation stage.

The erosion rate development over time, of the 1800l/h vegetation state, shows a reduction in the erosion rate for increasing r/w ratios, eventually reaching 0 w/hr at r/w is 8. After reaching an erosion rate of zero, the discharge was increased and erosion continued. This is visible in the green diamond shape dots in the figure. They mark a steady decrease in r/w ratios and an increase in the erosion rate. Eventually the erosion reduces in very sharp bends (r/w 2-2.4). At this point a cut-off occurred and the bend was abandoned.

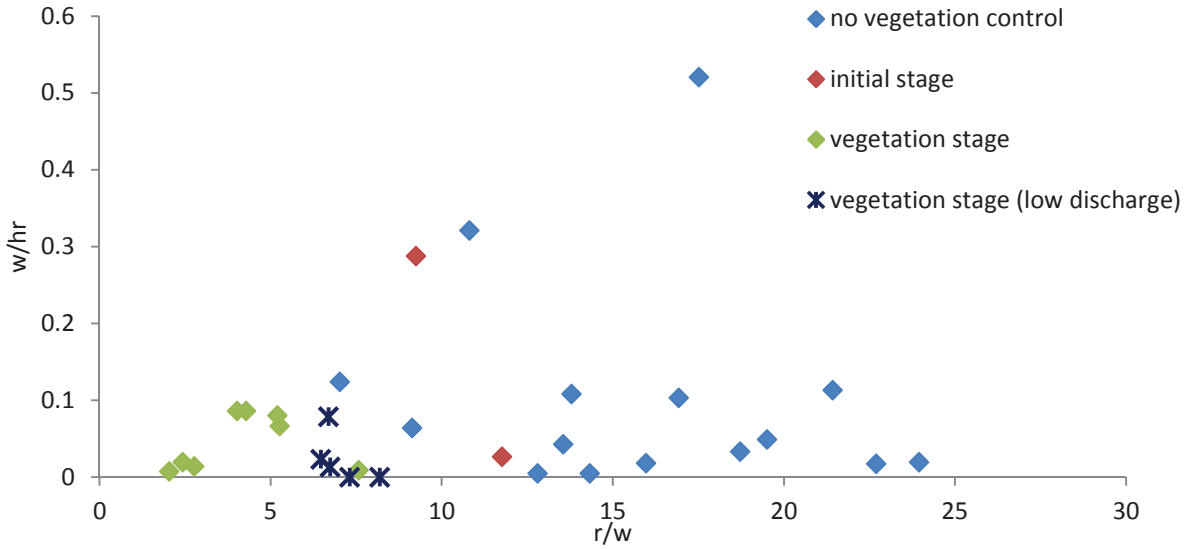

Figure 5.12. Erosion rate of the scale meandering river bank over time (10-75hr) in different stages of the river development.

5.2.3 Cut-offs

The cut-offs that occurred in the experiment were different for the initial state and vegetation state river. The difference is closely related to the changes in the morphologic development as a result of the introduction of vegetation. The initial stage cut-offs are described. This is followed by the low discharge vegetation state, vegetation stage and final state.

Initial stage

The development of the initial state and control experiment bends was characterised by a gradual floodplain directed movement of the bends. The expansion of the bends continued, until the gradient along the river became too low in relation to the downstream gradient. This resulted in increased flow over the low pointbar areas or swales. The flow over the point bar incised and formed a channel. The new channel had a gradient advantage over the old channel and eventually a cut-off occurred. Apart from an extended time span between chute cut-offs phases in the vegetation state (figure 5.3) the mechanism of the cut-offs differed from the initial stage cut-offs. Furthermore there was an occasional interference in cut-off mechanism in the low discharge vegetation state river.

Low discharge vegetation stage

In the 3 hour period of flow, after seed dispersal, the vegetation affected an active chute cut-off formed in the initial stage river. The vegetation tented to reinforce the central pointbar area section between the two active channels. Instead of flow going through the channel with the downstream gradient advantage and eroding the pointbar, the stability of the pointbar section allowed a division in the sediment transport through the two channels. This meant that majority of the bedload material was moved towards the inner bend by the secondary current. Eventually the channel was closed off with the flow going through the old channel. This can be seen in figure 5.8 C(I), the active cut-off in the first bend, and figure 5.8 D, the closed cut-off.

Vegetation stage

The changes that led to the cut-off over the floodplain in the central bend are described in more detail in relation to the morphologic development. The first stage in the alfalfa covered system bend development is the local erosion leading to an asymmetrical shape in the bend. The asymmetry shifts the accommodation space in the bend which resulted to scroll bar formation on the downstream end of the pointbar complex. The pool, that was upstream of the apex in the initial state bends has moved to the downstream side of the apex (figure 5.13A).

The second stage displays a continued local erosion of the bend. The created accommodation space was filled with scroll bars (figure 5.13 B). The bars were aligned differently than the older scroll complexes. The sediment that build up these more oblique bars was transported along the inner bend, from upstream, and from the outer bend side by the secondary current. Both sediment transport directions were observed, but no dominant mechanism was found. The upstream inner bend sediment flux was responsible for the splay like bar draped over the older scroll bars. The pool was present in the erosion zone of the bend.

In the next bend stage (figure 5.13 C) the local outer bend erosion continued. As a result of the steep bend, scrolls were formed on the downstream outer bend side. The inner bend complex received more sediment that build out splays covering the older deposits. In addition some new oblique bars were formed in the lee of the sediment splay. On the upstream side of the bend bar formation had started in a similar way, induced by the local outer bank erosion that created accommodation space.

The floodplain flow increased as a result of the upstream bar formation. This led to splay like sedimentation on the low areas of the pointbar. On the downstream end of the point bar the floodplain flow incised by headcuts.

In the final vegetation stage in (figure 5.13 D) the upstream bend has nearly closed of the channel. At this moment the headcuts had reached the further towards the upstream floodplain side. In the next

2 hours the headcuts reached the channel, thereby creating a cut-off over the floodplain. This stopped the morphologic development of the initial channel.

Figure 5.13 ***A*** *river at 53hours* ***B*** *river at 60 hours* ***C*** *river at 62 hours* ***D*** *river at 74hours. The flow direction is from left to right in all figures.*

5.2.4 Hydrodynamics

The addition of vegetation led to changes in the hydraulic development of the river system. First the changes in the wet over bank area and the general flow behaviour in relation to river morphologic units is presented. Secondly, the velocities at several locations and time steps are given. Finally, the roughness of the overbank flow is presented.

Wetted overbank area

The change in the overbank area that was inundated, as a result of the vegetation cover introduction, is illustrated in figure 5.14. There was a large reduction right after the vegetation distribution at 30 hours, where the inundated area reduced from 0.54 to 0.14. After the 40 hour mark there was again an increase in the wetted overbank area from 0.14 to 0.27 due to the increase in discharge. In the control experiment there was also a reduction in the amount of wetted overbank area. However, compared to the vegetation experiment, the reduction is more gradual. The exact changes in the wetted overbank area in terms of overbank flow and velocities are presented below for smaller subsections of the flume.

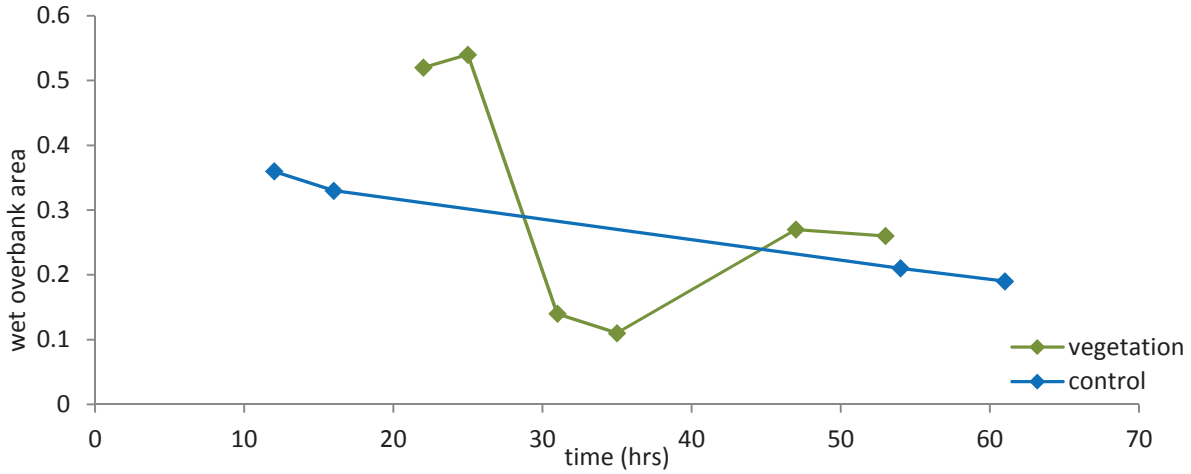

Figure 5.14. Wetted area of the non-vegetated control and vegetated river.

Channel and bend flow

The tracer in the channel moved preferentially through the centre. This was visible as a convex front with the most downstream tracer concentration maximum in the centre and the sides of the channel lagging behind. The same dispersion of tracer was observed for the initial and vegetation state systems. Furthermore, the short flood (2500 l/h) period resulted in the same flow in straight channel sections.

In bends the tracer patterns differed. The tracer moved straight onward from the upstream non-curved channel sections towards the outside of the bend. The tracer bulk moved along the outer bend of the channel with a small fraction fanning out over the pointbar front. This was the same for the river with vegetation, until the bends developed into sharp bends.

The flow through a sharp bend was characterised by a lingering of the flow in the knick-point of the bend. In addition the irregular bank margin (figure 5.10) created small dead zones where the tracer was held up for 2-3 seconds. After leaving the sharp bend a fraction of the water flowed over the beginnings of the sediment accumulation, that later closed of the channel (figure 3.32). In the lee of the bar there was a very strong deceleration of the flow. The tracer remained in these areas for 1-2 minutes compared to seconds over a normal no-vegetation or non-sharp inner bend scroll bar lee side. The flow over the higher floodplain side of the pointbar complex and the floodplain itself differed between the initial and vegetation state.

Point bar system flow

The same location in the flume (figure 5.8C(II)) is given (figure 5.15A and B). The differnce between the images is the addition of vegetation. The total river flow time difference between the non-vegetated and vegetated images is 1 hour. The location of tracer release and the discharge (1800 l/h) was the same for both situations. In the bare sediment river the flow is through the deep swale on the left, the main channel and over the pointbar. With vegetation the overal inundation of the overbank area was reduced. This led to visibly lower innundation levels on the overbank areas. This meant that the flow only went through lower the deep swale and through the main channel. Similar changes were found in other river bends in the system.

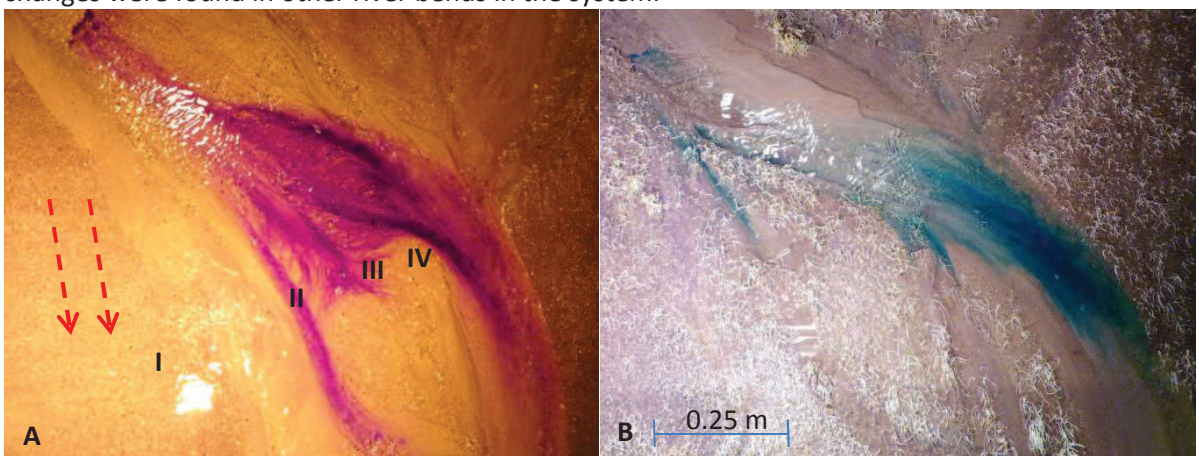

*Figure 5.15**A**. Flow over the un-vegetated central bend inner bend. The red arrows indicate the overbank flow direction. The red arrows indicate the direction of the floodplain flow. **B** Flow over the vegetated inner bend. The discharge is equal. The difference in flow time between the non-vegetated and vegetated image is 1hour.*

Overbank area flow

On the left upstream overbank area overbank flow was present due to the upstream inlet. The vegetation visibly reduced the overbank flow in this area from 30 hours onward. The overbank flow in the rest of the flume was generated in the bends. The upstream released tracer was driven by inertia so that it moved along the outer bank. The overbank flow was generated in the second section of a river bend, downstream of the apex, beacause a fraction of the tracer was transported onto the floodplain. Once on the floodplain it travelled in straight lines in the downstream direction (figure 5.15A). With vegetation the locations of overbank generation were identical to the bare sediment flume. However with vegetation there was a smaller inundated area (figure 5.14) and less observable overbank flow in general. Even the brief high discharge (2500 l/h) proved insufficient to create a level of overbank inundation comparable to the low discharge initial state.

Flow velocities in the meandering river

For the channel it was possible to use the Richardson and Carling (2006) velocity method (chapter 4.2.5). On the floodplains this was not possible, due to the long lingering of tracer. The two image tracer front displacement was used. The locations of the velocity measurements are indicated with Roman numbers in figure 5.15A.

The velocities in table 5.2 indicate that the velocities on the floodplain area of the flume were not dependent on the discharge and corresponding main channel velocities. The low stage initial river floodplain velocity is twice that of the other conditions, but this difference was not found in the velocities of an initial and vegetation stage high discharge floodplain flow. Furthermore no age dependency was present in the vegetation stage overbank velocities. Closer to the channel, the large swales displayed an increase in velocity for higher channel discharges. The small swale velocity was also discharge dependent, although to a lesser extent than the large swales. After the incorporation of vegetation the small swale velocity does not vary significantly.

The Richardson and Carling (2006) method channel tracer peak velocities, not presented here, were equal to the tracer front based velocities. The front velocities are presented here, in addition the two image based velocity is presented. In the initial stage river straight channel section, the increase in the flow velocities for a high discharge was 0.20 m/s for both velocity methods. In the vegetation state the channel velocities differed between both methods. The Richardson and Carling (2006) tracer curve methods indicates the same trend as the initial stage system velocities. This indicates an absence of dead zones in the channel. The two image tracer front movement method velocities are substantially lower indicating a difference between the applicability of both methods (chapter 6.1).
For all conditions listed in table 5.2 the average tracer front velocities through a bend were reduced compared to the straight section flow. The degree of velocity reduction is larger for a high discharge (0.25 m/s reduction) than for a low discharge condition (<0.1 m/s).

Location	1800(l/h) sand	2500(l/h) sand	1800(l/h) vegetation	2500(l/h) young vegetation	2500(l/h) veg old	2250 veg
Pointbar(III)	*0.12*	-	*0.06*	*0.06*	*0.05*	*0.07*
Small swale (IV)	*0.14*	-	*0.13*	*0.18*	*0.17*	*0.19*
Large swale (II)	*0.14*	*0.11*	*0.18*	*0.25*	*0.31*	*0.15*
Floodplain (I)	*0.08*	*0.02*	-	*0.03*	*0.03*	*0.03*
Channel (two image method)	*0.36*	*0.55*	*0.32*	*0.35*	*0.42*	-
Channel Richardson and Carling (2006) (noADZ)	*0.38*	*0.53*	*0.28*	*0.55*	*0.56*	-
Channel bend (noAdz)	*0.27*	*0.22*	*0.33*	*0.28*	*0.25*	*0.26*

Table 5.2. Overview of the velocities for different discharge and vegetation scenarios. The locations of the velocity measurements are indicated by the roman numbers in figure 5.15A.

Although there was minimal difference between the velocities in a vegetated and non-vegetated environment for a low and high discharge scenario the cross-sectional area of the flow differed for the overbank area. Since the overall wetted overbank areas was reduced the remaining floodplain flow was found in smaller areas of the overbank system. For example: on the floodplain a change from an approximate 0.4m wide flow area, for the sediment floodplain, to a confined 0.02m wide flow in the alfalfa environment. With an approximately equal upstream addition of tracer the vegetation scenario is characterised by a larger passing time of the tracer. In figure 5.16 the large swale (II) tracer passing is given.
It can be observed that the initial state tracer forms a swift rise up to a peak value with a rapid reduction, the total pass time of tracer was 4 second. The same locations pass time in a vegetation state is in the order of 40 seconds. This change resulted in the expanded tracer response in the figure.

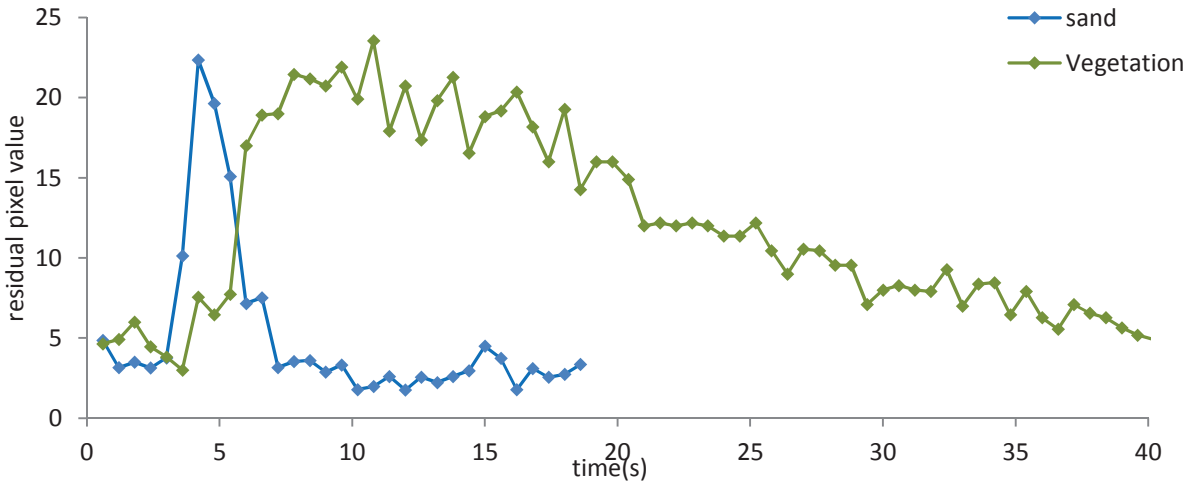

Figure 5.16. Tracer plume passing for the pointbar location with a discharge of 1800l/h for a bare sediment and alfalfa covered floodplain.

Overbank area roughness

The presented floodplain roughness value ranges (figure 5.17A, B) were computed by using the Reynolds number friction factor relation (equation 19) for a range of the water level values. The used levels were based on the DEM's and wetted area images. The ranges were 0.6 mm +/-0.4 mm for the non-vegetation flume and 1mm +-/ 0.5mm for the vegetated flume. In addition the roughness ranges are given for the water depth dependent Ferguson (2002) method (α=2) (equation 18) these friction factor values are indicated by the dotted lines for a 1-4 mm inundation range. The Chézy plot is used to explain the figure trends.

In the Chézy plot the lowest water level yields the lowest roughness value in all overbank scenarios. The resistance values and Reynolds numbers vary of a range, as a result of water level variation. The most rough scenario range is the 2500 l/h bare sediment floodplain. Less rough identical ranges are present for the 2250 l/h old and young vegetated floodplain. The least rough values are found for the 1800 l/h bare sediment floodplain. A comparison of the Reynolds number roughness range and the Feruson (2007) range indicates similar values are present for the Ferguson (2007) 2-4 mm range.

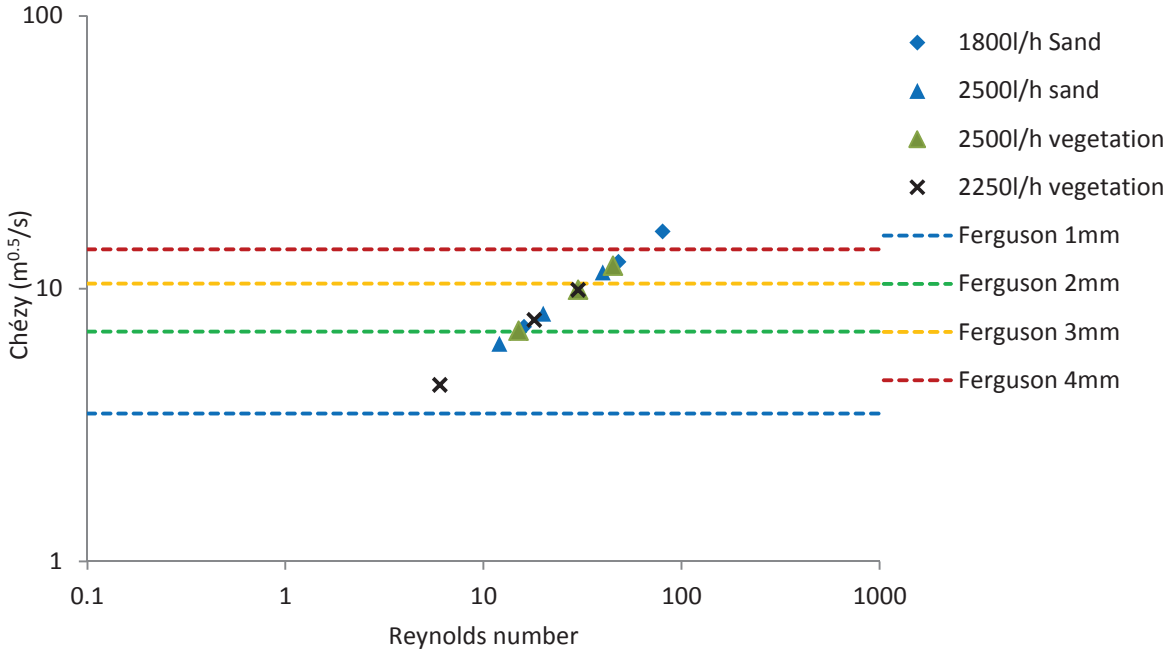

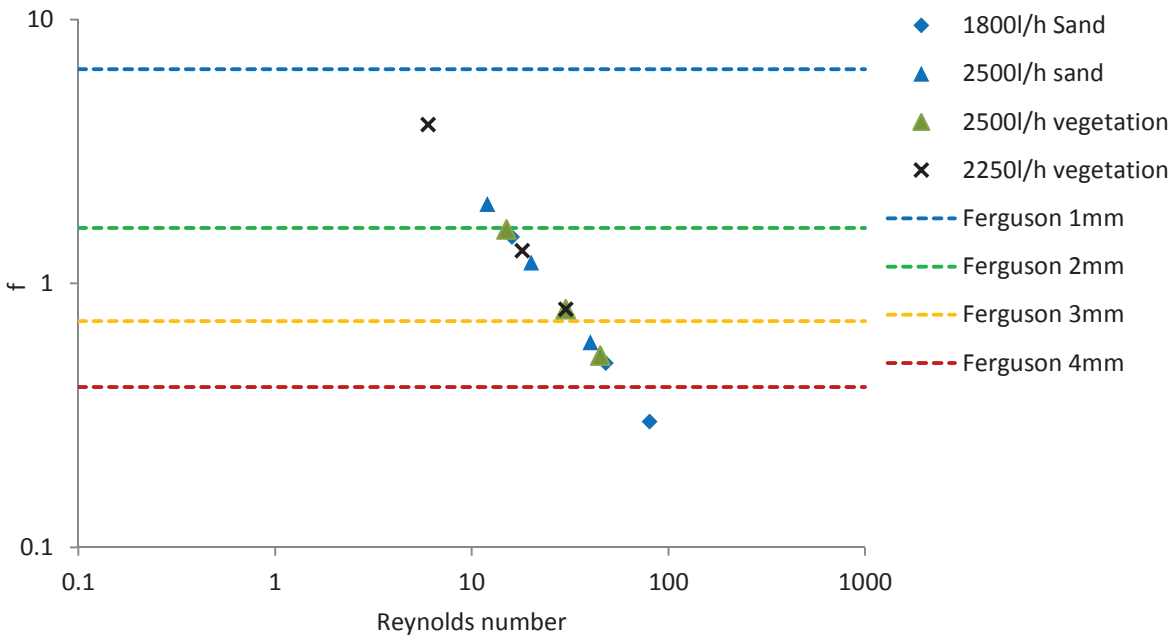

Figure 5.17 ***A****. The Chézy roughness values.* ***B****. Darcy-Weisbach friction factor values for the floodplain velocities. The calculation are presented for a 0.6 +/- 0.4 mm inundation level range for the bare sediment floodplain and 1 +/- 0.5 mm for the vegetation stage floodplain. The Ferguson (2007) prediction with α is 2 is also given for a range of inundation depths (1-4 mm).*

5.2.5 Riparian vegetation cover development

The introduction of a homogeneous vegetation cover to the meandering river after 30 hours of flow (figure 5.18A) allows the identification of several erosion and sedimentation driven vegetation pattern developments. The number of sprouted alfalfa seeds in the flume is on average 64% of the initial 1.5seed/cm^2 distribution after 3 weeks. In this section first the major changes in the riparian vegetation are given regarding general pattern formation. Secondly, the role of alfalfa sprouts as wooded debris in the experiment is described.

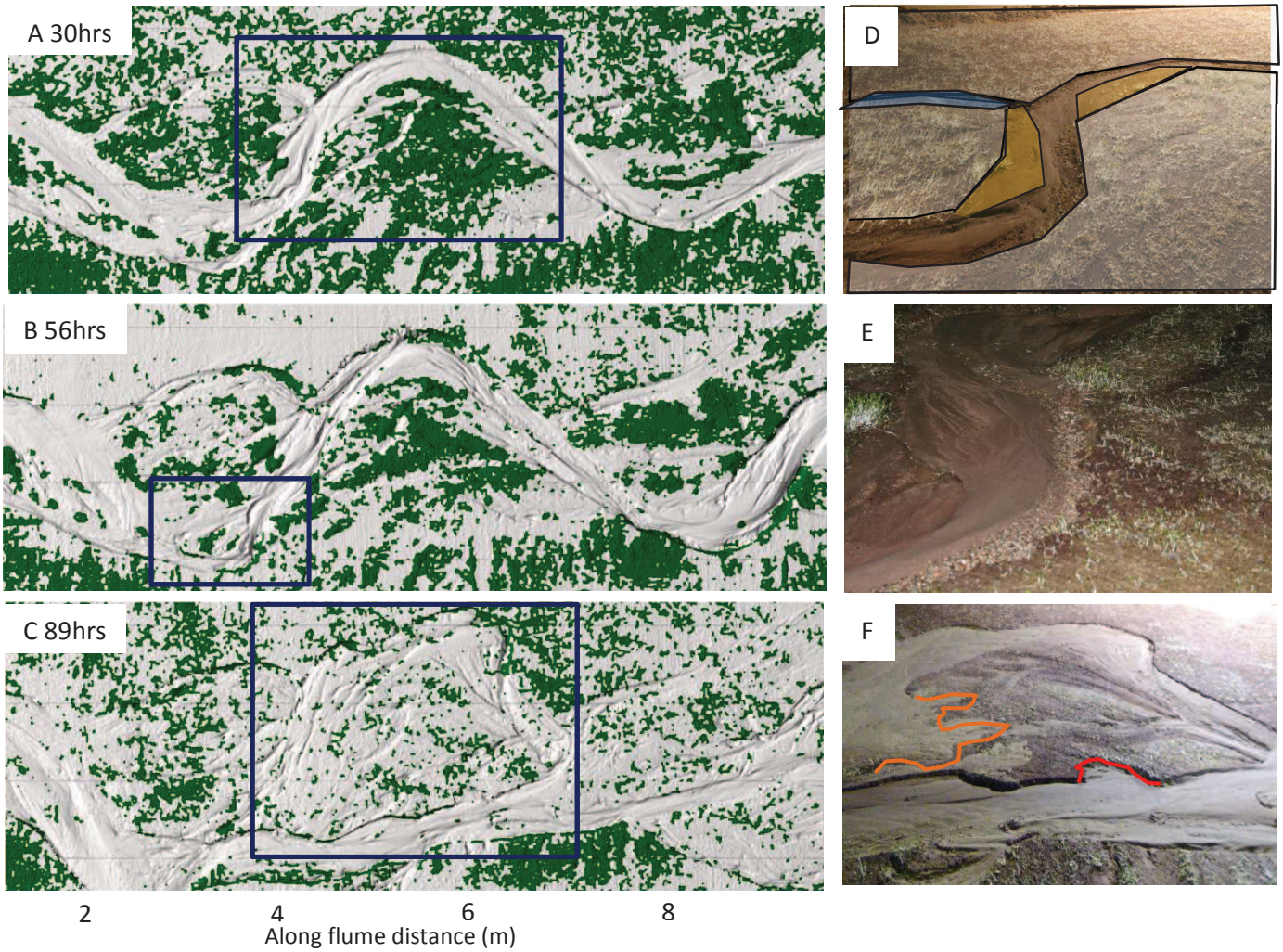

*Figure 5.18. Vegetation development over time **A**, **B** and **C**. Green indicates vegetation. Detailed vegetation development at several locations in the flume at the corresponding time steps. **D** Vegetation cover before flow. Yellow shaded areas indicate non-seeded point bars. The white shade indicates the vegetated floodplain. The blue shade illustrates a non-vegetated residual channel. **E** New formed deposits without vegetation cover. **F** Inactive channel in the floodplain. The red line is a headcut and the orange line a sediment splay over the existing vegetation*

The general development of the vegetation cover over time(figure 5.18A, B and C) showed that from 30 to 56 hours there was a general reduction of the amount of vegetation in the flume, due to extended inundation and rotting. The majority was lost in the upper left corner of the flume. Furthermore, it can be seen that there was an accumulation of pointbar deposits along the original vegetation boundary. This is given in figure 5.18D as the yellow areas in the image. The blue translucent area indicated a deeper old channel that continued to carry a small fraction of the flow and prevented the settling of seeds during the initial seed dispersal.

The new accumulations of inner bend deposits locally buried the margin of the existing vegetation, thereby shifting the vegetation cover margin further towards the floodplain in those locations (figure

5.19A). Other processes that buried existing vegetation where the infillings of the pointbar lows before the central bed cut-off (figure5.18F). Coupled to the formation of new pointbars is the receding vegetation margin along the outer bends of the flume as a result of erosion (figure 5.18B and C). Other erosional processes that removed vegetation where the central bend headcuts (figure 5.18 F).

In figure 5.18 C the cut-off over the floodplain has occurred that closed of river previously occupied channel. This formed a derelict structure in the landscape (figure 5.18F), without vegetation. This was similar to the blue area in figure 5.18D. It only became suitable for vegetation settlement after the flow disturbance disappeared from the abandoned channel. The old channel only became covered with vegetation after the second seed dispersal in the flume. Finally in the downstream section of the flume, the river eventually started to rework its own deposits instead of eroding the vegetation margin. This left curve like original floodplain margins to be present in the flume (figure 5.19B).

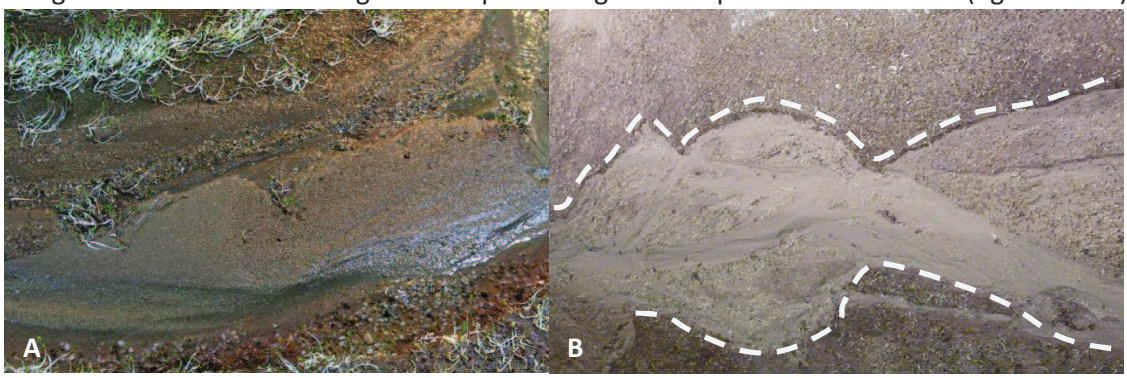

*Figure 5.19. **A** burial of vegetation by sediment on the pointbar. **B** Curved floodplain margins (white dotted lines) in the downstream section of the flume. The flow is from left to right in both images.*

Debris behaviour of alfalfa

Eroded alfalfa that formed clusters of sand and sprouts were either transported towards the downstream boundary, by rolling along the bed, or deposited on the direct downstream pointbar. Apart from the sediment and sprout clusters loose sprouts also entered the system. The individual sprouts were typically deposited on the pointbars. Once an accumulation of “debris” had formed more sprouts were captured and increased the accumulation size (figure 5.20A).

Once on the pointbars the sprouts divert flow around the cluster, thereby creating a lee zone for the flow directly behind the debris accumulation. The lee zone did not undergo morphologic change. On the margins of the lee zone the flow, going around the sprout accumulations, tended to create small scours on the pointbars. The size of the scours differed from small 1.5 long cm 2 mm deep depressions to larger, pointbar length sized, depressions (figure 3.40B). The scour formation by alfalfa on the pointbars was short lived. The vegetation clusters were removed from the pointbars within 1-2 hours. After a cluster was transported downstream, the scours on the pointbar were removed by the flow.

*Figure 5.20. **A** Detail of local erosion. **B** Overview of the erosion of the pointbar behind an accumulation of alfalfa sprouts. The flow is from top to bottom in both images.*

5.2.6 Overview of the experimental meandering river development

The development of the non-vegetated meandering river was characterised by the gradual outbuilding of meander bends by inner bend accumulation and outer bend erosion by entrainment and mass wasting. This continued development led to an increasing sinuosity. After the addition of vegetation the resistance of the outer bends to erosion increased.

The increased bank strength led to a reduced erosion rate of the outer bend. Furthermore there were localized zones in the bends where erosion occurred by undercutting. The local erosion led to a shift in the accommodation space in the bends and determined the sediment accumulation locations in the bends. The overall effects of this change were more asymmetric and sharper bends. The change in bend morphology manifested itself in the continued increase in the system sinuosity.

The changes in the river system, after the addition of vegetation, also had an effect on the overbank flow. The total wetted overbank area was reduced after the addition of vegetation. Furthermore the local inundation level was lower and overbank flow was reduced and confined to depressions in the floodplain. This meant that there was a shift in the discharge distribution towards the channel.

The resulting riparian vegetation pattern development was driven by morphologic development. The outer bank erosion led to a retreat of the vegetation margin in the floodplain direction. On the inner bend the accumulation of new bars increased the distance between the vegetation cover margin and the channel. Locally the vegetation was buried by sedimentation. The largest effect on the vegetation pattern was a cut-of over the floodplain that led to the incision of a new channel and the complete abandonment of the previous channel bed.

5.3 Annular flume

The annular flume setup was used to investigate various effects of scale vegetation in flume experiments. The conducted experiments range from a bare sand filled flume to different vegetation density vegetated experiments (chapter 4.2.3). Firstly the general flow and velocities in the channel and on the floodplain are presented. This is followed by bank erosion, failure mechanics and the morphologic development of the channel. Finally, the role of uprooted alfalfa on the channel is illustrated and the changes in the riparian vegetation cover are presented.

5.3.1 Hydrodynamics

Channel flow

The flow in the channel was sub-critical (Fr<1) and turbulent (Re>500) in the conducted runs. It was characterised by a secondary circulation cell, that was detected by using tracer. The flow cell moved water along the surface towards the outer bend. There the tracer moved towards the bottom and along the bed towards the inner bend. The secondary flow components are given in figure 5.21 A. With a high density vegetation cover the alfalfa was hanging over the channel margins. The flow in this scenario was observed to be slowed down by the vegetated outer bank channel bank margin.

In later stages of the channel development the outer bank secondary current return flow direction was changed. This occurred in both the bare sediment and the vegetation covered system after the formation of the centre channel ridge (chapter 5.3.2). This resulted in two different directions in which the tracer dispersed. The inner bend side of the ridge was still characterised by an inward and downstream directed component. However on the outer bend side of the ridge the flow was parallel to the outer bank margin and in the downstream direction (figure 5.21 B). In addition a slope in the water surface slope of the channel was observed.

At the outer bend margin the water level stood higher than on the inner bend in both the vegetation and non-vegetation environment. Due to the presence of vegetation and the soft sediment bed on the floodplain accurate measurements could not be made. When comparing the bare sediment runs to the vegetated runs qualitatively it can be stated that the water level setup at the outer bend is less in the vegetated flume state. On the inner bend the water level dropped to the floodplain level during the bare sediment runs, whilst with a vegetated floodplain this did not happen.

The flow on the interface between the channel and floodplain differed for the overbank scenarios as well. In the no-vegetation flume, eddies were present between the fast moving channel and more slow overbank flow along the outer bend margin (figure 5.21 A). These eddies were not present with vegetation on the overbank areas.

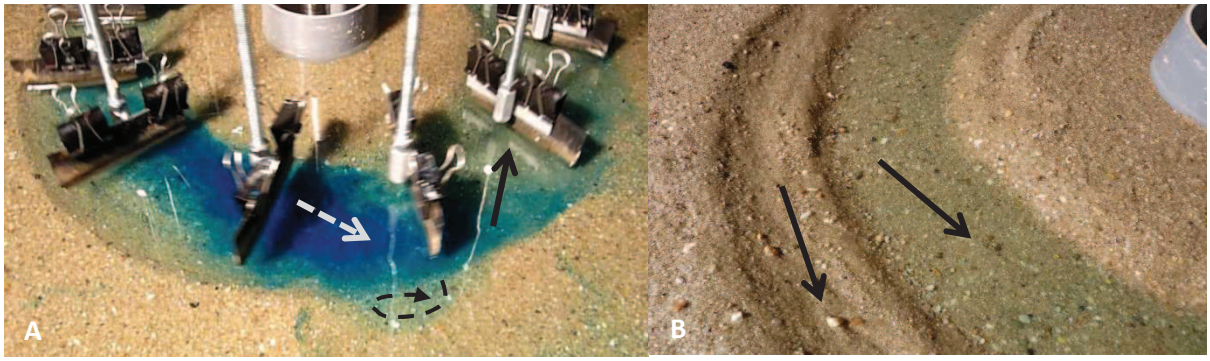

Figure 5.21. ***A*** *Secondary flow along the bed of the flume (black line) and surface (white dotted line). The outer bank eddy is indicated with the dotted line.* ***B*** *The direction of the flow (black lines) indicated in the empty flume.*

Channel velocity

The channel velocities are based on the timing of the arrival of the tracer front over one centre channel distance (1.25 m) for an undisturbed sediment bed with a 2 mm floodplain inundation level (table 5.3). A range of different forcing's were evaluated for different overbank composition scenarios.

With a below the beginning of motion channel forcing (0.25 m/s paddle velocity) flow velocities were approximately equal for all flume environments (0.10-0.13 m/s). With an increased forcing, the channel velocities increased for all floodplain composition scenarios. The magnitude of velocity increase differed per flume scenario. The increased 0.29 m/s paddle forcing, in combination with a vegetation cover, resulted in larger flow velocities than the no-vegetation increased forcing average velocity. Furthermore, a lighter vegetation density resulted in a larger increase in velocity, 0.17 m/s compared to the dense vegetation cover velocity 0.14 m/s. In the no-vegetation environment there was only a slight increase and no difference in the average flow velocity was present between the initial and equilibrium channel morphology. In addition it was found that an increase (2 mm) in the floodplain inundation depth only marginally affected the channel flow by a 0.05 m/s increase in flow velocity.

Paddle forcing velocity (m/s)	Vegetation density (*seed/cm*^{2})	U_{av} (*m/s*)	Details
0.25	0	0.10	Initial channel
0.29	0	0.11	Initial channel
0.41	0	0.12	Initial channel
0.25	0	0.11	Final no vegetation
0.41	0	0.11	Final no vegetation
0.25	1.5	0.13	Standing vegetation
0.29	1.5	0.17	Standing vegetation
0.25	3.0	0.12	Overhanging vegetation
0.29	3.0	0.14	Overhanging vegetation
0.41	3.0	0.16	Overhanging vegetation

Table 5.3. Average channel velocities in the annular flume for a range of paddle forcing's and overbank composition scenarios.

Region of Influence on the vegetated floodplain

The channel exerted a degree of influence on the vegetated cross-sectional floodplain environment, although eddies were absent. The channel flow formed a region of influence (ROI) in the floodplain. The swaying of vegetation and other small differences between the images marked the influence region. The ROI was detected by taking ten consecutive images and determining the difference in pixel values between them. The raw data was soothed using a median filter. This was done for the low (figure 5.22 A) and high (figure 5.22 B) vegetation density. The age of the vegetation (15 days) is the same for all velocity and water level conditions.

In general there was a decrease in the influence when moving from the channel margin, the 0 cm mark in the figures (5.22 A and B), to the distal part of the floodplain. For each vegetation density scenario a larger inundation depth resulted in a longer distance over which the channel actively affected the floodplain. The same applies to an increase in the channel velocity. A combination of both an increased velocity, as well as a higher inundation depth, yielded the largest ROI. In the different density scenarios the maximum distance over which the influence was present was equal, at approximately 5 cm (25 *h* for the 2mm and 12.5 *h* for the 4 mm runs) from the outer bank channel margin. The variation in disturbance values, further on the floodplain, can be regarded as background noise.

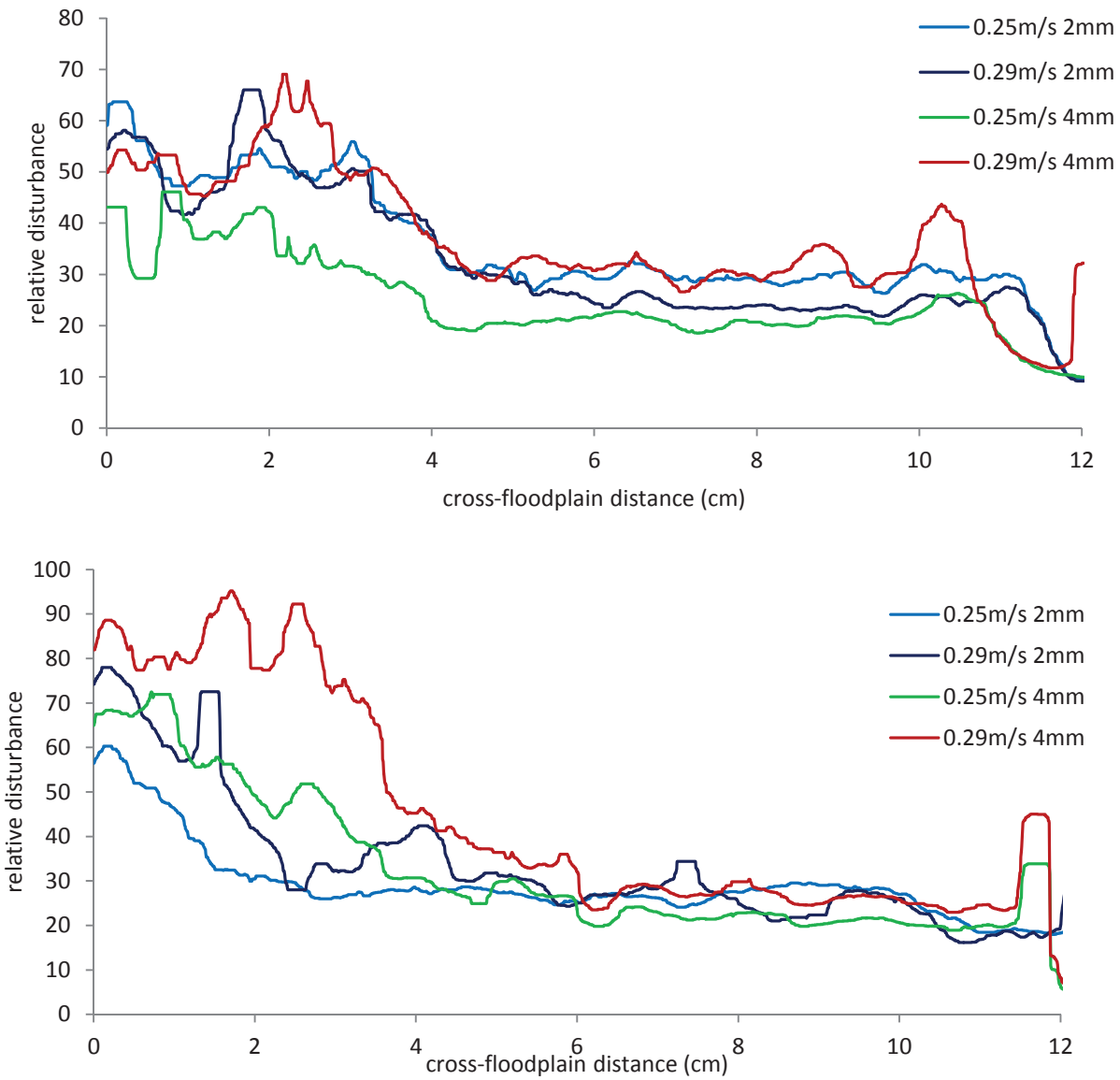

*Figure 5.22.**A** Low vegetation density vegetation cover region of influence from channel flow. **B** High vegetation density cover relative disturbance on the floodplain from channel flow. The velocity in the legend is the paddle forcing velocity the inundation level on the floodplain is also indicated .*

Overbank flow

With different inundation levels on the floodplain (2 and 4 mm), vegetation densities (1.5 and 3 seeds/cm^2) and ages (6-16 days), various circulation patterns were found on the outer bank floodplain. The individual circulation cell flow was identical for all conditions. There was a flow component directed from the channel onto the floodplain. This flow component re-joined the channel some distance from the floodplain directed flow. If the direction of flow in a single cell is in the downstream direction, it is upstream directed in the neighbouring cell. This means two circulation cells consisted of a zone of divergence, floodplain directed, and convergence, channel directed flow. The circulation patterns did not vary with an in-or decrease in the channel forcing velocity within the validity range of the annular flume. An overview of the different circulation cells is given for a 0.25 m/s paddle forcing of the channel flow (figure 5.23). The distance between the floodplain and channel directed flow and the cross-floodplain distance spanned is expressed both in centimetres and in inundation levels on the floodplain (n*h).

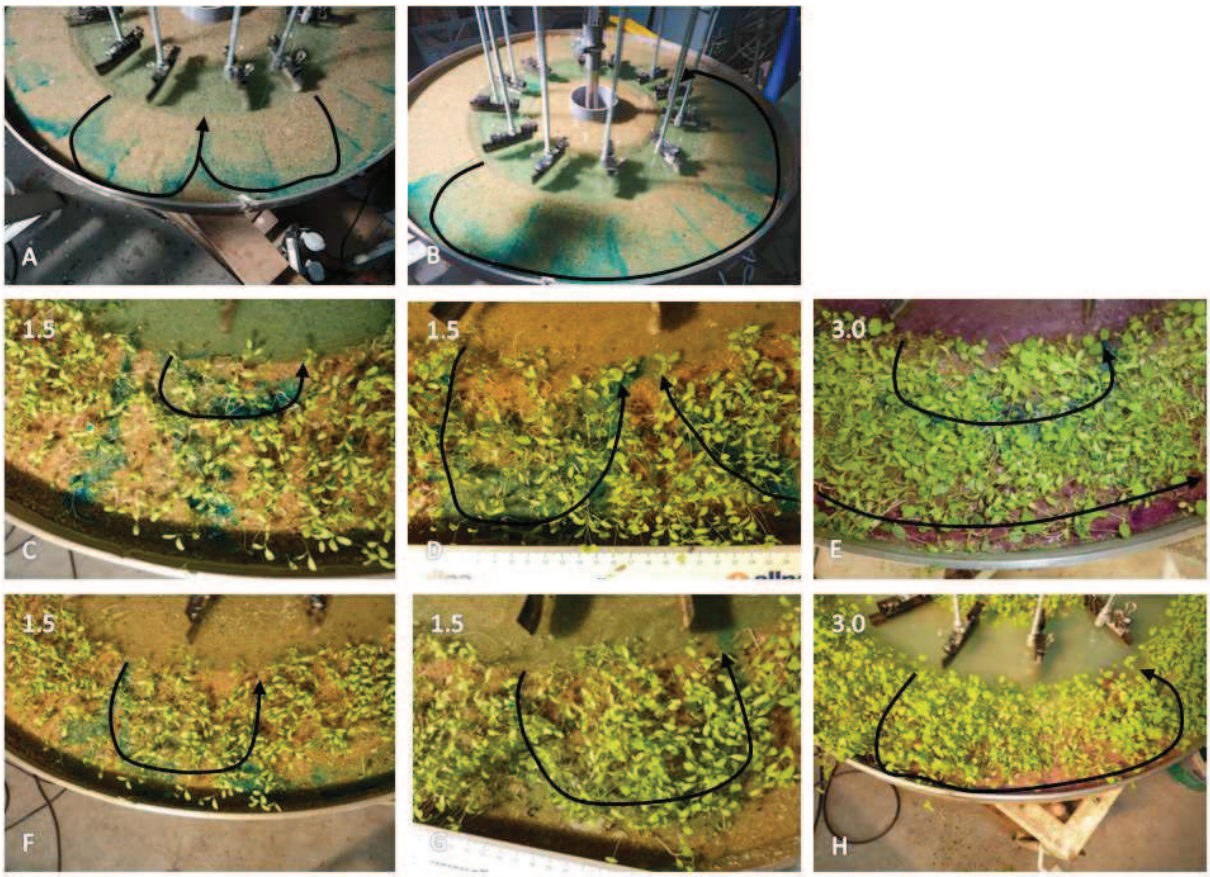

Figure 5.23. ***A*** *2 mm floodplain inundation* ***B*** *4 mm floodplain inundation* ***C*** *1.5 seed/cm^2 6 day old vegetation 2 mm inundation,* ***D*** *1.5 seed/cm^2 15 day old vegetation 2 mm inundation* ***E*** *3 seed/cm^2 15day old vegetation 2mm inundation* ***F*** *1.5 seed/cm^2 6 day old vegetation 4 mm inundation* ***G*** *1.5 seed/cm^2 15 day old vegetation 4 mm inundation and* ***H*** *3 seed/cm^2 15 day old 4 mm inundation.*

A low (2 mm) level inundated sandy floodplain resulted in small cells that spanned the entire cross-sectional distance (15 cm) of the floodplain. The distance between the divergence and convergence zone was roughly 12 cm (60 *h*). Instead of multiple small cells the increased (4 mm) water level on the floodplain yielded just two cells that spanned half a floodplain length, 125 cm (312 *h*). The flow in these large cells was focussed along the metal wall of the flume. After the incorporation of vegetation the size of the circulation cells differed.

Both the 2 and 4 mm, low vegetation density, inundated floodplain circulation displayed small circulation cells along the channel margin. The magnitude of these cells was on the inundation level and the age of the vegetation cover (figures 5.23 C, F and C, D). A 2 mm inundation level and young (6 day old) alfalfa created a flow cell close to the channel margin (10 *h*). The distance between di-and converging zones was approximately 12 cm (60 *h*). After 15 days of vegetation growth, the circulation cells spanned the entire cross-sectional distance of the floodplain, 15 cm (75 *h*). The width of the cells remained similar to the young vegetation environment cell (12 cm, 60 *h*). With a larger floodplain inundation depth the floodplain circulations cells, for the two vegetation ages, were the same. They both spanned the complete cross-sectional floodplain (37 *h*) with roughly 12 cm between the floodplain directed and return flow (30 *h*).

The 2 mm inundation depth for the high density vegetated flume floodplain flow consisted of two smaller flow cells. The flow circulated over the floodplain, reaching the centre of the floodplain (37 *h*). It re-joined the main channel in a convergence location at a distance of 12 cm (60 *h*) from the divergence zone. The small circulation cell is visible in figure 5.23 E as a blue tracer line. At two locations in the flume, a larger floodplain directed flow diverged at the most distal part of the floodplain. This flow moved over a distance of half a flume (625 *h*) before it converged and joined the channel. The larger floodplain circulation cell is the purple tracer line (figure 5.23 E). With the larger

inundation level several larger flow cells were present on the floodplain. The distance between the diverging and converging zones was 30 cm (75 *h*). Furthermore the cell covered the entire cross-sectional floodplain length of 37 *h*.
The development of the flow cells, as presented in the figures above, required an approximate 2-3 minutes period. Furthermore the floodplain flow was characterised by a distinct oscillating in a direction perpendicular to the main flow. The effect of the oscillations in the tracer movement and the flow velocities are described in more detail in the section below.

Overbank flow velocity

The flow velocity on the outer bend floodplain was monitored for a low (2 mm) and high (4 mm) inundation level. In addition the channel forcing range was varied. The velocities are given for a proximal 3 cm, centre 8 cm and distal 13 cm section of the floodplain. The presented velocities are the average values of two measurement repetitions. The channel bed was the initial horizontal bed. The conditions on the floodplain were sub-critical (Fr<1) and laminar (Re<500) in all of the presented scenarios.

Paddle velocity (m/s)	Location	$h_{floodplain}$ (*m*)	U_{av}Sand (m/s)	U_{av}Young 1.5 seed/cm^2 (m/s)	U_{av}Old 1.5 seed/cm^2 (m/s)	U_{av}Young 3.0 seed/cm^2 (m/s)	U_{av}Old 3.0 seed/cm^2 (m/s)
0.25	Proximal	0.002	0	0	0.01	0	-
0.25	Centre	0.002	0	0	0.002	0	-
0.25	Distal	0.002	0	0	0.002	0	-
0.29	Proximal	0.002	0	0	0.001	0	0
0.29	Centre	0.002	0	0	0.005	0	0
0.29	Distal	0.002	0	0	0.002	0	0
0.25	Proximal	0.004	0.029	0	0.006	0	0
0.25	Centre	0.004	0.021	0	0.001	0	0
0.25	Distal	0.004	0.017	0	0.002	0	0
0.29	Proximal	0.004	0.027	0	0.003	0	0.005
0.29	Centre	0.004	0.029	0	0.001	0	0.006
0.29	Distal	0.004	0.023	0	0.001	0	0.005

Table 5.4. Overview of the annular flume overbank velocities. Sand referrers to non-vegetated flume scenario. The indices young(6 day old) and old (15day old) to vegetation runs.

In the bare sediment floodplain velocities (table 5.4) the inundation level on the floodplain formed a limitation on the floodplain flow velocity. This is the 0 m/s value in table 9.2 and indicates the absence of a measurable flow with low inundation levels. With the high inundation level the velocity was measurable and in the 0.02-0.03 m/s range. The channel flow forcing only marginally increased the velocity of the flow. In the cross-floodplain direction the average velocities in the centre and proximal part were roughly equal, but the distal section was slower.
With a vegetated floodplain different parameters were of importance in relation to the overbank velocities. The vegetation covered overbank velocities in the flume were dominantly dependent on the age of the alfalfa sprouts. The effect of the age essentially determined whether or not flow was present on the floodplain. In case of overbank flow, with a measureable velocity, the low density measurements indicate a factor 10 reduction compared to the no-vegetation overbank flow.
The main difference in the vegetation composition between the young (6 day) and old (15 day) alfalfa was the structure of the stems. Young alfalfa stems were draped along the bed, whilst older stems stood up straight. Other effects like the inundation depth and channel forcing did not alter the vegetated velocity with a low density cover. Similar to the bare sediment flume run, the cross-sectional floodplain proximal velocities tended to be higher than the distal ones. The difference between a light and a dense vegetation cover was the absence of measurable velocities for old

vegetation runs, with a low inundation level. Furthermore the high density high inundation velocity was larger than the low density environment velocities.
In all of the above presented runs, with a measurable overbank velocity, the tracer movement was characterised a cross-floodplain, channel and floodplain directed, paddle related oscillation. The velocities of these oscillations were approximately 0.005 m/s in the cross-floodplain direction for all above presented flume environments. A single oscillation, in a tracer based overbank velocity measurement is indicated in figure 5.24. The white dotted lines indicate the average degree of lateral fluctuation on the floodplain.

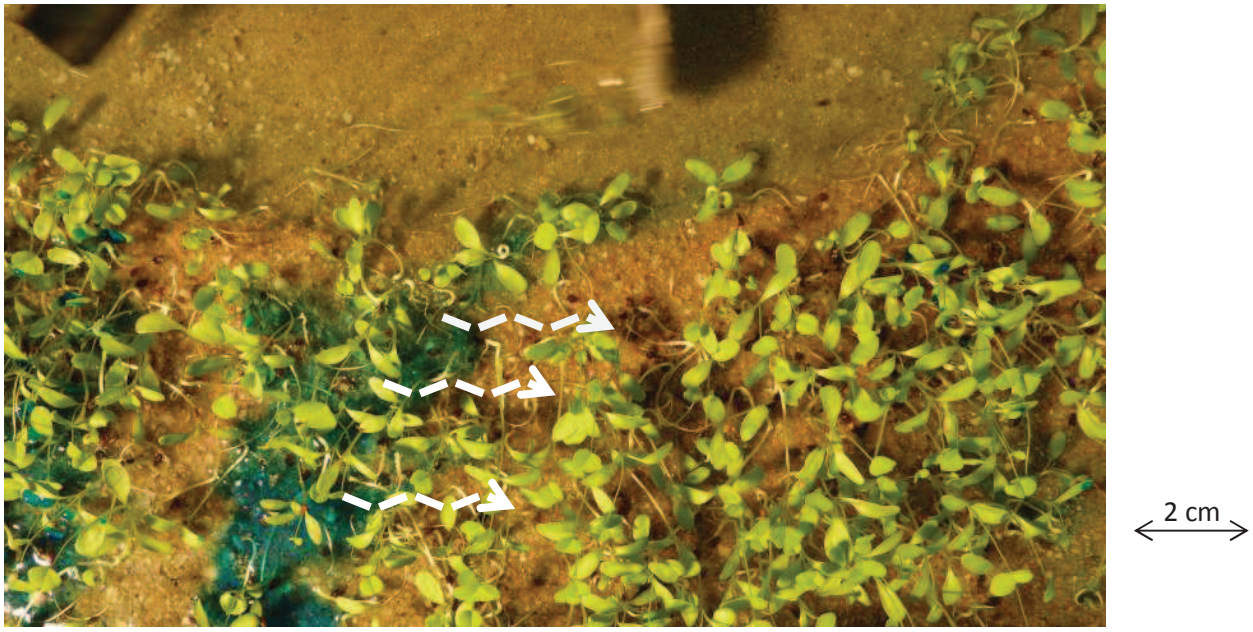

Figure 5.24. Tracer movement oscillations are indicated by the red dotted lines. The average degree of the fluctuations is indicated by the lines.

Overbank roughness

The above presented velocities (table 5.4) were used to determine the hydraulic resistance of the floodplain. The floodplain roughness was computed using equations 18 and 19. With the Darcy-Weisbach value the Chézy coefficient was computed via equation 20.In figures figure 5.25 A and B the same general trends are present. The Chézy value figure is used for a more detailed look at the results.
There is a clear distinction to be made in terms of resistance values between the vegetation (1.5-8 $m^{0.5}/s$) and the bare sediment floodplain (12-17 $m^{0.5}/s$). The sediment only roughness overbank values are higher and within the Ferguson (2007) range (with α is 2). The vegetation covered system run values have lower roughness values, these lie below the predicted Ferguson (2007) range. Additionally the Reynolds number indicates a transition from a vegetation ($Re<20$) to a bare sediment ($Re>50$) composition floodplain.
The variation in the roughness value range, for the 1.5 seed/cm^2 density, by incorporating the proximal central and distal floodplain sections indicates that there is a significant degree of variance within the roughness measurements.

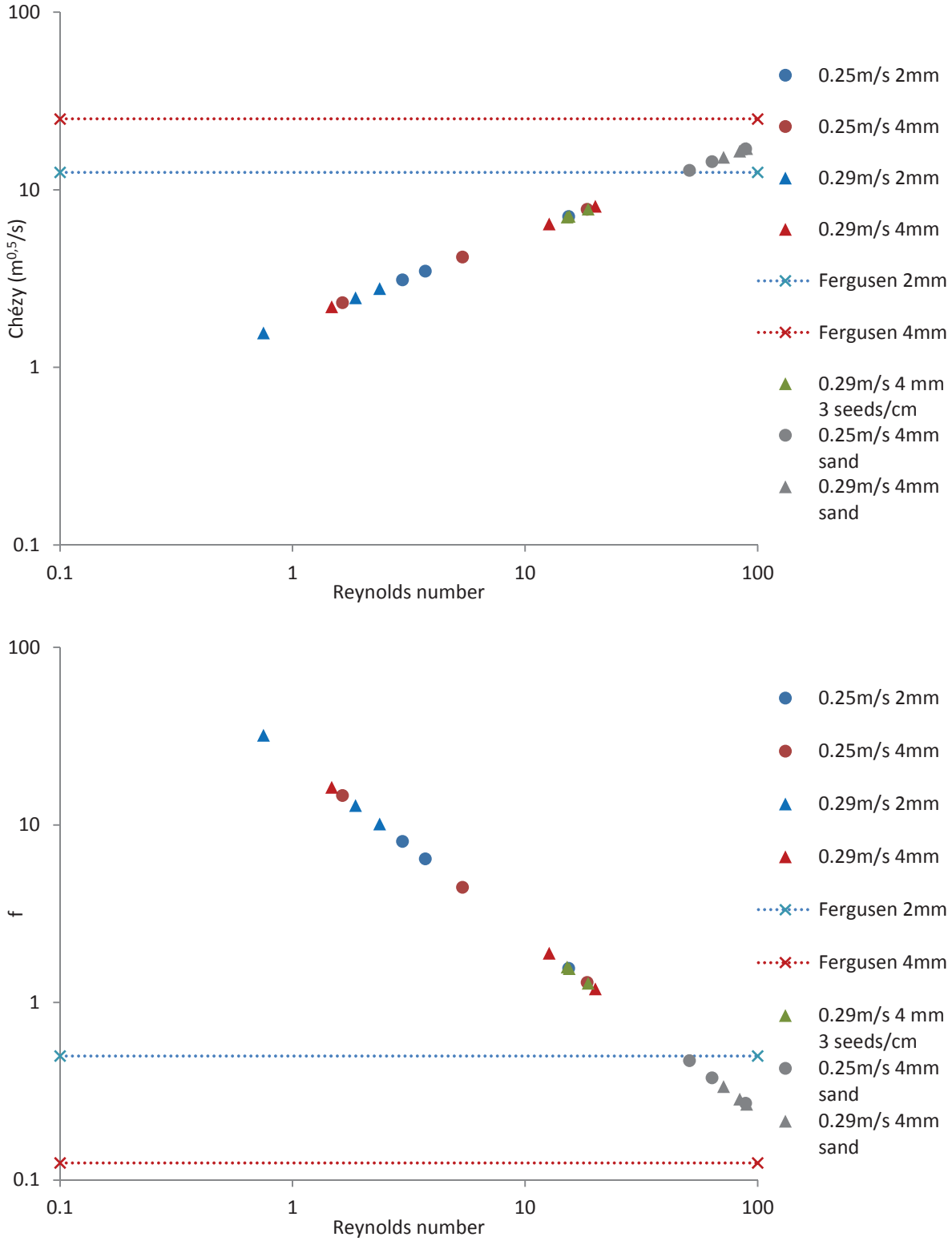

Figure 5.25. ***A*** *Chézy value (equation 19 and 20) plotted against the Reynolds number for the annular flume experiments with and without vegetation.* ***B*** *Darcy-Weisbach friction factor (equation 19) plotted against the Reynolds number. The paddle forcing velocity*

5.3.2 Morphological development

The morphologic development of the annular flume channel is given for the non-vegetated flume. This serves as a frame of reference for the vegetated floodplain runs presented next. The high density vegetation runs is presented first. This allows the identification of the maximum vegetation realted effects. This is followed by the low density run that displayed a more pronounced bed development.

Non-vegetated annular flume

The erosion of the outer bank in the annular flume was studied for a range of channel flow velocities with a 2 mm floodplain inundation level. An overview of the bank erosion in the flume without vegetation is given in figure 5.26. The runs 1, 2 and 3 were conducted at the beginning of motion (0.29 m/s paddle velocity).

The erosion of the outer bank proved to be a non-continuous process. In all of the runs presented, a stepped retreat of the channel margin can be observed. The retreat of the outer bank halted at the same distance in all runs. This maximum retreat was found at the 16 mm mark. The same 16 mm maximum was also found with an increased mobility of the sediment bed (0.41 m/s paddle velocity). The time, over which the stepped erosion took place, was reduced for a high flow condition. The high flow eroded to the 16 mm boundary in 4.5 minutes compared to the 10.5-14 minute period for the beginning of motion runs.

The mechanisms of bank failure and thus outer bank erosion were the same for all runs above the beginning of motion. The sediment of the outer bank, when mobile, tended to move directly down slope by mass wasting. At the bed it was moved as bed load in the downstream and inner bend direction. Some of the finer grains of sediment were directly entrained of the bank and carried downstream.

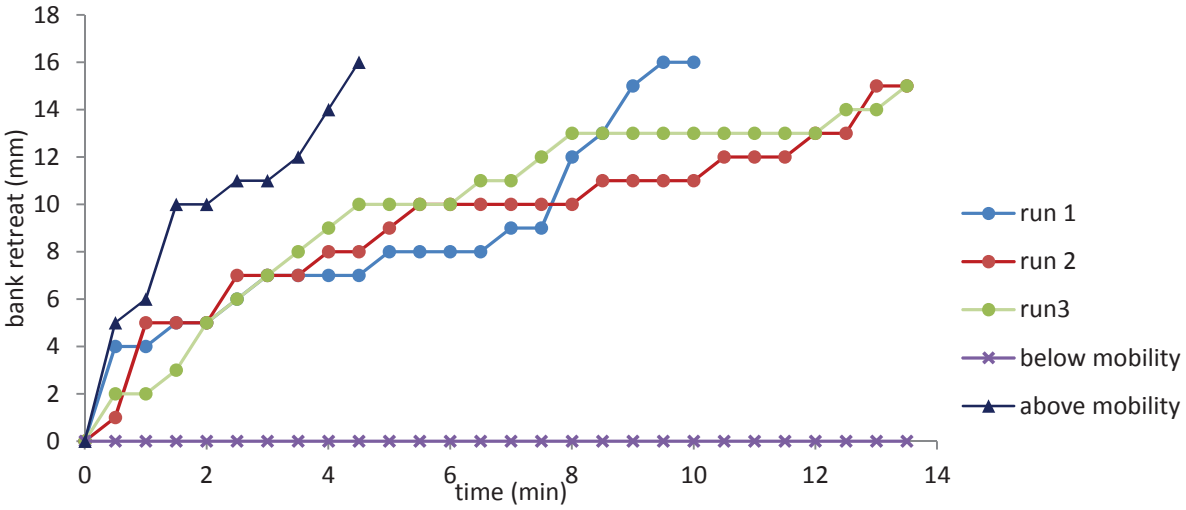

Figure 5.26 Retreat of the annular flume outer bank. Three runs at the beginning of motion as well as far above and below beginning of motion run are plotted.

The eroded sediment moved both down the outer bank slope and downstream. However due to the circular nature of the flume the eroded sediment in the downstream direction was replaced by sediment from the upstream direction, thereby forming a ridge on the base of the channel (figure 5.28 A). The ridge of sediment moved slightly in the inner bend and downstream direction during the first 10 minutes of the run, until an equilibrium bed profile formed. In figure 5.27 the equilibrium profile is displayed. The ridge in the centre of the channel and the floodplain directed retreat of the outer bank margin is present in the cross-sectional equilibrium profile plot. The inner bank remained stable.

After 10 minutes a final step in the outer bank erosion occurred. This created small local depressions of the outer bend with an approximate length of 12 cm. Along the outer bend ridge small lobes

formed. These lobes migrated in the downstream direction. The formation of the outer bank depressions and sedimentary lobes marked the end of morphologic development of the channel. The slope of the outer bend in the final stage was 0.31 (dy/dz). The sorting of grains was absent in the equilibrium profile.

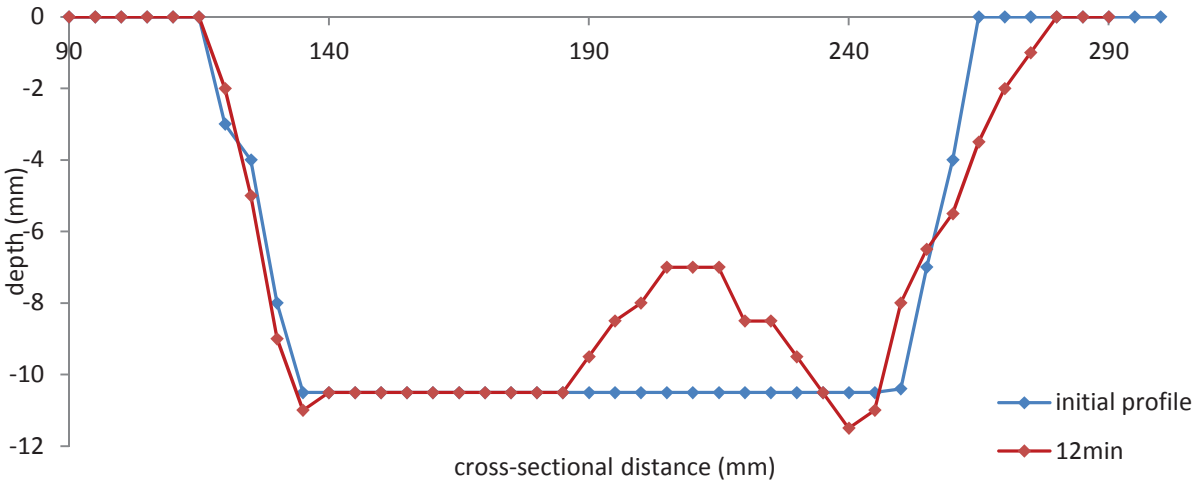

Figure 5.27. Bare sediment filled flume morphologic development. The cross-section in blue is the initial channel, the red line is the equilibrium bed profile. The paddle occupied the area between 140 and 240 mm in the cross-sectional transect.

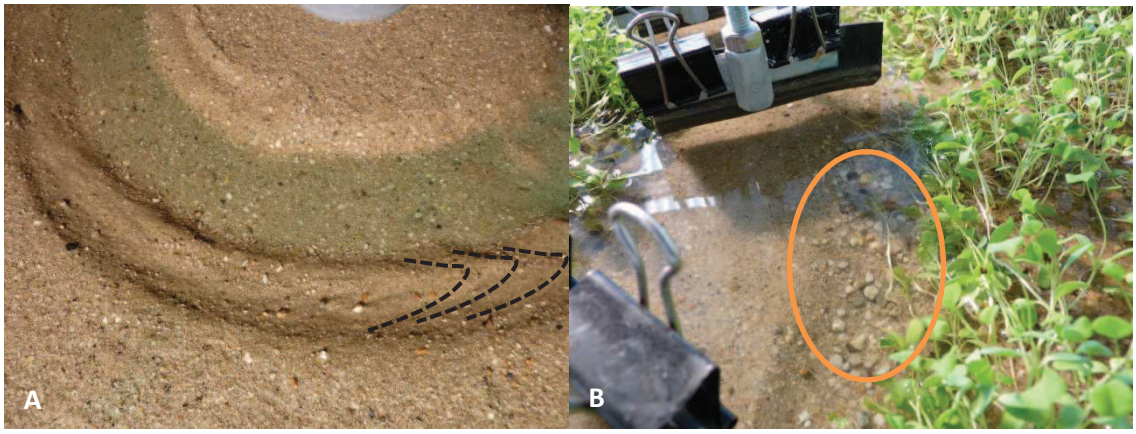

*Figure 5.28.**A** The final morphology profile for a no-vegetation scenario, the dotted lines indicate the fronts of the sedimentary lobes in the system. **B** High density equilibrium profile with coarse sediment along the outer bend.*

High vegetation density runs

It should be mentioned that the paddles of the annular flume resulted in mechanical uprooting of the vegetated channel margins in both vegetation density scenarios. After several rotations a fraction of the overhanging alfalfa was removed from the system. The mechanical removal of alfalfa left substantial amounts of vegetation in place along the entire channel margin (figure 5.28 B).

With a high density vegetation cover on the floodplain no erosion of the outer bend occurred after running the flume for a range of flow conditions over extended periods of time (>2hr at the beginning of motion). Erosion remained absent with velocities beyond the validity range of the annular flume (>0.5 m/s). The higher flow velocities resulted in an excess amount of water being forced towards the outer bend and did not represent river bend flow. The high density vegetation along the outer bend displayed a series of changes that can be divided into four stages (figure 5.29).

Initially the channel had straight sides (figure 5.29 A) as a result of the template used to prevent seeds from entering the channel (chapter 4.2.3). After filling the flume to a 2 mm floodplain

inundation level the margins of the channel reduced their slopes to the angle of repose, (dy/dz) at 0.575 (figure 5.29 B). With flow in the channel the alfalfa sprouts were bend in the downstream direction. After bending over, the leafs of the alfalfa were below the water surface. After 15 minutes of flow it could be observed (figure 5.30) that there was a decrease in the bed level along the outer channel margin (x=250mm). In the centre of the channel the bed level rose. This formed a longitudinal ridge in the centre of the channel (figure 5.28 B), similar to the sand run presented above. The ridge moved slightly in the direction of the inner bend over time. The inner bend also accumulated un-sprouted alfalfa seeds. The final stage displays the outer bank still in place with only some minor changes in the morphology of the channel bed (figure 9.1 3D). Over time (80 min) the outer bend depression slightly increased in depth. At the base of the depression coarser grains were observed (figure 5.28 B). The final profile outer bend was angled (dy/dz) at 0.486. The morphologic development of the high density vegetation cover bed is given in detail for a run with the velocity at the beginning of motion (0.14 m/s) and a 2 mm inundation depth (figure 5.30).

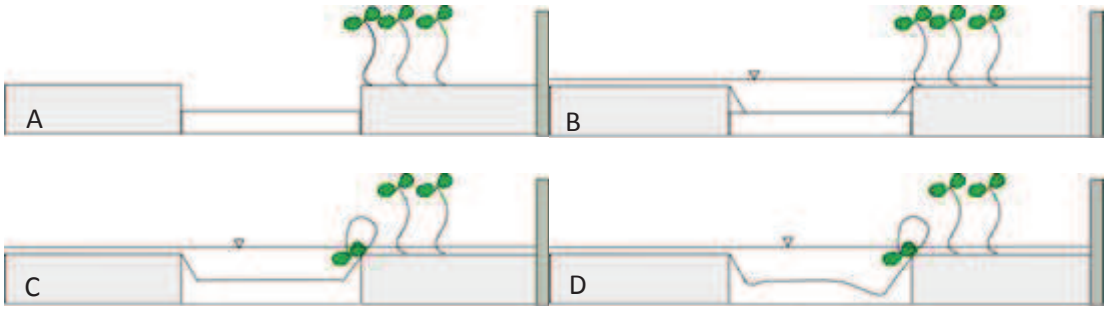

Figure 5.29 ***A****. Initial channel without water.* ***B*** *after filling the channel the outer and inner bend angel decreases.* ***C*** *Alfalfa bends over and shelters the outer bank.* ***D*** *A slight depression has formed along the outer bend margin, but no erosion occurred. The outer bank is on the right side in each image*

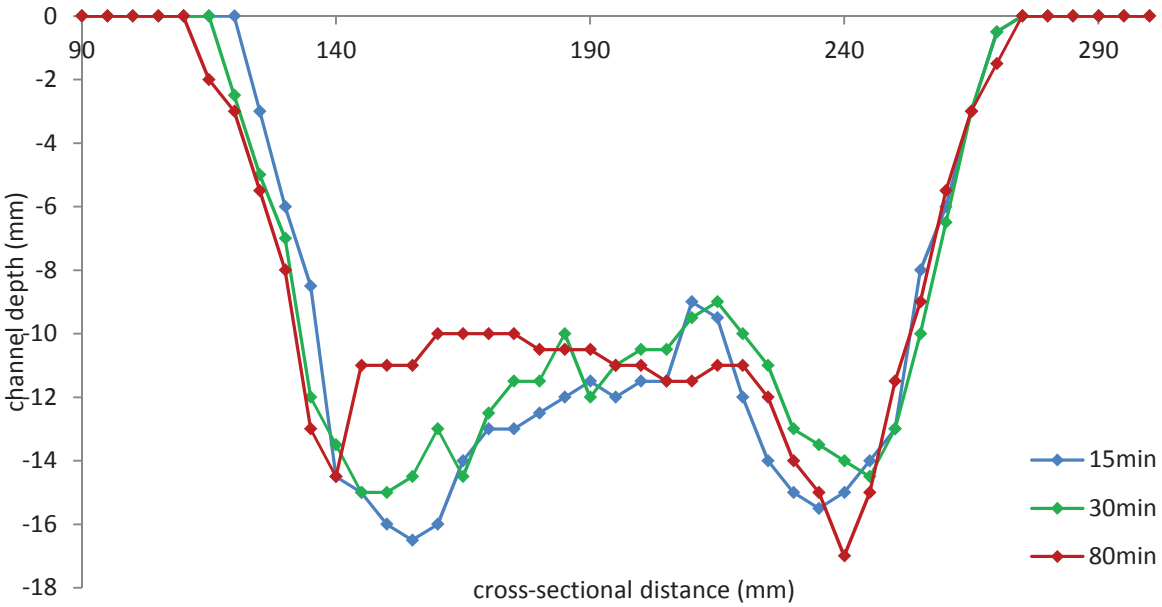

Figure 5.30. Morphologic development of the annular flume for a high vegetation density floodplain cover. The outer bend is on the right side of the plots. The paddle is present between 140 and 240 mm in the cross-sectional direction

Low vegetation density runs

The low density vegetation cover on the floodplain (1.5 seed/cm^2) did not rule out erosion of the outer bank. The retreat of the outer bank is plotted in figure 5.31 for a channel velocity of (0.17 m/s), equivalent to the beginning of motion. The development of the outer bank shows a clear stepped retreat of the channel margin. The small 1 mm increments occur nearly instantaneous. The overall erosion driven retreat of the outer bank was 3 mm compared to the 16 mm bank erosion in the no-vegetation scenario. The main failure mechanism of the outer bank, in the first 20 minutes of flow, were downslope mass wasting and once on the bed downstream movement of the sediment. There was no preferential erosion present around the alfalfa stems or between vegetated patches.

After the first 20 minutes of flow the outer bank of the channel had a steeper, vertical (dy/dz=1), slope than the bare sediment and high density runs. The erosional process of the outer bank changed. Mass wasting and entrainment remained dominant, but now there was a clear preferential erosion around the alfalfa stems. This resulted in clusters of eroded sprouts entering the channel.

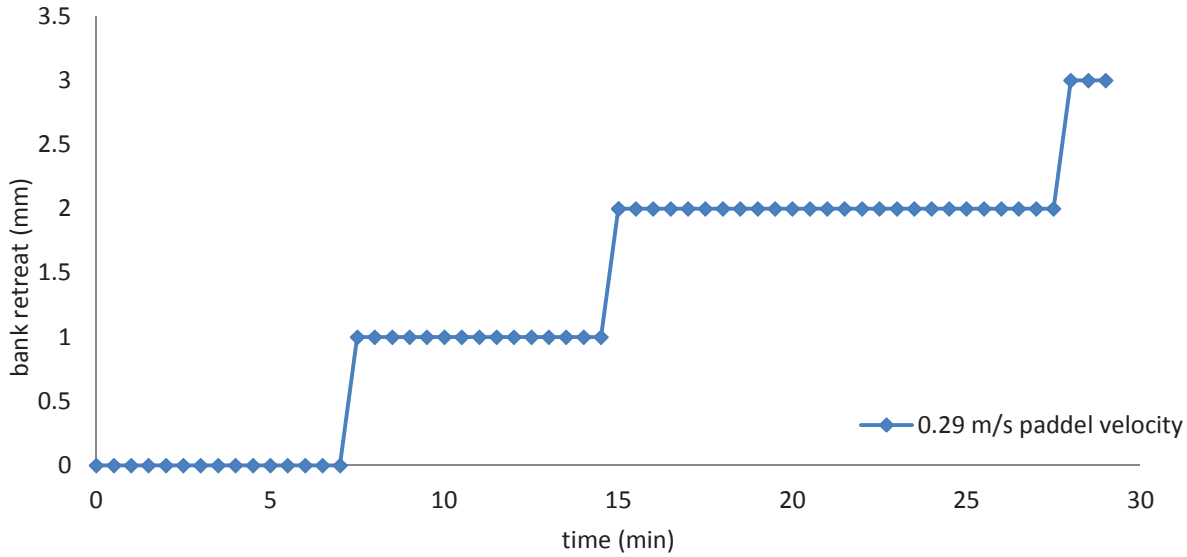

Figure 5.31. Erosion of the 1.5 seed/cm^2 vegetated outer bank with a channel flow of 0.17 m/s and a 2 mm floodplain inundation level. The stepped bank retreat increments occurred within the 30 second measurement interval.

The development of the channel morphology with a light vegetation cover for a run, at the beginning of motion, is given in figure 5.32 (blue and green line). The general development closely resembled the dense vegetation scenario. The outer bend was deepened and a central ridge formed. Over time the outer bend depression became deeper. In contrast to the dense vegetation scenario the central ridge was moved further towards the inner bend. In addition the outer bend channel margin became nearly vertical. The 30 minute profile (figure 5.32) is the equilibrium for the beginning of motion run. The depression along the outer bank margin and the steep outer bank can be seen in figure 5.33 A. Furthermore the lighter vegetation density in the figure is apparent, so is the absence of sheltering of the bank by overhanging vegetation along the channel margin. In addition the central ridge is visible in the picture. After increasing the velocity (0.63 m/s paddle velocity), further development of the channel was observed (red line figure 5.32).

The outer bend depression deepened and all the excavated sediment was moved towards the inner bend. Along the outer bend margin coarse sediment was present and locally the metal base of the flume became visible. The eroded sediment was delivered to the inner bend together with un-sprouted alfalfa seeds. After 30 minutes of 0.63 m/s paddle velocity forcing an equilibrium profile was formed. The equilibrium profile was characterised by the paddles brushing along the top of the inner bend sediment accumulation. The slope of the inner bend accumulation (dz/dy) was 0.16.

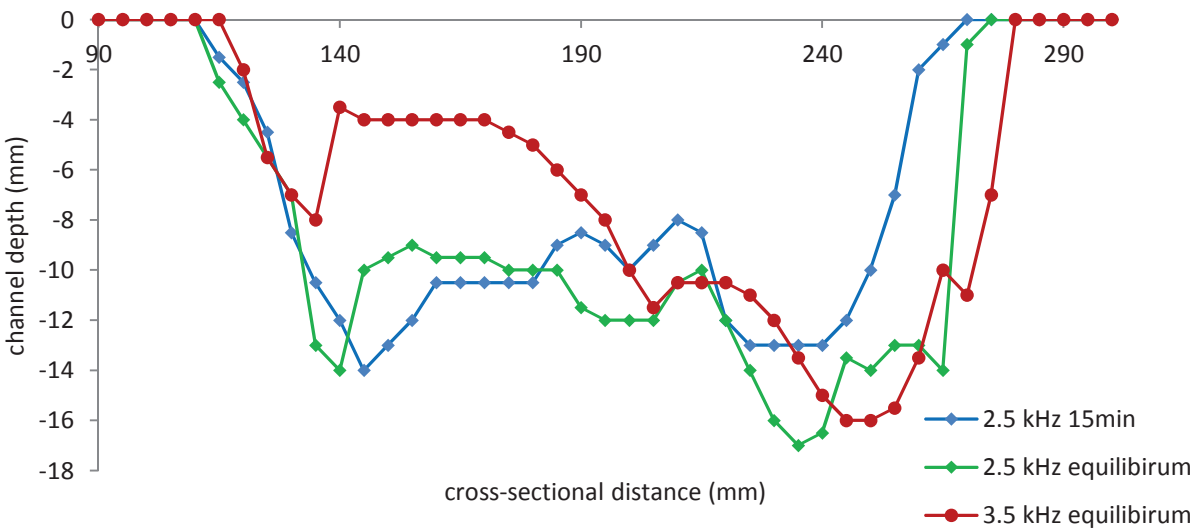

Figure 5.32. Morphologic development of the channel bed for the light vegetation density scenario.

*Figure 5.33.**A** Annular flume bed after 15 minutes of flow. Note the steep outer bend, indicated by the white arrow, and the un-sprouted seed accumulation along the inner bend. **B** Equilibrium profile for the increased (0.63 m/s paddle velocity) forcing run. The flow is from top to bottom in both images.*

Overbank morphology

The bed sediment was mixed with 20 volumetric percentage of silica flour (M6). The deposition of fine white silliclastic sediment in the flume was studied for the two different floodplain inundation depths in the high density environment. The vegetation cover consisted of >15 day old vegetation.

With the low stage inundation depth in the flume the channel coloured white instantly. However the amount of suspended silica in the channel reduced rapidly in a 5 minute interval. This was observed as a decrease in the white turbidity of the water. The overbank flow of the flume did not acquire a significant amount of silica flour. After running the flume for 2 hours, the overbank area of the flume did not display fine sediment traces.

With a higher floodplain inundation depth the overbank flow visibly contained silica flour. The concentration of silica in the floodplain water and channel rapidly reduced. After 2 hours of constant flow deposition along the channel margin had occurred. A narrow band of 2.5 cm displayed a whitish line between the grains and had a distinctive colour difference compared to the distal part of the floodplain (figure 5.34). The channel morphology resembled the equilibrium profile that is given in figure 5.30.

Figure 5.34. Silica flour deposition along the channel margin. The floodplain sediment along the outer bank displays a fine white filling between the sand grains on the left of the white dotted line.

5.3.3 Riparian vegetation cover development

Alfalfa that made its way into the channel, either by bank erosion or mechanical uprooting by the paddles, can be regarded as wooded debris (chapter 2.2.2). The debris sprouts were occasionally trapped by vegetation along the outer bank. This resulted in long interlinked alfalfa chains across the width of the channel in the downstream direction. Other sprouts settled to the bottom of the flume.
The leafs of the submerged stems locally affected the flume sediment bed in the channel. The effect consists of a small 5 mm long and 1 mm deep local depression right behind the leafs of the debris alfalfa (figure 5.35 A) Other uprooted alfalfa clustered together in tumbleweed like balls. These balls of sprouts were rolled in the downstream direction by the paddles (figure 5.35 B). Some of the un-sprouted seeds made their way into the channel. Once in the channel they were transported towards the inner bend.

Figure 5.35 ***A****. Local erosion of the channel bed behind a debris sprout of alfalfa. Flow is from left to right* ***B*** *rolled balls of uprooted alfalfa.*

Vegetation patterns in the Annular flume

In both the high and low density vegetation covers, approximately 89% of the seeds had sprouted thereby forming the riparian vegetation on the floodplain. The development of the sprouts was characterised by a 6 day initial growth period. After the first 6 days the growth continued over a three week period. The changes in the continued growth period were a slight increase in stem length, 5-6 cm after 6 days to a 7-8 cm length around day 15. Furthermore the older alfalfa sprouts started to form additional leafs. The second difference between the 6 and 15 day vegetation was that the young vegetation draped over the sediment bed of the floodplain, whilst older vegetation stood up straight.
Due to the influence of the flow on the vegetation cover patterns or an absence of riparian vegetation patterns were present. The high density vegetation cover prevented the erosion of the outer bank. Therefore no patterns developed in the vegetation cover. The light density homogenous cover changes were related to the morphologic development of the channel (chapter 5.3.2). The main drivers of riparian vegetation pattern change were erosion and sedimentation. Along the outer bend margin erosion was present and on the inner bend side sedimentation formed non-vegetated sedimentary deposits. When regarding the flume morphology at the end of the above mobility run a non-vegetated sand bar deposit was present along the inner bend (figure 5.36). On the outer bank the vegetation margin retreated slightly, due to erosion.

Figure 5.36. Vegetation patterns in the low density high forcing run. The white shaded areas indicate the vegetation margin. The yellow indicates the bare sediment inner bend bar accumulations. The un-shaded area is the annular flume channel.

5.3.4 Overview of the annular flume development

The annular flume experiments indicated that the addition of a dense (3.0 seed/cm^2) vegetation cover ruled out erosion of the outer bank, thereby limiting the morphologic development. With a lighter vegetation cover density (1.5 seed/cm^2) the erosion of the outer bank was maintained. Furthermore the added bank strength increased the outer bank slope. These changes allowed a continued morphologic development of the channel that was characterised by a deep outer bend scour and an inner bend bar.

Other vegetation induced effects were present on the overbank area of the flume. The presence of vegetation within the 6-10 day age prevented measurable overbank flow velocities. Older vegetation (16 days) did not prevent measurable overbank velocities. The resulting values indicate that the presence of a 1.5 seed/cm^2 alfalfa cover causes a factor 10 reduction in the overbank velocities (0.003 m/s) compared to a non-vegetated system (0.025 m/s) with an equal inundation level.

5.4 Chilworth flume

The Chilworth experiments aimed at determining the hydraulic resistance of a natural vegetation composition in a controlled environment. This was done for a range of flow conditions and flume compositions. In this chapter the composition of the natural vegetation in the flume is presented for different flume run environments. This is followed by the Richardson and Carling (2006) method velocities in the flume and the hydraulic resistance of the vegetation cover. The flow was sub-critical (Fr<1) and turbulent (Re>500) in all runs.

5.4.1 Vegetation composition and density

The vegetation in the 52 m long flume consisted of different species. Near the upstream inlet (1-5 m) grass was present along the flume bed. In the next section (5-7 m) large birch trees were present, with a 15-20 cm diameter. Some small 1-2 year oak saplings populated the margins of the upstream flume channel. At 7 m the cover along the bed changed from grass to a detritus layer consisting of fallen leafs. In this section (7-40 m) brambles dominated the undergrowth section together with small shrubs. Thin stemmed (3-10 cm) diameter birch and beach trees formed the top of the vegetation.

Downstream of r_4 (chapter 4.2.4) a large ash tree and a willow like species dominated the vegetation composition. The undergrowth consisted of hazel nut shrubs. The vegetation in the flume is given for the left side (figure 5.37 A) and right side of the flume (figure 5.37 B). In addition detailed images of the vegetation composition along the bed of the flume are given in the figures 5.37 C and D. Later runs were conducted with the litter layer removed and the trees cut down (figure 5.39).

An estimate of the undisturbed vegetation density at chest height was made by using a Matlab script based threshold on RGB images (figure 5.38). It should be noted that the stem size of the trees increased towards the bed and smaller shrubs and detritus were also present. This means the vegetation density at the submerged section of the flume was larger than the presented chest height values.

*Figure 5.37. **A** The undisturbed flume from the left and **B** right side of the flume. Two detail photographs of the composition along the bed, whilst running the flume (**C, D**). The arrows indicate the detail image location.*

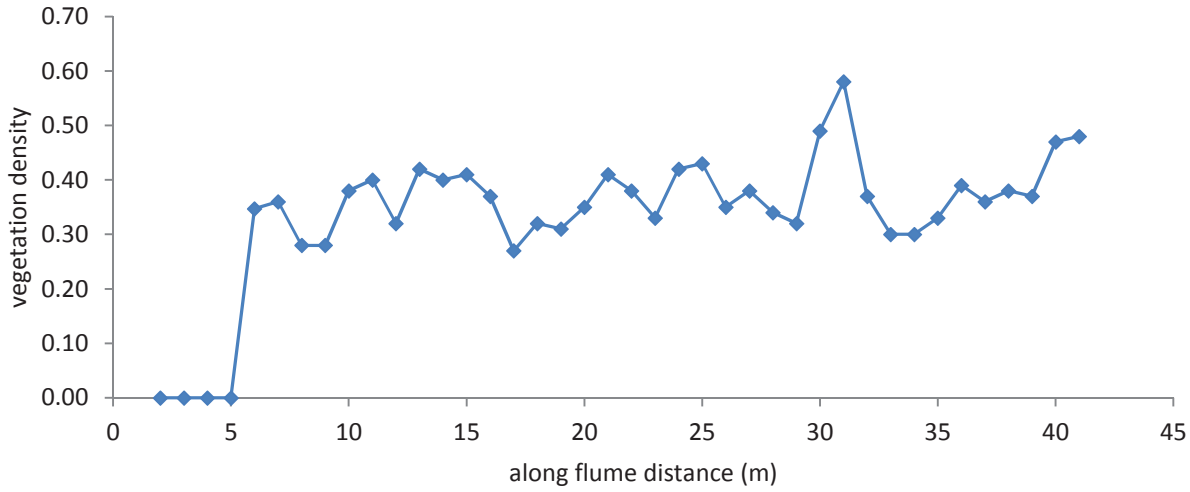

Figure 5.38. The vegetation density fraction at chest height in the flume when moving from the upstream inlet to the downstream weir on the right side of the flume.

Figure 5.39. The flume with the litter layer and bulk of the trees removed leaving the thickest trunks intact.

5.4.2 Cross-sections, water levels and slopes

An overview of the conducted runs and corresponding conditions, as well as the measured parameters is given in table 5.4. The presented data was obtained after the system was left to attain an equilibrium in the water level slope. Therefore steady flow conditions are assumed to be present in the flume.

Run (T)	Vegetation composition	Upstream weir opening (turns)	Downstream weir state	Wetted cross-section (m^2)	Slope (m/m)	Hydraulic radius	U_{av} (m/s)
1	Trees + litter	3	Down	0.45	0.0023	0.13	0.023
2	Trees + litter	4	Down	0.45	0.00165	0.13	0.023
3	Trees + litter	8	Up	0.75	0.002	0.20	0.442
4	Trees + litter	24	Up	0.94	0.0025	0.25	0.070
5	Trees + litter	24	Up	0.93	0.0023	0.21	0.070
6	trees + litter	12	Up	0.82	0.0021	0.20	0.064
7	Trees + litter	8	Up	0.74	0.0019	0.18	0.049
8	Trees	3	Down	0.34	0.00018	0.10	0.040
9	Trees	3	Up	0.57	0.000287	0.16	0.026
10	Trees	4	Up	0.59	0.00034	0.16	0.032
11	Trees	8	Up	0.76	0.000179	0.20	0.025
12	Trees	24	Up	0.97	0.00039	0.24	0.100
13	Empty	8	Up	0.74	0.000072	0.20	0.025
14	Empty	24	Up	0.91	-0.00009	0.22	0.125
15	Empty	4	Up	0.61	-0.00016	0.17	0.036
16	Empty	3	Up	0.58	0.000341	0.16	0.042

Table 5.5. Overview of the conducted runs and measured parameters in the Chilworth flume.

The water level slopes (table 5.4) were based on the upstream flume water level measurement locations (r_2 and r_3). The slope reduced for increasingly higher flow stages in a single flume vegetation composition. A reduction, factor 10, in the surface slope was present after removing the trees and again after cutting out the stumps. The run 14 and 15 water level slopes were negative in the system. The below presented computations are based on the most upstream (r_2) cross-sectional profile hydraulic radius values. An overview of the different water levels in relation to the flume cross-section, for the runs is given in figure 5.40.

The water level in the system increased as a result of opening the upstream gate. In the different flume compositions, with an equal upstream boundary condition, the water levels were similar. The highest levels were found for the completely opened upstream weir (24 rotations). The intermediate weir opening runs (8 and 12 rotations) and low flow scenarios (3 and 4 rotations) resulted in lower inundation levels of the flume. The outlier, in the below presented figure 5.40, is T8. The wetted perimeter at the cross-section is plotted against the tracer front arrival time velocity based flume discharge (figure 5.41).

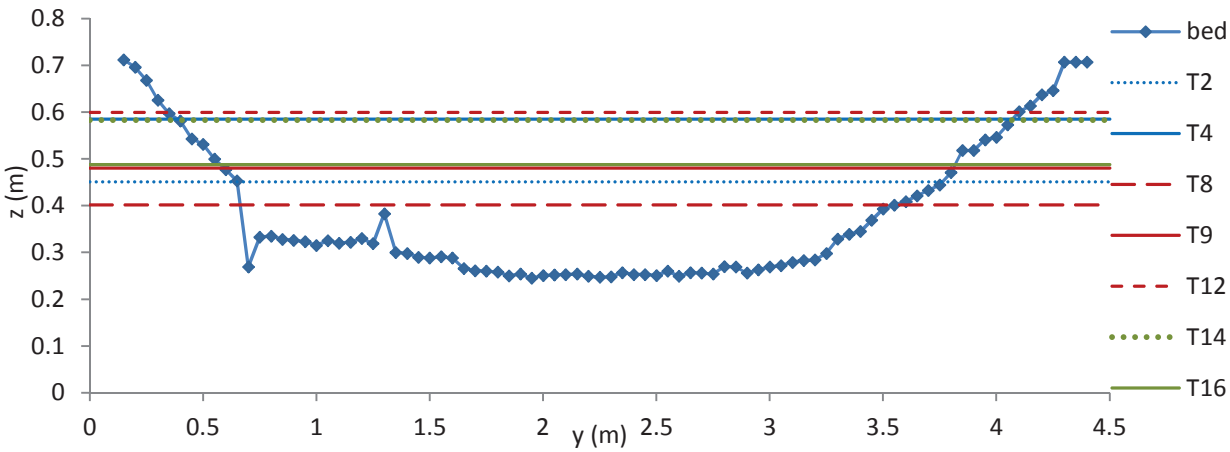

Figures 5.40. The water level mark in the flume for the different run conditions listed in table 9.4.The zero height reference level is the r_1 ruler placed at the concrete inlet bed.

The three different flume composition scenarios vary over a range of *R* versus *Q* values (figure 5.41). The high flow runs (index max in figure 5.41) group together around R=0.23, with a similar discharge of 0.12 m^3/s. The intermediate tree and litter runs have a similar *R* value (0.2), but varied over a wider range of discharge values (0.045-0.11 m^3/s). The other compositions (tress only and empty) display a variation in the hydraulic radius for a similar (0.02 m^3/s) discharge. The discharge values of these compositions were lower than the tree and litter flume discharge. The lowest flow runs, those with a lowered tailgate (index down in figure 5.41), have the lowest hydraulic radius and similar discharge values. The raised tailgate low flow conditions (index up figure 5.41) differ in discharge.

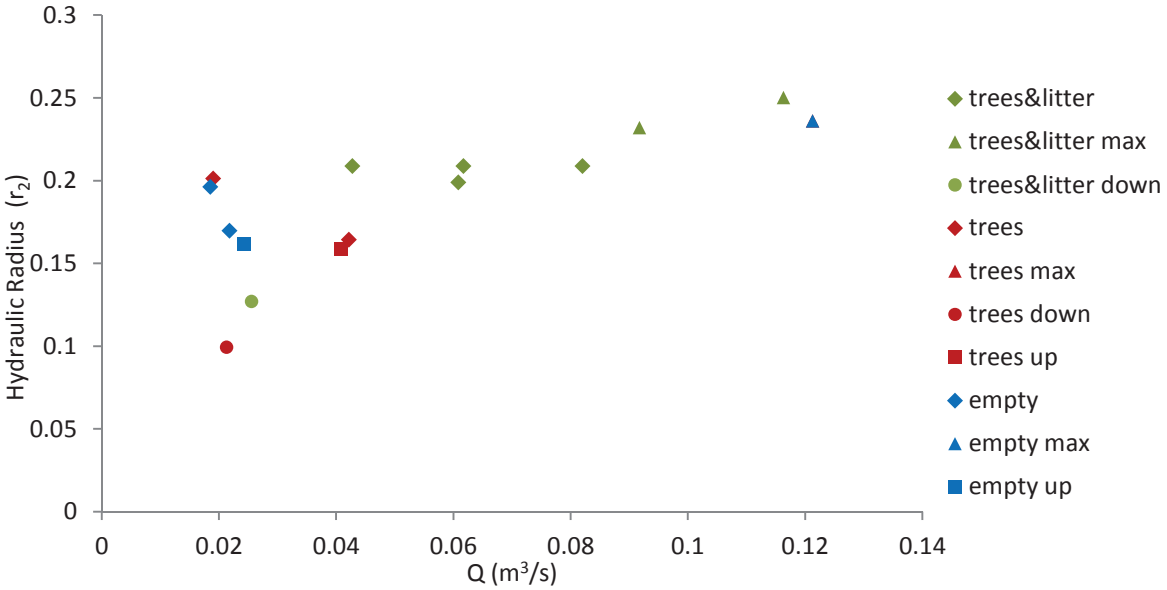

Figure 5.41. Hydraulic radius (at r_2) plotted against the cross-section and velocity based discharge. Triangles are the high flow conditions, circles the lowered low flow tailgate runs and squares raised tailgate low flow runs. The diamonds are the intermediate conditions.

5.4.3 Flow, tracer dispersion and velocities

The tracer front dataset is more elaborate than the peak set. Therefore the tracer front values are presented in this report. The difference in arrival times between the peak and the front is illustrated in figure 5.42. The tracer arrival times indicate a higher tracer front velocity than the peak value arrival time velocity for all flow and composition scenarios. The tree and litter velocities of the tracer peak are similar (0.07 m/s) and varied stronger for the front (0.08-0.12 m/s). The tree only flume high stage flow is comparable to the tree and litter value, but the intermediate tracer front values are reduced. In addition the peak velocity values in the system are lower.

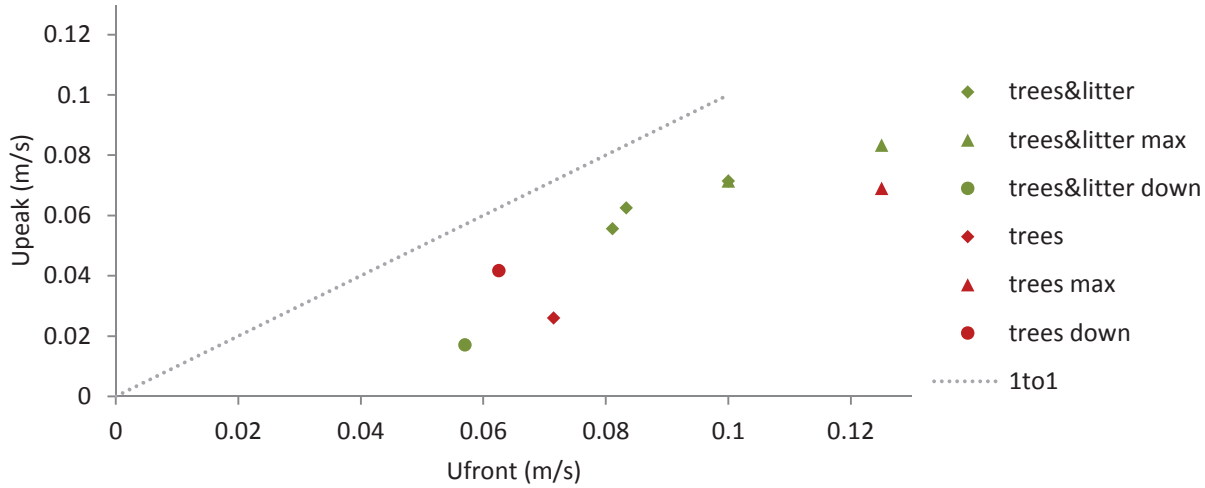

Figure 5.42. The peak tracer velocity plotted against the tracer front velocity for the intact flume and the trees only scenario. The triangle indicate the highest flow stage and the circles a downstream lowered weir.

Observations of the tracer dispersal in the tree and litter composition indicate that the tracer front itself marked a clear line in the flume perpendicular to the downstream direction. No preferential flow paths could be observed around more dense vegetated patches of the flume. However in the tree only flume there were clear preferential flow paths around tree stump areas. This resulted in a long and short front tracer front arrival time at the measurement location. The difference between the two was in the range of 2 minutes. The difference in arrival time could not be observed for the peak values. In the below presented results the slower arrival time was used for the tracer front velocities.

Other visual observations in the flume learned that the litter layer stayed intact when wetting the flume and running it over the entire flow stage range of the tree and litter runs. Furthermore the amount of leaf displacement during the runs itself, for both low and higher stage flow conditions, can be neglected. The effect of the leaves on the flow was present by the eddy shedding from the leaf tips. The same eddy shedding was observed around shrubs stems and tree trunks. The small shrubs and stems did not display bending in the flow direction.

In figure 5.43 the fluorometer analysed sample data trends are given for experiment T2. Both the upstream and downstream measurement location fluorescence curves indicate the arrival of the tracer as a steady rise up to a peak value and a gradual, but longer, decline to a background concentration value. The shape of the first curve is more confined in time than the downstream response. In addition the fluorescence values are larger for the r_2 measurement location.

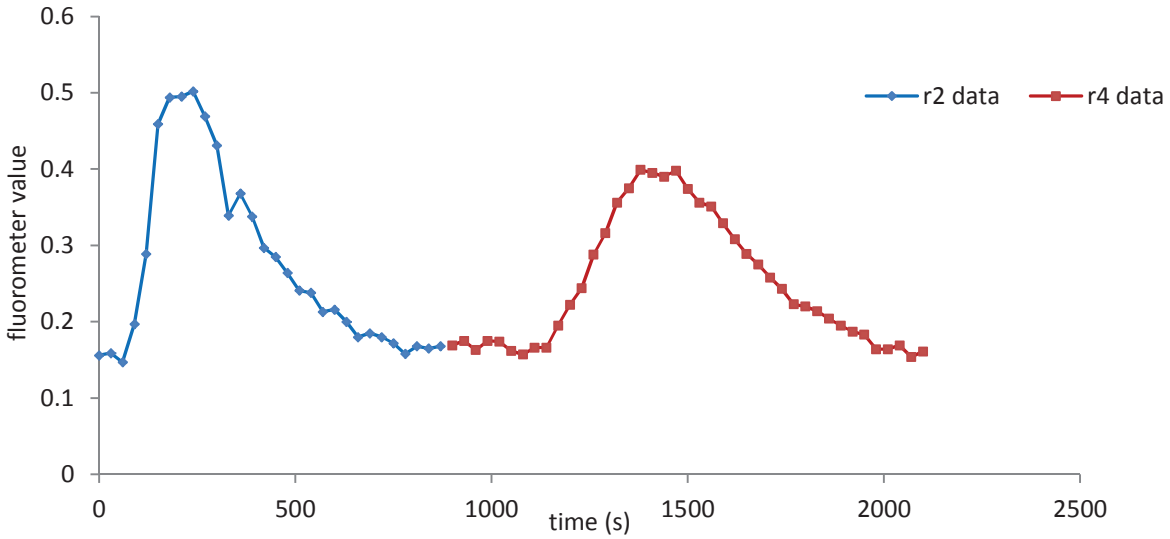

Figure 5.43 Fluorometer data of run T2 for the upstream r_2 (blue) and downstream r_4(red) locations.

The shear stress in the flume (equation 4) was plotted against the Reynolds number (figure 5.44) for the tracer front and peak based velocities in the flume between r_2 and r_4. The tracer front values for the tree and litter flume are found over a smaller Reynolds number range than the tree only scenario. The difference between the peak and front velocity is found in the Reynolds number values within a single flume composition. Furthermore, when comparing the magnitude of the shear stress, it can be seen that it is larger in the intact flume (3-3.5 Pa) than in the removed tree composition(0.5 Pa).

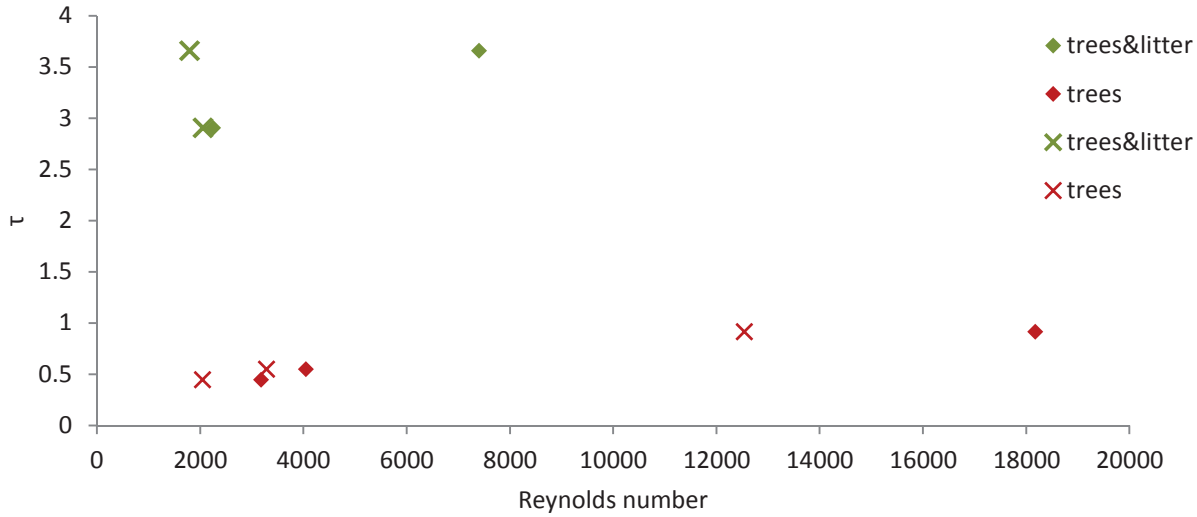

Figure 5.44 Shear stress plotted against the Reynolds number. The diamonds indicate the tracer front and the crosses the peak.

5.4.4 Hydraulic resistance

The roughness of the flume bed was determined for the initial rise or the first arrival time of the tracer between the measurement locations r_2 and r_4. This yields a roughness value without the consideration of ADZ's. Since the dataset of the peak arrival time is more elaborate than that of the peak only, the tracer front roughness based results are given below. This means the roughness of the peak based, lower velocity, roughness is more rough than the below presented results. The empty flume dataset (r_1-r_2) is presented in order to allow a degree of comparison between the three scenarios. The resulting Chézy (equation 5) roughness for the flume is given in figure 5.45 A and the equation 20 based Darcy-Weisbach friction factor values in figure 5.45 B.

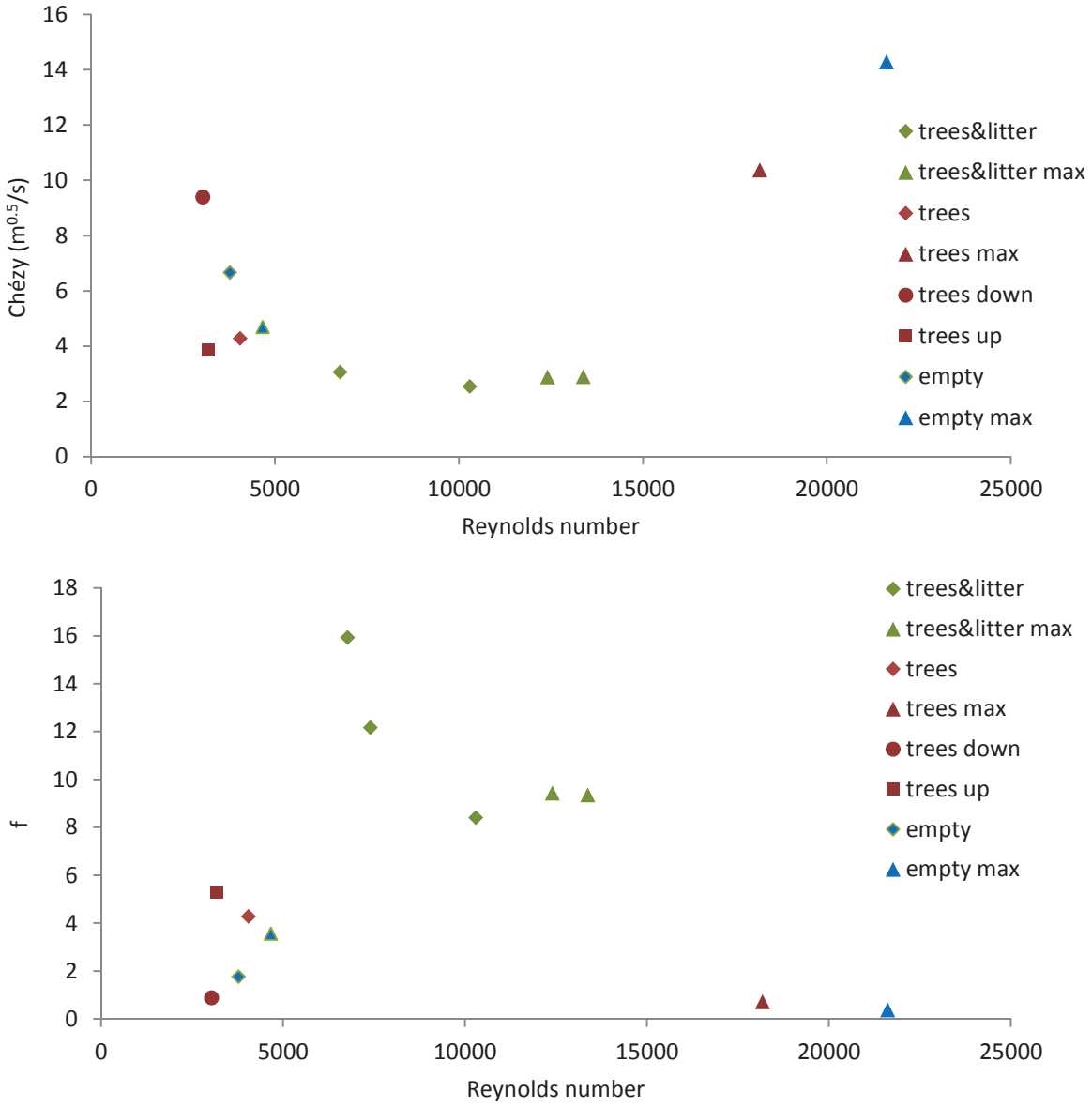

*Figure 5.45.**A** Chézy roughness values based on the tracer front for the Chilworth experiments. **B** Darcy-Weisbach factors. The triangles indicate the high flow stage and the circles the lowered downstream weir runs.*

The trees and litter roughness values (figure 5.45A) for the tracer front do not display a large increase in roughness for higher water level conditions. The average roughness laid around a Chézy of 5 $m^{0.5}/s$. When taking the ADZ into account, not presented here, a more rough value of 3 was found. The most rough condition (1.3 $m^{0.5}/s$) was found for the low flow stage with the lowered

downstream weir (green circles). Without the litter layer the range of roughness values are increased as were the roughness values themselves.

The high flow stage tree only run tracer front value of 10 $m^{0.5}/s$ was found. This indicates a large reduction compared to the tree and litter layer run value of 5 $m^{0.5}/s$. The roughness reduced again after removing the trees to 14.3 $m^{0.5}/s$. Furthermore the overall system turbulence increased for the progressively more empty flume scenarios. In the low flow stage range the changes were different.

The low flow stage, downstream lowered weir runs (circles), gave a similar degree of difference compared to the raised gate runs, with 9 $m^{0.5}/s$ for the tree only and 1.3 $m^{0.5}/s$ for the tree and litter layer. With a raised tailgate (squares) the empty and tree only runs had a roughness value in the range of the intermediate flow condition runs, These lie between 4-6 $m^{0.5}/s$. The empty runs were on the higher value end of the range.

The Darcy-Weisbach friction factors (figure 5.44 B) essentially represent the same trends as the Chézy value plot they are derived from. However, it should be noted that the values for the tree and litter flume were high, within the 8-18 range. The tree only run roughness vales were reduced compared to the tree and litter flume, but were still high. The empty flume values were in the range of 0.90-0.090, with the lowest value for the high flow condition. So, for each progressively more cleared out flume scenario the spread in the roughness increased and the roughness values reduced. The largest roughness reduction was found after the removal of the litter layer. This indicates the importance of the litter layer in the overall system roughness with relatively low inundation ranges and flow velocities.

5.5 Baptist vegetation resistance modelling

The different experimental setups vegetation roughness can also be computed by using the Baptist et al. (2006) vegetation resistance model (chapter 2.2.1). In this chapter the experimental conditions based model predicted Chézy coefficients are given. In case of the scale experiments just the overbank area is considered. The parameters used for modelling the specific environments are listed in table 5.2.

Parameter	Chilworth trees&litter	Chilworth trees	Annular flume 1.5 seed/cm^2	Annular flume 3.0 seed/cm^2	Eurotank 1.5 seed/cm^2
Stem drag	1.5	1.5	Equation (28)	Equation (28)	Equation (28)
Ks (m)	0.1	0.1	D84	D84	D84
Dv	0.5	0.3	0.01	0.021	0.01
Hv (m)	Hv=R	Hv=R	Hv=h	Hv=h	Hv=h
Cb (m$^{0.5}$/s)	Equation (17)	Equation (17)	Equation (17)	Equation (17)	Equation (17)
v (Pa/s)	1.3*10^{-6}	1.3*10^{-6}	1.3*10^{-6}	1.0*10^{-6}	1.0*10^{-6}

Table 5.6. Model input parameters for the specific flume environments.

5.5.1 Chilworth flume

The Baptist et al. (2006) model was calculated for the Chilworth flume intact and trees only condition. The model parameter input is the data in table 5.6. The stem drag was kept constant at 1.5 according the Järvelä (2002) study. The vegetation density for the intact flume is 0.5 and 0.3 for the trees only scenario. The flow in the flume is regarded as non-submerged vegetation flow, this means $h=h_v$.

The model based roughness (figure 5.46) indicates that the model underestimated the roughness in the flume environments. The difference between the model prediction and the measurements was larger for the intact flume runs (factor 5) than the tree only runs. These trends in the model result roughness are opposite to the measured based value trends. An increase in Chézy was found for more turbulent flow in the trees and litter runs, whilst the model predicted a decrease.

With only the trees in the flume the low flow stage prediction differed significantly from the measurement based roughness, however the high flow stage model roughness (12.05 m$^{0.5}$/s) showed good agreement with the measurement based data (10.36 m$^{0.5}$/s). In order to get model results similar to the measured values a k_s of approximately 1.6 is required for the tree and litter runs and the low stage tree only runs.

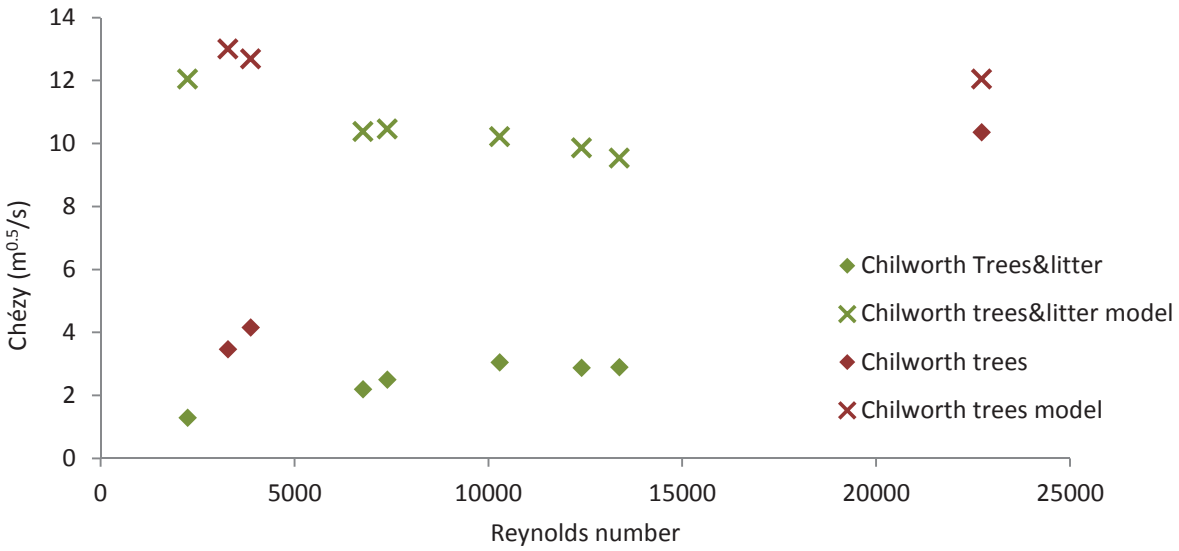

Figure 5.46. The Chilworth experimental measurement based and model base roughness.

5.5.2 Scale experiments

The scale experimental roughness was determined by correcting the W-C law for the laminar flow conditions (equation 17). This means a slope and a viscosity were required. The meandering river experiments *S*=0.01 was used, and for the annular flume *S*=0.0057. Two different inundation levels (1-2 mm) are given for the meandering river experiments due to the uncertainty in the local water depth.

The model performance (table 5.7) resulted in an underestimation of the Reynolds number relation based flow resistance of the scale vegetation. The difference in the results is the largest for the vegetation covered annular flume runs (factor 6-8). The model results indicated a less rough system with Chézy 25-30 $m^{0.5}/s$, whilst the Reynolds number relation indicates a very rough system (Chézy 5-7 $m^{0.5}/s$).

The bare sediment floodplain roughness is the W-C equation with the correction for laminar flow. The results of the Reynolds number relation and the model predictions differ a factor 2 for the annular flume. In the meandering river experiment the difference is similar for both the bare sediment as the vegetation covered system (factor 1.5-2). The difference between the model roughness and for a vegetation covered scenario and a bare sediment environment was very small in all flume runs. The difference in the 1mm 2500 l/h vegetation and bare sediment scenarios was only a very slight reduction in the roughness (0.1 $m^{0.5}/s$). The predicted reduction in roughness is not found in the Reynolds number relation based vegetation and initial stage 1mm conditions. A more detailed analysis of the difference between the model output and measurements is given in chapter 6.3.2.

Scenario	Measurement based roughness ($m^{0.5}/s$)	Model predicted roughness ($m^{0.5}/s$)
Annular 1.5 seed/cm^2 2 mm floodplain water level	3.1	24.4
Annular 1.5 seed/cm^2 4 mm floodplain water level	5.5	29.7
Annular sand 4 mm floodplain water level	15.9	30.0
Euro 2500 l/h vegetated 1 mm floodplain water level	9.1	19.1
Euro 2500 l/h vegetated 2 mm floodplain water level	14.0	24.6
Euro 2500 l/h sediment 1 mm floodplain water level	8.9	19.2
Euro 2500 l/h sediment 2 mm floodplain water level	11.4	24.7

Table 5.7 The scale experimental Reynolds number based roughness and the Baptist et al. (2006) model output.

6. Discussion

In this section the velocity measurement inaccuracies are presented. The main focus of this chapter is to compare the results of the separate flume experiments (chapter 5) and connect them to each other and the literature review in chapter 2. First the velocity measurements are presented. This is followed by the riparian vegetation driven morphologic development in the meandering river and annular flume. The effects of the scale riparian vegetation are in detail presented in terms of engineering effects, abiotic and biotic factors. The resulting riparian vegetation patterns in the meandering river are connected to literature prescribed patterns. Finally the hierarchical control of scaled riparian vegetation and meandering river systems is presented.

6.1 Velocity measurement inaccuracy

The Richardson and Carling (2006) method, with discrete sampling, has an uncertainty in determining the exact moment of the front arrival time and the peak of half a sampling interval. For the experiments conducted in Chilworth this means a 15 seconds uncertainty that translates to a +/-0.01 m/s in- or decrease in the average velocity. This means the uncertainty can be neglected.

The second uncertainty in the Richardson and Carling (2006) method is the velocity with an unmixed front. In the tree and litter runs the front was mixed, however an un-mixed front was present in the empty and tree only runs in the outdoor flume. The two minute difference in the tracer front arrival time results in a +/-0.1 m/s velocity uncertainty. This is a substantial uncertainty compared to the total velocities.

The maximum difference, between to measurements in the scale experiments, was 0.3 seconds, which translates to a +/- 0.1 m/s uncertainty in the channel velocities of the meandering river. This is up to 30% of the measured velocity value. This means that the presented velocities are susceptible to a large uncertainty. The alternative, two image difference, tracer front analysis method does not have the timing uncertainty that the tracer curve based Richardson and Carling (2006) method presents. Therefore the front based velocities are better represented by the second application method. In case of the channel flow velocities in chapter 5.2.4 it means that the more accurate representation of the velocity is found for the two image method.

6.2 Scale experiment flow and morphology

6.2.1 Experimental river morphology

The addition of vegetation to the meandering decreased the bank erosion rate, but allowed a maintained morphologic meander development. The continued development resulted in a more sinuous and sharp bended system. The central channel bend developed into a bend with two sharp curves. In previous experimental river experiments, this was not observed. The addition of a homogeneous vegetation cover resulted in a reduction in the number of active channels and the formation of sinuous systems (Gran and Paola, 2001, Tal and Paola, 2007, Van de Lageweg, 2009). The Braudrick et al. (2009) river, with constant alfalfa addition to the floodplain, produced a sinuous river. Van Breemen (2011) had continued erosion in a meandering river environment, but there the bends did not became sharp.

A similar meandering river development is found in the Van Dijk et al. (2012) meandering river, with the addition of silica flour. The formation of a plug bar (Van Dijk et al., 2012) closely resembled the development of the central river bend in this study. The general meandering river pattern, with double and sharp bends, was not found in this experiments. The double headed bends are found in natural systems, like the river Allier in France (figure 6.1 A and B). A comparison of the river Allier and scale river pointbar morphology indicates a difference in the morphology of two systems. The experimental river oblique oriented scrolls past the bend apex are different from the bend parallel scrolls in the river Allier. This suggests a different interaction between flow and morphology in both systems.

The sharp experimental river bends are found in other natural meandering river systems (Ferguson et al., 2003, Nanson, 2010). However natural sharp river bends suffer from a lack of research into the

flow mechanics and subsequent morphodynamics (Blanckaert, 2010, Nanson, 2010). A corresponding river bend morphologic development is only found in other scale experiments. In a sharp bend scale experimental flume study by Blanckaert (2010) the bed remained mobile whilst the inner and outer bend were fixed (r/w=1.3). The resulting bed topography displayed a bar pool pattern with a transverse bed slope. The depth in the bend pool was 3 times higher in the rest of the system. On the downstream end of the bend the system became shallow again. This is similar to the experimental bed topography of the vegetation state river (at 56 hours figure 5.8 D). The experimental river had a deep outer bend pool upstream of the inner bend bar. The inner bend bar itself was present downstream of the bend apex and the rest of the system was more shallow. The similarity in the morphology indicates a potential for comparable bend flow mechanics in both scale experiments.

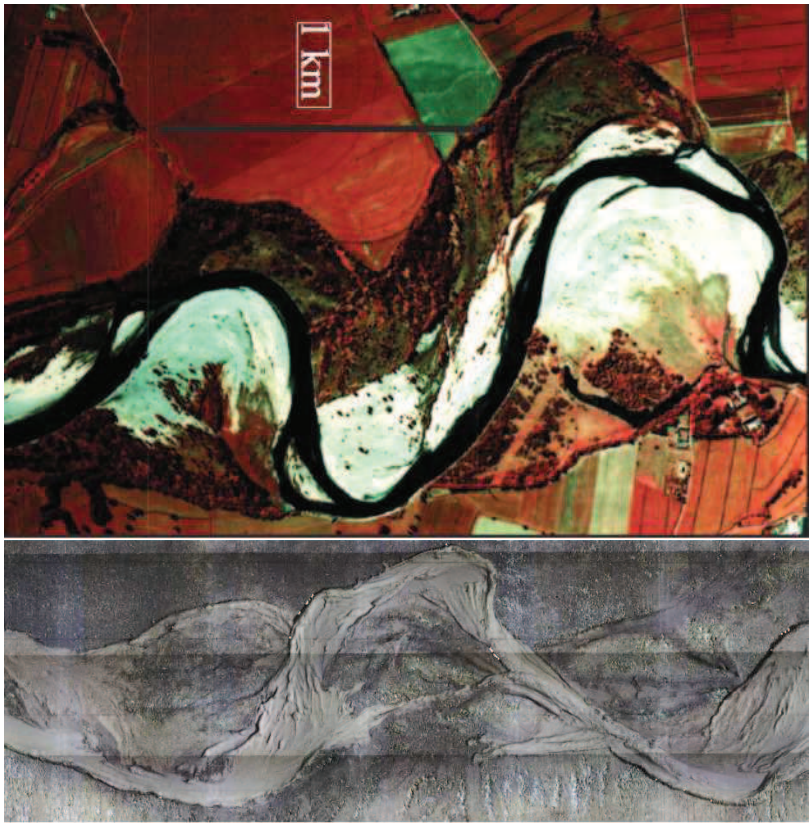

Figure 6.1. ***A*** *The river Allier in France with a double bended bend (Kleinhans and Van den Berg, 2010), the image is mirrored.* ***B*** *The experimental meandering river at 70 hours. Flow is from left to right in both images.*

6.2.2 Annular flume morphology

In the annular flume the bed morphological development differed between the bare sediment and vegetation cover systems. The difference is due to the effect of added bank strength by vegetation. The added vegetation reduced the lateral erosion and thus the width of the system. The reduced width led to more pronounced bed development. This is similar to earlier experimental pattern research (Gran and Paolo, 2001, Tal and Paola, 2007) and given by bar theory. The change in bank strength, leading to less wide systems and alternate bar formation (Struiksma et al., 1985).

In addition there was a difference in the bed development between the used vegetation densities. The low density cover high paddle forcing allowed the formation an inner bend bar and outer bend scour, similar to the Teske (2011) steep clay outer bank channel bed morphology. This development was absent in the high density vegetation runs (chapter 5.3.2). The difference between the morphologic development of the high and low density vegetation runs could be due to the slope of the outer bends and the roughness of the outer bend. Blanckaert et al. (2010) found that the secondary flow strength reduces for less steep and more rough outer bends. The potential reduction in the secondary flow strength could explain the difference in morphologic bed development for the

different density high forcing runs. The second difference between the high and low density runs is the absence of outer bank erosion with a 3 seed/cm^2 vegetation cover.
In natural system riparian vegetation is able to produce a sheltering effect along the outer bend margin (Millar, 2000), this was most likely present in the annular flume run. The overhanging alfalfa sheltered the outer bend and prevented erosion. So the potential effect of outer bank roughness is apparent in the annular flume, for with a more rough outer bend there was no erosion of the outer bend and little bed morphologic change.
When regarding the morphologic development of both the meandering river and the light density annular flume the effect of riparian vegetation on the morphology can be identified. The main driver of these morphologic developments was the reduced outer bank erosion, due to the added bank strength by vegetation. The incorporation of vegetation led to the following changes in the overall river morphology:

-Sharp and asymmetric bends
-More sinuous system

Other morphologic changes that were also present in the annular flume were:

-Steeper outer banks
-Deeper outer bank pool's

6.2.3 Channel bend flow

The similarities between the morphology of the vegetation stage experimental river and the Ferguson (2003), Blanckaert (2010) and Nanson (2010) morphology suggest the presence of a flow separation zone along the outer bank of the sharp bends. The presence of a separation zone in natural systems is indicated by w/h<10 (Nanson, 2010). In the river experiment the w/h ratios were only below 10 for the vegetation stage system. The presence of this zone is confirmed by the lingering of tracer along the sharp outer bends.
The Annular flume w/h ratio is in the same range as the sharp meandering experimental river bends (w/h<10), but did not display flow separation. The absence of flow separation is indicated by the morphologic changes in the vegetated flume bed. The formation of the central ridge by the secondary current, created a zone along the outer bend bed with just a downstream flow direction. In the high paddle velocity low density run the secondary flow was strong enough to move this ridge towards the inner bend and form a transverse bed slope in the flume.
So the separation zone, found by Ferguson et al. (2003) and Nanson (2010) in natural systems with w/h<10 and in the scale setups by Blanckaert (2010) is found in the vegetation state experimental river. However the annular flume, although in the same w/h range, did not display effects of flow separation zones in the channel morphology.

6.2.4 Transverse bed slope

The changes in the bend sharpness, of the scale experimental setups, manifest themselves in the secondary current and thus the morphology of the transverse bed slope. According to equation (1) (Talmon et al., 1995) the transverse bed slope increases for a larger depth, as well as a decrease in the r/w ratio. The model predicted increase in slope for a reduced r/w ratios is given in figure 6.2 for the meandering river environment. The prediction is also give for the initial annular flume parameters. Furthermore, apart from the depth and r/w ratio, the steepness of the outer bend is able to increase the secondary current strength (Blanckaert et al., 2010). In the experimental setups the bends became both sharper and deeper. So, as a result, a larger transverse bed slope gradient was found in the vegetation stage experimental river compared to the control and initial stage systems (figure 6.2). The annular flume slope for the vegetation cover run lies within the meandering river vegetation stage. On the high end of the transverse bed slope are two vegetation stage data points as well as the Teske (2011) slopes.

The relative timing of the changes in river bend parameters and the corresponding change in the transverse bed slope was also found in the annular flume light density high forcing run. In both flume experimental systems the order of bend changes and transverse bed slope response is as follows:

(1) Bank strength increases after vegetation dispersal
(2) Reduced erosion over time
(3) The outer bend becomes more steep, sharp and deepens (low discharge vegetation river and annular flume)
(4) Secondary current increases in strength
(5) After increasing the discharge (meandering river) and velocity (annular flume) the channel bend deepens.
(6) Secondary current increases in strength
(7) The formation of steepest transverse bed slopes occurs.

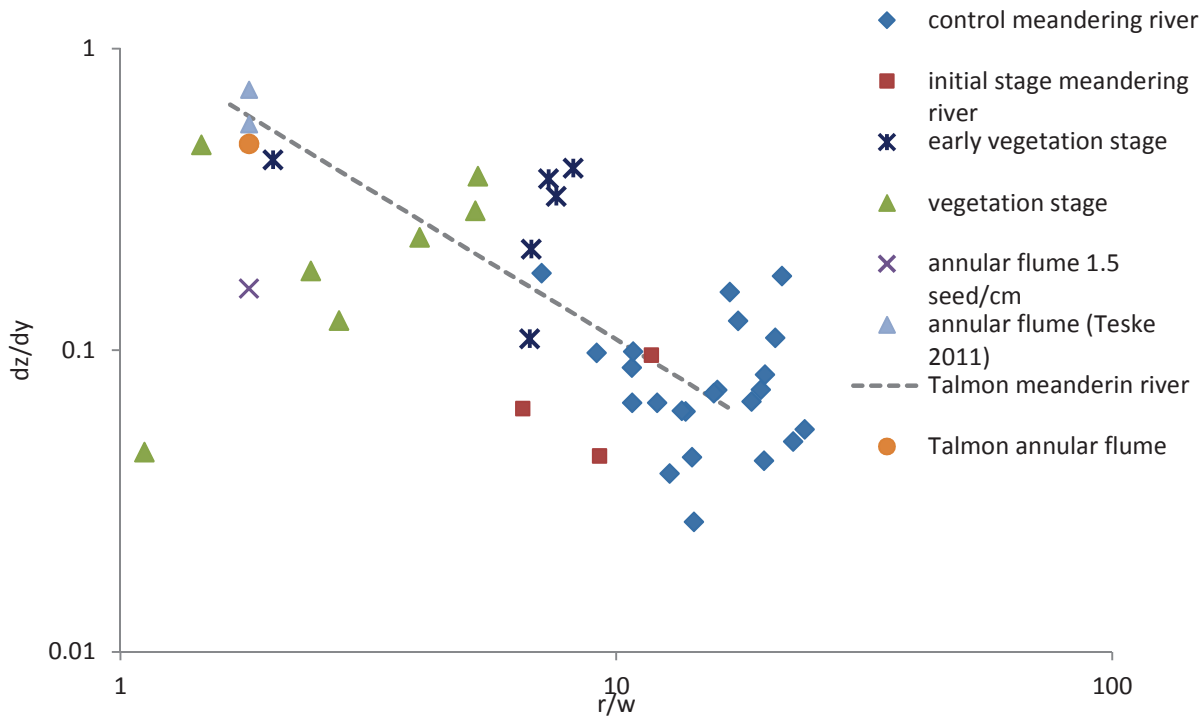

Figure 6.2. The transverse bed slopes in the scale experiments together with the Talmon et al. (1995) prediction for the annular flume and meandering river experiments. In addition the Teske (2011) slopes are given for the fixed bank annular flume.

6.2.5 Overbank flow and discharge division

The overbank flow patterns and discharge division in the meandering river experiment can be compared to the literature (chapter 2). The overbank flow in the system was generated by inertia moving a faction of the channel flow onto the floodplain in the downstream section of a bend. Once on the floodplain, it travelled in the downstream direction. This is similar to the results of Shiono et al. (1998).

Since noise in the water level measurements prevented a quantitative discharge distribution in the system, only a qualitative flow division description was given. It was found that after the implementation of a vegetation cover a smaller area of the flume was inundated (figure 5.14). Furthermore the tracer on the floodplain was more confined in local depressions. Since the velocity was approximately equal on the floodplain and the cross-sectional area was smaller continuity dictates that the discharge was reduced. These changes indicate that a larger fraction of the discharge was transported through the channel instead of over the overbank area. This is similar to the discharge division found by Knight and Brown, (2001).

The reduction in the wetted area and deepening of the channel bed were also found by Tal and Paola (2007). The shift in the discharge division in the Tal and Paola (2007) experiments was partly contributed to an increase in overbank roughness. However, the experiments conducted for this thesis indicate an absence of a significant quantitative reduction in the flow velocities on the floodplain in the meandering river experiments (chapter 5.2.4). This means the deceleration on a vegetated fixed bed floodplain, as observed by Jahra et al. (2012) was not found in the meandering river.

The absence of a reduction in the overbank flow velocity measurements could be linked to the timing of the vegetation induced morphologic change, for it are the morphological changes that accommodate a larger fraction of the discharge in the channel. Since the changes in the channel depth and outer bank steepness occurred in both the experimental river and low density annular flume run within less than one hour. The discharge division shift would have occurred before the measurements were made. The second contribution to the discharge shift was due to a vegetation induced hydraulic resistance. This effect was observed in the low discharge vegetation stage development. There was a clear reduction in the overbank flow velocity on the upstream left floodplain area. Not only was the discharge division shift towards the channel observed right after the implementation of vegetation, after 30 hours, it was again observed with an increase of the constant discharge to 2250 l/h at 45 hours. On the overbank there was only a minor increase in the wetted area, from 0.11 to 0.27, whilst the channel and overbank flow velocity remained equal.

Finally it was found that there was an increase in the channel velocity between the constant discharge and the brief flood. There was no difference between the initial and vegetation state velocities for the two image based values. This means the Straatsma and Baptist (2007) increase in channel flow velocities for more rough floodplains was not found in the scale meandering river.

To summarize, the division of discharge in a vegetated meandering environment is characterised by larger fraction of the discharge in the channel and a reduced overbank contribution compared to the non-vegetated environment. The main drivers of the discharge shift are the morphologic river response as a result of added bank strength and an increased hydraulic resistance.

6.3 Engineering effect scaling

The scaling of the experiments focussed on the representation of a riparian vegetation cover. So the scaling of alfalfa to real riparian vegetation is evaluated in terms of the representation of real vegetation engineering effects, abiotic and biotic parameters. The different experimental results are compared to each other and the literature in each sub-section.

6.3.1 Bank strength and failure

Annular flume and block erosion experiments

The outer bank retreat in the annular flume can be compared to the block erosion experiments (Van de Lageweg, 2009, Van Breemen, 2011). In these experiments, also known as Friedkin experiments, of Van Breemen (2011) erosion of the high density vegetated block occurred whereas in the annular flume no erosion took place. This is because the 1.5 seed/cm^2 annular flume density is the same as the Van Breemen (2011) high density (chapter 4.2.1). In the Friedkin experiments the reduction of the block volume is a gradual process. This translates to steady erosion rates during the experiment. However in the annular flow the retreat of the outer bank was not gradual. A stepped retreat was present in both the light vegetation and no-vegetation runs.

Another differences was the absence of preferential erosion of less dense vegetated patches in the annular flume. This difference could be related to the higher flow velocities in the Friedkin experiments. Higher velocities could have been able to locally erode and transport larger sections of the blocks. Alternatively the angled flow in the Friedkin experiments could be responsible for a focussed local erosion. In the annular flume the outer bank was more gradually eroded by a uniform secondary current and constant downstream flow components, thereby creating an even and more slow retreat of the bank. A final prominent difference between both experimental setups is the annular flume paddle forcing. As the channel widened the distance from the paddle edge reduced and thus the strength of the flow along the channel margin, thereby creating the maximum retreat boundary.

Annular flume and meandering river

The Annular flume determined vegetation density and the morphological development of the meandering river, with this vegetation density, indicates the flume translates well to the meandering river experiment. Furthermore it confirms the suggestion of Van de Lageweg et al. (2010) to use a light density vegetation cover in order to maintain morphologic development. The scaling of the annular flume and Eurotank experiments, by added vegetation induced bank strength, becomes apparent when plotting the erosion rates of the annular flume experiments in the Eurotank plot (figure 6.3).

The annular flume data is found on the low end of the r/w scale. The non-vegetated erosion in the annular flume rate lies on the top end scale of the meandering river experiments. These high w/hr values are found for the initial hours of the river development and indicate the establishment of the meandering river. The annular flume is set at an initial state that is also rapidly moving towards an equilibrium. The second difference is that once the annular flume has reached this equilibrium no more morphological development takes place, whereas the meandering river continues to renew itself by cutting of bends. The vegetation covered annular flume data plots within the range found in the Eurotank, although slightly on the lower end of the horizontal scale due to the small r/w ratio of the flume.

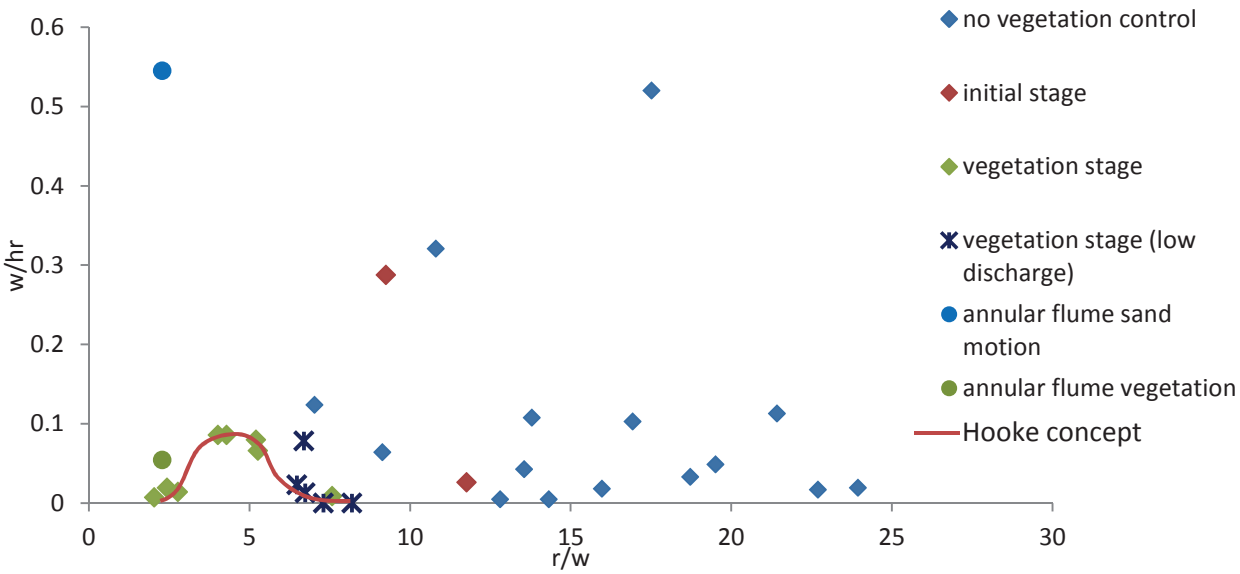

Figure 6.3. The bank erosion expressed in width per hour plotted against the radius width ration for the different flume setups.

The conceptual Hooke (1984) rate of movement curve for bedrock meanders is indicated in figure 2.3. A comparison between the conceptual curve and the control experimental erosion rates indicates that the observed bend development does not fit the conceptual curve. The measurement data varies over a wide range of r/w. The vegetated stage bend development is different. In case the low discharge stage and higher discharge (vegetation stage) data are connected a relatively smooth curve is present (figure 6.3 orange line). The blue stars are found in the low discharge vegetated stage bend development. These data points depict the initial asymmetric bend development (initiation stage Hooke, 1984). The green diamonds in the plot are the higher discharge data point. These point are found in the period of maximum bend development (growth period Hooke, 1984). The smaller r/w ratio points indicate the final stage of the bend development that was characterised by the formation of a plug bar (termination stage Hooke, 1984).
In general it can be stated that in the flume experiments, conducted for this research, a clear reduction or even elimination of the erosion of the outer bank was found as a result of the addition of a vegetation cover to the respective flume floodplains. Furthermore the annular flume proved a viable option to determine the appropriate vegetation cover density.

Bank failure

The mechanisms of bank failure for the scale experiments without vegetation were entrainment and mass wasting. After the introduction of vegetation the failure mechanisms started to differ. In the Annular flume entrainment and mass wasting remained dominant. Over time some preferential erosion did occur along the stems of the alfalfa. The dense annular flume vegetation cover provided enough roughness along the bank to prevent entrainment, as described by Abernethy and Rutherford (1998) for natural rivers. In the meandering river undercutting of the outer bank started to play a role as opposed to the previously found saturation of bank sediment (Van Breemen, 2011). The absence of undercutting in the annular flume was due to the limit at which the paddles provide sufficient flow to erode the outer bank. Furthermore there was a limited space available to undercut the outer bend due to the metal base. This means that instead of continued erosion an equilibrium profile forms.
The undercutting of the bank was the key bank failure mechanism in the vegetation stage meandering river. It resulted in smaller clumps of vegetation and soil aggregates entering the system. These eroded clumps have been shown to be immobile in natural rivers for low flow conditions and offer a degree of protection along the toe of the bank (Micheli and Kirchner, 2002). In the scale

experiment the eroded floodplain material did not provide substantial protection of the bank toe, for it was almost instantaneously broken up and moved in the downstream direction.
The undercutting, in the meandering river experiment, occasionally caused an instantaneous failure of a larger fraction of the outer bank. This is similar to the results of Micheli and Krichner (2001) for grassy meadows. The change from entrainment to undercutting suggests that the dominant contribution of the scale vegetation is the root tensile strength (Micheli and Kirchner, 2002).
The root reinforcement of alfalfa has been recognised qualitatively as the dominant factor in scale experiments (Gran and Paola, 2001, Braudrick et al., 2009). Root reinforcement was indeed found to be a quantitative factor in shear stress measurements (Van de Lageweg, 2009, Van Breemen, 2011). However in the experimental meandering river the alfalfa growth was affected by the local flume environment, in terms of lighting and inundation (chapter 5.2.5). The roots were therefore not likely to reach down more than 4-6 mm as opposed to >10 mm in the annular flume and Van Breemen (2011) experiments. Furthermore vegetation disappeared rapidly from the system leaving only a reddish soil like (less than 2 mm thick) upper layer substance.
This might suggest an absent added bank strength in those locations of the Eurotank, but this was not found. For the changes in the river (chapter 5.2.1), in the vegetation covered areas and red soil only areas, were identical. So instead of root reinforcement a biological binding of the sediment could prove sufficient to increase bank strength in scale experiment. Whether or not the vegetation and soil effect are equal in their respective reinforcement of the bank should be further investigated.

6.3.2 Hydraulic resistance

First of all it should be noted that the high end of the Darcy-Weisbach friction factor scale translates to smaller changes in the low end Chézy friction factor values. This affects the ranges of the different friction factor expressions in this report. In this section the Chilworth results are compared to other full scale experiments in order to determine the validity of the experiments as a control to the scale environments. This is followed by the scaling of the Chilworth and scale experiments. Finally the Baptist et al. (2006) modelling of the different flumes is evaluated.

Chilworth with literature

The roughness values found in the full scale flume experiment can be compared to other flume studies. A qualitative comparison between the results indicates that, similar to the study by Järvelä, where a sub-layer of grasses proved to significantly increase the overall roughness, the main contribution to the roughness in the flume can be indexed as: (1) the litter layer and undergrowth (2) the stems. Unlike the results of Armanini et al. (2005) no bending of vegetation was found for higher flow conditions in the flume. This could explain why the roughness in the flume with trees and litter was relatively constant with Chézy around 2.8 $m^{0.5}/s$. A qualitative comparison of friction factors can be made as well.
The Chilworth flume roughness, with trees and litter layer, of f=8-16 lies above the Järvelä (2002) flume study values of f=8, for leafy willow branches. The trees only roughness f=1-5 lies above the leafless willow branch roughness f=0.8. So the respective decrease in the overall roughness is similar in the Chilworth and Järvelä (2002) experiments, but the Chilworth facility roughness is a factor 2-5 larger. The reason for the decreased roughness in the Chilworth flume lies in the site specific roughness contributions. The main contributor to the roughness in the Chilworth flume is the litter layer that consisted of fallen leaves and the small shrubs along the base of the flume.
The resulting tree and litter layer Chézy value of 2.8 $m^{0.5}/s$, for the arrival of the tracer front, can be compared to model study values of larger river systems. In the model study of Staatsma and Baptist (2008) a 3-10 $m^{0.5}/s$ Chézy range was applied to the most dense sections of the floodplain. The Chilworth experiments thereby illustrate that a the measured natural vegetation cover resistance is on the low end of the presented model study range. In addition it should be noted that the with the incorporation of the ADZ in the velocity, the roughness in the flume for an intact vegetation cover is

further reduced. This means a lower Chézy value could be found for dense vegetated areas and indicates the need for more natural system roughness measurements.

Roughness in scale experiments

Laminar flow resistance has been studied extensively for pipe flow. However the open channel flow equivalent has received less attention in geomorphologic and engineering fields (Yen, 2002). The methods presented in this report are a Reynolds number scaling, similar to pipe flow and an expression of the roughness as a function of the water depth and grain size (Ferguson, 2007). Although both methods present values in a similar range, for the non-vegetated annular flume (chapter 5.3.1), no decisive conclusion can be made on the reliability of both method values. In addition the Ferguson (2007) method is based on a calibration factor alpha (1-4) that further increased the uncertainty. Therefore the Reynolds number scaling, as a function of both water depth and velocity, it is deemed the most suitable method of determining the roughness in the scale experiments.

The Annular flume and scale meandering experiment results indicate that the roughness for flow in an equal vegetation cover density environment is almost a factor two larger in the meandering river, 7-12 $m^{0.5}/s$ compared to 1.5-8 $m^{0.5}/s$. The bare sediment floodplain displays the opposite trend with a factor two larger Chézy value in the annular flume, whilst the meandering river roughness did not vary significantly. The controlled annular flume environment displayed a clear velocity reduction as a result of a vegetation introduction.

In addition it should be noted that the Annular flume vegetation velocity was depended on the vegetation age, whereas this factor was absent in the meandering river experiment. So with these effects present (annular flume age and Eurotank water level) the quantitative term comparison should be regarded with these uncertainties in mind.

Chilworth and scale experiments

The Chilworth Chézy roughness values, for the intact flume, indicate a more confined range of roughness values and a more rough environment than the meandering river scale experiment. The lowest values of the annular flume setup are within the Chilworth value range. The tree only range (table 6.1) spans approximately the same roughness value range as the meandering river with a vegetation cover on the floodplain. Although these values illustrate a degree of similarity between the different flumes, large uncertainties in the roughness value computation of the scale experiments indicate a direct comparison should regarded with caution.

Experiment	Chilworth (trees and litter)	Chilworth (Trees)	Eutotank (vegetation stage)	Annular flume (1.5s eed/cm^2)	Järvela (2002)
Chézy ($m^{0.5}/s$)	2.2-2.9	4-10	7-12	1.5-8	3.13
Darcy-Weisbach (f)	8-16	0.9-4.3	0.5-1.6	1.2-32	8

Table 6.1 Roughness values in the experiments and the Järvelä (2002) values.

So the Chilworth and Järvelä (2002) experiments scale relatively well in terms of Chézy values and indicate the similar contributors to the flume roughness. The Yen (2002) methods of laminar flow roughness in the annular flume produced roughness values in the same range of Chézy values as the intact Chilworth flume. This indicates an approximate scaling of a 1.5 seed/cm^2 alfalfa scale vegetation cover in a controlled flow environment. However, when incorporating this scale cover in an experimental meandering river no reduction in velocity and thus roughness was detected. Based on visual observations and changes in the inundation level in the meandering river and the annular flume experimental measurements it can be stated that a feedback exists between riparian vegetation and the hydraulic regime. This feedback manifested itself as a reduced overall overbank

flow in the vegetated overbank areas that led to a larger fraction of the discharge being transported through the systems main channel.

Baptist model performance

The values of the Baptist et al. (2006) model for the Chilworth experiments were above the actual measured values in all conditions (figure 6.4). The difference should be even larger in case the ADZ based velocities were to be used. The difference between model output and measured values was less for the trees only scenario. The high flow stage showed a good agreement with the model output. This illustrates the models applicability to the cylindrical representation of vegetation it was designed for (Baptist et al., 2006).

The model prediction for the scale experiments differed significantly (table 5.7), although the presented Baptist et al. (2006) model results were based on the laminar flow corrected White-Colebrook equation (equation 17) and variable stem drag expression (equation 28). The model remained essentially insensitive to the velocity of the flow. This leaves the water height was the only scenario depended parameter variable in the model. The standard Baptist el al. (2006) model bed roughness computation, White-Colebrook (equation 17), does not represent shallow gravel bed flow well. The relatively high output of the W-C law is indicative for the final output of the Baptist et al. (2006) model. A better estimation of the roughness is found in the Ferguson (2007) expression (equation 18). Therefore the Ferguson (2007) roughness prediction was used instead of the conventional laminar flow corrected W-C law. These model results, with the Ferguson (2007) expression and the conventional W-C formulation, are presented over a range of vegetation densities for the light density 4 mm floodplain level inundation (0.003 m/s overbank velocity) annular flume (figure 6.4).

The model (figure 6.4) does present a reduction in the Chézy value for increased vegetation densities (figure 6.4). From densities of 0.1 onward there is a substantial decrease in the Chézy value. However the reduction due to the vegetation in the roughness in the scale experiment is very slight. This is because only a very small fraction of the flume was covered by stems 1%. So the validity of the Baptist et al. (2006) model for laminar flow conditions is yet to be determined, but this analysis is limited by a basic way of accurately representing the roughness value in a specific open channel laminar flow environment (Yen, 2002).

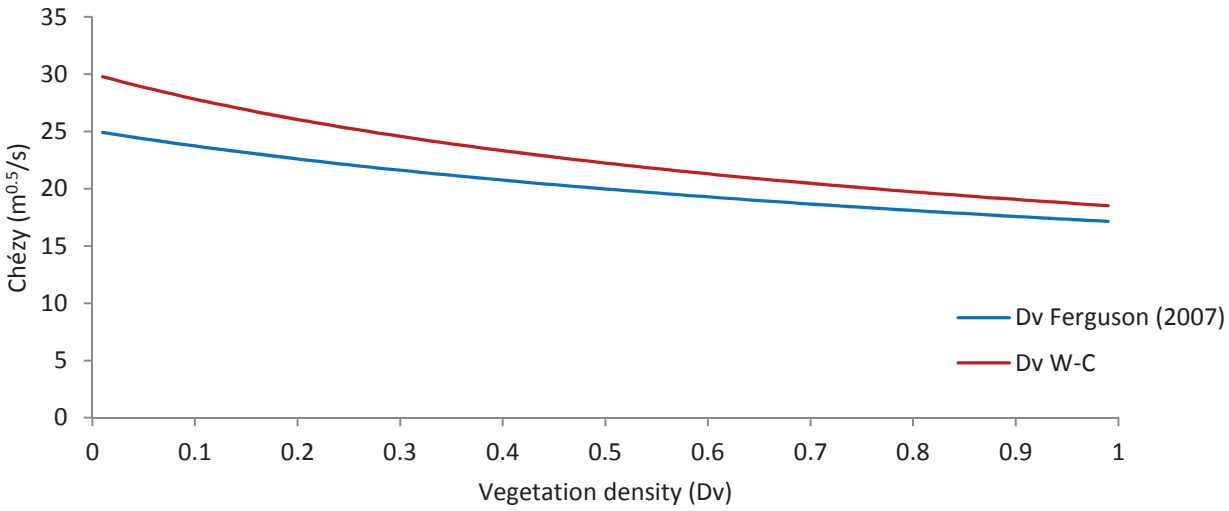

Figure 6.4.The Baptist et al. (2006) model output for the 4 mm inundated annular flume with a varying vegetation density. The red line is the conventional Baptist et al. (2006) model corrected with a laminar flow stem drag and White-Colebrook roughness expression. The blue line is the same Baptist et al. (2006) laminar flow corrected model, but with the Ferguson (2007) laminar flow roughness estimation.

6.3.3 Sediment trapping

In the annular flume the sediment trapping ability of alfalfa, related to the presence of overbank flow and suspended sediment transport, was investigated. Although the flume has proven to be able to create overbank morphology, with a fixed clay floodplain (Teske, 2011), substantial morphologic development was absent in the conducted experiments. This is due to several factors. The first is the limited morphologic development of the bed compared to the flume environment of Teske (2011). The absence of bed development results in a rapid decrease of suspended material availability in the channel and thus eliminates the transport of sediment to the floodplain and the formation of overbank morphology. The second limitation in the annular flume is the reduction of the floodplain directed flow. The sediment and vegetation on the flume floodplains greatly reduced the overbank flow velocities, compared to the Teske (2011) clay system. Although this flow reduction might be beneficial to the settling of fines it also reduced the flow in the circulation cells, thus limiting the supply of suspended sediment rich material. This is important, because the main sediment delivery mechanism in the flume, for floodplain formation, is advective transport (Adams et al., 2004) as opposed to turbulent diffusion. The development of overbank morphology in the annular flume indicates that in scale experiments the blocking and reduction of flow prevents the delivery of fines to the overbank area. This means the trapping effect is not found in the conducted scale experiments.

6.4 Biotic factor representation

The experimental vegetation did not experience soil and texture related growth stress. Furthermore seasonal variations were absent. The use of a constant discharge prevented hydrologic disturbance of vegetation without river morphologic change, this is unlike the natural system development described in the conceptual plot figure 2.16 (Stella et al., 2011). The remaining biotic factor (succession) and the scaling of the development time scale is presented in this sub-section.

6.4.1 Succession and rejuvenation

In natural environments succession plays an important role in riparian vegetation development. The selected vegetation dispersal regime of a single species in the flume experiments rendered the natural succession of vegetation absent in the experiment. However, when regarding the four stages in natural system succession (Naiman et al., 1998), there is a successional stage that is similar to the alfalfa development in flumes. In the second successional stage one species is dominant over all other ones and it is this species that displays growth over time. This closely resembles the development of alfalfa sprouts. In the first six days there is growth of one species and no flow in the flumes. After six days the vegetation no longer continues to grow. So it is similar to a stationary stage 2 real vegetation cover.

In all other experiments described in chapter 2.3 the alfalfa was regarded as a constant factor after the 6 day mark up to the point of withering (3 weeks). Furthermore the alfalfa had a constant effect on the bank strength and hydraulic roughness within the 3 week period (Gran and Paola, 2001, Tal and Paola, 2007, Braudrick et al., 2009). However, even though the experiments in the Eurotank and the annular flume were seeded with the same seeds, the resulting vegetation was different. This difference expressed itself in terms of, length, root size, composition, number of sprouted seeds and sprout shape. The most important difference between the two environments affected the flow dynamics in the experiments (chapter 6.5).

In the annular flume the 6-day day old vegetation cover reduced the flow velocities, due to the roots packed to the ground. After the 15 day mark the sprouts were standing straight and overbank flow velocities were measured. Furthermore the general flow patterns on the overbank areas differed between the young and old vegetation state. This means that, when describing it in terms of succession, the initial 10 day period is similar to a vegetation composition with a thick undergrowth, stage 3 (Naiman et al., 1998) whilst after the 10 day mark it resembles stage 2. So a reversed succession is potentially present in scale experiments. This means that opposite to the natural

development, in which a higher successional state indicates a more dense vegetation composition environment, the scaled succession is comparable to a succession step back. This is equivalent to a less dense vegetation composition (Naiman et al., 1998).
In the Eurotank this development was not found, because the sprouts were whitish and stood up straight from the period of initial seed development onward. This suggests that, although the properties of alfalfa can be expressed quantitatively, there is a wide variability in cover and the effects. This greatly reduces the comparability of conducted experiments for this report as well as to the available literature and natural systems.

6.4.2 Development time scale

The vegetation was introduced without active flow in the river. Therefore the timescale of vegetation development, in relation to that of the river, can be regarded as an instantaneous change. This is not scalable to natural system. When comparing this to for example the river Allier (Geerlings et al. 2006) the development of the river bends is a process on a century scale. The succession of pioneer vegetation to a mature state is roughly half this period in the range of 30-60 years.
In case of the Rhine delta the scaled experimental river covers a millennium worth of morphologic change (Van Dijk et al., 2012). So in general it can be stated that the scaling of the development time scale of vegetation, in relation to natural systems, is river specific. In case of an instantaneous and homogeneous seed distribution implementation of vegetation, there is no scaling to nature. However since the aim of the vegetation cover was to isolate the engineering effects in the already meandering system, it illustrates the essence of scale experiments rather than a poor representation of natural vegetation development.

6.4.3 Large wooded debris

In real river uprooted trees have the potential to fix bars (Gurnell and Petss, 2006) and trap sediment (Edwards et al., 1999). In scale experiments some of these properties could also be contributed to alfalfa, as presented in chapters 5.2.4 and 5.3.3. The alfalfa sprouts tended to orient themselves with the leaves in the downstream direction similar to natural system LWD (Edwards et al., 1999). Furthermore the local scouring behind the leafs (Perona et al., 2012) is also present as is the trapping of additional sprout debris. So based on the results it can be stated that uprooted alfalfa displays some aspects of LWD in real river. However the uprooted sprouts, unlike natural systems, did not dominate the formation of a local morphology. They only added a small scour in their lee that was superimposed on the local morphology. Unlike natural systems the debris was stationary, due to the constant discharge. Whereas in natural system discharge variation removes LWD from pointbars (Bendix and Hupp, 2000). The scale LWD remained stable once deposited, up to a shift in the local morphology. The shift led more focussed flow onto the LWD site thereby removing it from the bar. Since the LWD effects did not influence the river development it can be deemed as an insignificant effect in the scaled vegetation biotic factor representation.

6.5 Vegetation patterns

Although the homogeneous pattern does not represent a natural seed dispersal by either wind or flow (Gurnell and Petts, 2006), it allows the isolation of the effect of the river on the vegetation pattern. The low flow stage, whilst seeding, forced the vegetation to the higher flume areas. Without morphologic drivers able to manifest themselves, the high density annular flume cover, no vegetation patterns were formed. Over time both the flow in the Eurotank and the annular flume led to the development of patterns in the homogenous vegetation cover. The two morphological drivers were inner bend sedimentation (Bendix and Hupp, 2000) and outer bend erosion (Edwards et al., 1999). This focussed the formation of riparian vegetation around the bed development. Excess sedimentation led to local burial of vegetation. Burial removed vegetation from the system (Bendix and Hupp, 2000). It occurred in the inner bends and in the central bend during later stages of the bar formation that closed of the channel. It led to local changes in the riparian cover.

The larger riparian vegetation patterns consisted of the non-vegetated pointbar fronts (Bendix and Hupp, 2000, Stella et al., 2011) and the abandonment of channels (Stella et al., 2011). The non-vegetated pointbars were also found by Tal and Paola (2007). The cut-off bend in the experimental meandering river was not found in previous experiments. It is similar to the bend found in the field study of Stella et al. (2011) figure 2.22. The younger area (abandoned bend) was not covered with vegetation and was present in the older vegetation covered floodplain. In the downstream section the reworking of younger non-vegetated deposits left the pristine floodplain undisturbed and left curved vegetated margins. This is similar to an older terrace in a natural flume environment (Bendix and Hupp, 2000).
A pattern based comparison with the model study of Perucca et al. (2006), figure 5.18 D and figure 2.23a_2, shows that the same inner bend vegetation patterns is present. Unlike the model results of Perucca et al. 2006 the experimental pattern is not related to drought stress or flood disturbances.
So the development of these vegetation patterns in the flume illustrates that for these specific patterns succession and additional vegetation dispersal are not required. Furthermore river morphodynamics related erosion and sedimentation are dominant in experimental riparian pattern formation.
It can be summarized that the main contributors to experimental pattern formation are outer bend erosion and inner bend accumulation. These two processes create an floodplain directed shift of the vegetation cover on the outer bank margin and increases the distance between the inner bank vegetation margin and the channel. The resulting pattern consists of non-vegetated inner bend deposits next to the vegetation margin.

Experiment related vegetation pattern interference

In addition to the river related vegetation pattern development some processes affected the vegetation cover in the Eurotank facility. A factor that affected the cover was the partial inundation of the sprouts when running the flume. In the areas that were subjected to overbank flow the sand in the flume darkened and turned reddish brown. The timing of discoloration was 2 hours of flow time. The formation of a brown coloured overbank area was coupled to a deterioration of the alfalfa sprouts in those areas. Over a period of 5 days the vegetation cover disappeared in those regions. The areas, when not inundated, remained able to sustain re-seeded vegetation.
The Eurotank facility was lighted by standard office light. Due to the fixing of the lamps the flume was not uniformly lit. This expressed itself in the vegetation cover. In the areas where both TL-light and daylight were reaching the alfalfa the vegetation tended to be slightly taller and greener. In addition the vegetation in the better lit areas seemed to be more resilient to inundation.
Finally a species of white fungi manifested itself on the distal right side of the floodplain. It did not affect the vegetation cover or areas where flow was present. The aggressive *fusarium wilt* fungi, that was present in earlier experiments, was absent during the research conducted for this report.

6.6 Hierarchical control of the experimental meandering river development

The original Naiman et al. (1998) hierarchical control (figure 2.1) on riparian forest development was modified to illustrate the effects of riparian vegetation on the scale meandering river development (figure 6.5). The most important factor is indicated by the number one index:

1) The hydrologic regime (d) determines, together with the existing river planform (g), where riparian vegetation forms during seed dispersal (chapter 4.2.2). It also affects the rotting of vegetation by inundation of the overbank areas. In later stages the river dominates the formation of patterns in the vegetation cover (g) by erosion and sedimentation.
2) The riparian forest characteristics affect the geologic structure via bank strength (f) (chapter 6.3.1). They also determine the hydraulic resistance of the overbank area (d) (chapter 6.3.2). The hydraulic regime affects the magnitude of the bank strength effect (a).
3) The biotic factors determine the characteristics of the riparian cover in terms of condition, lifespan, rotting and root length (e) (chapter 6.4).
4) When regarding the overbank areas the role of the vegetation cover on the hydraulic resistance is difficult to quantify. It was found that the growth of the alfalfa sprouts (succession) has a potential effect on the overbank flow resistance (c) (chapter 6.3.2).

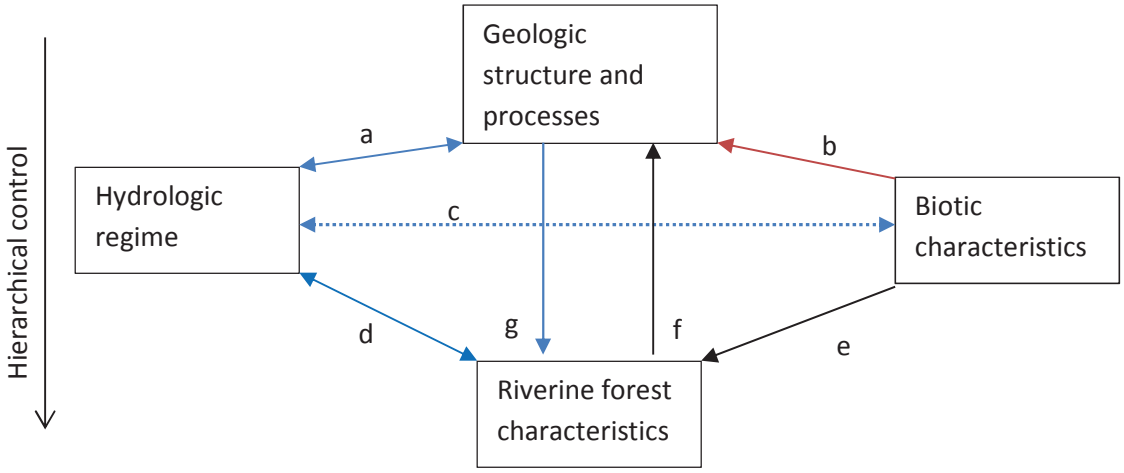

Figure 6.5 The Naiman et al. (1998) hierarchical control for the meandering river experiment. Black arrows are the same as in the original plot. Blue arrows are altered or new links and potential new links (dotted). Red arrows are original plot links that were not found in the scale experiments.

6.7 Further research recommendations

The above presented analysis of the experimental results indicates that the incorporation of scale vegetation, into morphological experiments, is coupled to growth related potential changes in the properties of vegetation. In order to accurately describe the added roughness of vegetation experiments without external interference to the vegetation cover and morphological feedback should be conducted. These experiments have to be compared to better laminar flow roughness equations. Furthermore the Chilworth roughness measurements indicate that the undisturbed flume produces a very rough flow environment. The lack of comparability to other natural vegetation environments illustrates the need for more natural vegetation composition measurements. Finally the unique controlled continuous bend flow properties of the annular flume and the applicability in relation to river morphological scale experiments indicates a future potential for research with this flume.

11. Conclusions

The conducted scale experiments illustrate details of the interactions between an alfalfa scale riparian vegetation cover and experimental meandering river dynamics. New insights in the engineering effects, biotic and abiotic factors of scale experiments in relation to real riparian vegetation environments were found. This chapter presents an overview of the main findings in relation to the main questions. The sub-questions focussed on the scale representation of several literature suggested effects of vegetation on a meandering river.

What is the added roughness of scale and real riparian vegetation on floodplain flow?
The hydraulic resistance of a natural vegetation cover with a litter layer along the base of the flume is in the low end of the Chézy range (2-5 $m^{0.5}/s$). In scale experiments the resistance of vegetation is difficult to quantify. Furthermore previously neglected effects, the state and age of the vegetation, play a dominant role in controlling the roughness of the overbank system. In a controlled annular flume flow environment the vegetation induced roughness is present and results in a Chézy value range decrease from 12-17 to 1-7 $m^{0.5}/s$.

What is the distribution of discharge over the floodplain and channel in a vegetated compared to a non-vegetated flood regime situation?
The effect of vegetation on the discharge division is an increase in the amount of discharge through the channel. The redistribution of discharge is observed as a general reduction in the wetted overbank flume area and concentration of the overbank flow into local depressions. The main mechanisms behind the vegetation induced discharge shift are added bank strength and an increased hydraulic resistance.

What is the effect of a riparian vegetation cover on a scale meandering river pattern?
The vegetation cover increases bank strength. It thereby reduces the lateral bend displacement and focusses the outer bend erosion. The focussed erosion creates more asymmetric, deeper and sharper bends as well as steeper outer bank channel sides. These changes increase the strength of the secondary current, which results in steeper and higher transverse bed slopes.

How does riparian vegetation affect the inner bend accretion and outer band erosion?
The scale vegetation slows down and focusses the outer bend erosion. This alters the accommodation space in the river bend and moves the inner bend scroll bars downstream of the apex. Furthermore vegetation changes the failure mechanism from entrainment to undercutting.

What is the role of the eroded outer bend vegetation on the channel?
Uprooted alfalfa sprouts are deposited on the pointbars downstream of the erosion sites. There, a local sheltering effect and small scours are found in their lee. In addition the trapping of other eroded sprouts by existing clusters is present, but no severe effects in relation to the overall river dynamics or morphology are present in scale experiments.

How does the, literature suggested, riparian vegetation sediment trapping effect influence the formation of overbank morphology?
In a controlled flume environment, designed to create overbank morphology, the vegetation severely limits bed sediment transport. This leads to a reduction in the amount of suspended fines. Together with a slower floodplain flow the supply of fine sediment to the overbank area is reduced. This limits overbank morphologic development. The trapping effects of riparian vegetation is insignificant in the conducted flume experiments.

What is the effect of a scale meandering river on riparian vegetation pattern development?
The main drivers of vegetation pattern development are erosion and sedimentation. Erosion on the outer bend side drives the existing riparian vegetation cover margin in the floodplain direction. The inner riparian vegetation cover margin is locally buried by excess sedimentation. Over time inner bend accretion moves the channel further away from the vegetation margin. After a cut-off occurs an abandoned non-vegetated channel is present in the vegetated floodplain.

It can be summarised that the most prominent effects of riparian vegetation on the meandering river development are the vegetation induced bank strength and hydraulic resistance. The dominant factor is the stabilization of the banks by vegetation. This leads to changes in the bend erosion that determine the overall system morphologic development. In addition the hydraulic resistance of the vegetated floodplain redistributes the discharge, which leads to a larger fraction of the flow in the channel. This knowledge could improve the implementation of vegetation in re-meandering and floodplain management projects.

8. Acknowledgements

I would like to thank my supervisor dr.M.G.Kleinhans for providing an abundance of ideas and the support in developing the annular flume experiments. My second supervisor W.M.Van Dijk MSc. for his input in the meandering river experiments and analysis of the data. Furthermore the Utrecht based experiments would not have been possible without the help of Anne Baar, Wietse van de Lageweg. KNAW assistant Eveline van der Deijl. The technical staff of the of the Physical Geography department: Chris Roosendaal, Henk Markies and Marcel van Maarseveen. The Experiments conducted in collaboration with the University of Southampton were made possible thanks to prof.dr.P.A.Carling, dr.J.Leyland and technician P.M.Morgan.

9. Summary

The vegetation along a meandering river system is known as riparian vegetation. The river and vegetation systems have been studied mostly separately by two different fields. The river flow mechanics and morphologic development related research has been conducted by engineers and earth scientists. The vegetation cover has been studied by ecologists and biologists. There is little overlap between both fields. In this report an attempt has been made to bridge a part of that gap. The main objective of this study is to determine the effects of riparian vegetation on meandering rivers

Meandering rivers are characterised by their sinuous shape that displays a dynamic development over time by the lateral movement of the bends in the system. Riparian vegetation (from the Latin *riparius* meaning to the river) is present along these meandering river margins. The effects of riparian vegetation on the river are known as engineering effects. Three different engineering effects are indicated. The reinforcement of the outer bank by the roots of the vegetation. An increased flow resistance due to vegetation on the higher parts of the pointbar and floodplain. The final engineering effect is the trapping of fine material on the overbank areas of the river.
A riparian vegetation cover is influenced by the river. The river aides in the dispersal of seeds and determines the availability of moisture and the suitability of the soil for vegetation growth. Together the interactions between the river and the riparian vegetation give rise to the formation of riparian vegetation patterns.

The recent development of scale experimental meandering rivers (Van Dijk et al., 2012) presents a powerful platform to investigate the river and vegetation interactions. In order to investigate the effect of riparian vegetation a self-formed scale meandering river was used where a homogeneous vegetation cover of alfalfa (*Medicago Sativa*) was added after the meandering river had formed. Detailed aspects of the meandering river and scale vegetation interactions were studied in a unique annular flume. This flume is capable of creating controlled and constant channel and overbank flows in a circular channel. This allowed the identification of the effects of vegetation on bank strength and the related erosion. Furthermore the inundation of the vegetation covered overbank areas allowed fluorescent tracer based velocity measurements. Finally a full scale outdoor flume, with a natural vegetation cover, served as a frame of reference to the scale experimental roughness values. Three different flume compositions were used: the non-disturbed vegetation cover with an intact litter layer, a tree trunk only flume with a removed litter layer and a cleared out flume.

In the meandering river experiment the incorporation of a homogeneous vegetation cover on the meandering river floodplains led to a reduced and focussed erosion of the outer bends. The bends developed into more asymmetrical and sharper bends as a result of the focused local undercutting of the outer bend. This led to an increase in the system sinuosity. The asymmetric development also led to inner band accumulation on the downstream end of the apex. Furthermore the outer bend became more steep and deepened. This resulted in a higher pointbar with a larger inner bend transverse bed slope. In addition the vegetation cover focussed the flow into the channel in the upstream part of the river.
The continued morphological development of the river led to the formation of riparian vegetation patterns. These patterns consisted of the floodplain directed retreat of the vegetation margin by erosion in the outer bends. On the inner bends new non-vegetated

pointbar deposits formed along the vegetation margin. Locally the burial of vegetation was found on the pointbars.
The same effects of vegetation were identified in the annular flume. With a light (1.5 seed/cm^2) vegetation cover density there was reduction in outer bend erosion. This led to a steeper and more deep outer bend. The channel development consisted of the formation of inner bend bar accumulations. This meant the same vegetation pattern development was found in the flume. The addition of fine suspended sediment to the flume did not yield substantial overbank morphologic development. The vegetation covered floodplains limited the flow velocities on the overbank areas. Furthermore they caused a blocking effect to the floodplain directed flow. The lower overbank velocities in the annular flume translated to higher roughness values for the vegetation covered runs.
In the full scale vegetation flume it was found that the litter layer, consisting of leaves and shrubs, was to a large extent responsible for the system's hydraulic resistance. The removal of the litter layer increased the Chézy coefficient values.

Based on the scale experimental results it can be concluded that the introduction of riparian vegetation affected the river by engineering effects. The most prominent was the reduced lateral erosion by the addition of bank strength in the scale experiments. The controlled annular flume experiment overbank velocity measurements indicated a quantitative increase in the roughness due to vegetation. An approximate quantitative scaling between the scale experimental values and those of the full scale flume was found.

The experimental results indicate that a better understanding of riparian vegetation and meandering river interactions could make a more efficient use of the bank strength effects of natural riparian vegetation in for example re-meandering projects. In addition the full scale natural vegetation roughness measurements, with a litter layer, indicated that the contribution of the litter layer is significant on the overall roughness of the system. This has a potentially large influence on flood routing in river systems.

10. List of symbols

A_r/A = *shear surface area occupied by roots*
c_r = soil strength term (kPa)
c' = effective cohesion (kPa)
C = Chézy coefficient for hydraulic resistance ($m^{0.5}/s$)
C_b = bed roughness ($m^{0.5}/s$)
C_d = stem drag coefficient
C_f = dimensionless friction factor
d_r = root diameter (m)
D = diameter of cylinder (m)
D_{50} = median grain size (m)
D_{84} =16^{th} percentile of the coarsest sediment (m)
D_{90} = 10^{th} percentile of the coaesest sediment (m)
D_f = dispersive properties of river reach
f = Darcy-Weisbach friction factor
F_p = pullout force (kPa)
g = gravitational acceleration, 9.81 m^2/s
h = average water depth (m)
h_v = vegetation height (m)
IP = interaction parameter
k = von Karman constant (0.4)
k_s = Nikuradse coefficient (m)
L = Length of measurement section (m)
L_r = root length (m)
m = number of cylinders per m^2
q = discharge (m^2/s)
r = radius of river bend (m)
R = hydraulic radius (m)
Re = Reynolds number
S = slope (m/m)
t = reach mean travel time
T = ADZ residence time
T_r = tensile strength of roots (kPa)
u = average flow velocity (m/s)
u_c = flow through submerged vegetation zone (m/s)
u_u = velocity above submerged vegetation (m/s)
u_{cb} = flow through non-submerged vegetation zone (m/s)
u_* = shear velocity (m/s)
U_m = momentum based velocity
w = average river width (m)
W = weight of the failure block (kPa)
y_p = horizontal pointbar length (m)
z_p = vertical pointbar height (m),
z = height above bed (m)
z_0 = roughness height (m)

α = coefficient
β = angle of the failure plain (°)
θ = non-dimensional shear stress
θ_d = shear distortion from vertical (°)
θ_s = ANGLE of WAT (°)
κ = Von Karman constant, 0.4
λ_w = adaptation length of water (m)
λ_s = adaptation length of sediment (m)
μ_w = pore water pressure (kPa)
ρ =density of water, 1000 kg/m^3
ρ_s =density of sediment, 2650 kg/m^3
τ' = tangential stress (kPa)

τ_b = bed shear stress (N/m)
τ_d = second concentration peak arrival time
τ_f = shear stress at failure (kPa)
τ_t = total shear stress (N/m)
τ_u = first concentration peak arrival time
τ_v = vegetation shear stress (N/m)
ρ = density of fresh water 1000 kg/m^3
ρ_s = density of sediment 2650 kg/m^3
σ = normal stress (kPa)
ϕ' =angle of internal friction (°)

11. References

Abernethy, B., Rutherford, I.D., 2001, The distribution and strength of riparian tree roots in relation to riverbank reinforcement.
Hydrological processes, Vol.15, p.63-79

Adams, P.N., Slingerland, R.L., Smith., N.D., 2004, Variations in natural levee morphology in anastomosed channel floodplain complexes.
Geomorphology, Vol.61, p.127-142

Armanini, A., Righetti, M., Grisenti, P., 2005, Direct measurements of vegetation resistance in prototype scale.
Journal of hydraulic research, Vol43, no.5, p.481-487

Baptist, M.J., 2003, A flume experiment on sediment transport with flexible submerged vegetation.
International workshop on RIParian FORest vegetated channels: hydrolic, morphological and ecological aspects

Baptist, M.J., Babovic, V., Rodríguez Uthurburu, J., Keijzer, M., Uittenbogaard, R.E., Mynett, A., Verwey, A., 2006, On inducing equations for vegetation resistance.
Journal of hydraulic research, Vol.0, No. 0, p.1-16

Bertoldi, W., Drake N.A., Gurnell, A.M., 2011, Interactions between river flows and colonizing vegetation on a braided river: exploring spatial and temporal dynamics in riparian vegetation cover using satellite data.
Earth surfaces processes and landforms

Bendix, J., Hupp, C.R., 2000, Hydrological and geomorphological impacts on riparian plant communities.
Hydrological processes, Vol. 14, p.2977-2990

Berendsen en Stouthamer, 2001, Paleaogeographic development of the Rhine-Meuse delta, the Netherlands
Van Gorcum Assen 2001

Blanckaert, K., de Graf, W.H., 2001, Mean flow and turbulence in open-channel bend.
Journal of hydraulic engineering, October

Blanckaert, K., de Vriend, H.J., 2003, nonlinear modelling of mean flow redistribution in curved open channels.
Water resources research, Vol.39, No. 12

Blankaert, K., 2010, Topographic steering, flow recirculation, velocity redistribution and bed topography in sharp meander bends.
Water resources research, Vol. 46

Blanckeart, K., Duart, A., Schleiss, A.J., 2010, Influence of shallowness, bank inclination and bank roughness on the variability of flow patterns and boundary shear stress due to secondary currents in straight open channels.
Advances in water resourches, Vol. 33, p. 1062-1074.

Bornette, G., Tabacchi, E., Hupp, C., Puijalon, S., Rostan, J.C., 2008, A model of plant strategies in fluvial hydrosystems.
Freshwater biology, Vol.53, p.1692-1705

Brierly, G.J., Ferguson,R.J., Woolfe, K.J., 1997, What is a fluvial levee?
Sedimentary Geology, Vol. 114, p.1-9

Cazanalcli,D., Smith, N.D., 1998, A study of morphology and texture of natural levees – Cumberland Marshes, Saskatchewan, Canada.
Geomorphology, Vol.25, p.43-55

Crosato A., 2007, Effects of smoothing and regridding in numerical meander migration models.
Water resourches research, Vol. 43

Crosato, A.,Mosselman, E., 2009, Simple physics-based predictor for the number of river bars and the transition between meandering and braiding.
Water resources research, Vol.45

Eaton, B.C., Millar, R.G., 2004, Optimal alluvial channel width under a bank stability constraint.
Geomorphology, Vol.62, p.35-45

Eaton, B.C., Giles, T., R., 2009, Assessing the effect of vegetation-related bank strength on channel morphology and stability in gravel-bed streams using numerical models.
Earth surfaces and landforms, Vol. 34, p.712-724

Edwards, P.J., Kollmann, J., Gurnell, A.M., Petts, G.E., Tockner, K., Wards, J.V., 1999, A conceptual model of vegetation dynamics on gravel bars of a large Alpine river..
Wetlands ecology and management, Vol. 7, p.141-143

Ferguson, R.I., Parsons, D.R., Lane, S,N., Hardy, J.H., 2003, Flow in meander bends with recirculation at the inner bank.
Water resources research, Vol.39, No.11

Ferguson,R., 2007,Flow resistance equations for gravel- and boulder-bed streams.
Water resources research, Vol.43

Geerling, G.W., Ragas, A.M.J, Leuven, R.S.E.W., van den Berg, J.H., Breedveld, M., Liefhebber, D., Smits, A.J.M., 2006, Succession and rejuvenation in floodplains along the river Allier (France)
Hydrobiologia, p. 71-86

Geerling, G.W, Kater, E., van den Brink, C., Baptist, M.J., Ragas, A.M.J, Smits, A.J.M., 2008, Nature rehabilitation by floodplain excavation: The hydraulic effect of 16 years of sedimentation and vegetation succession along the Waal River, NL.
Geomorphology, Vol.99, p.317-328

Gran, K., Paola, C., 2001, Riparian vegetation controls on braided stream dynamics.
Water resources research, Vol.37, No.12, p3275-3283

Gurnell, A.M., Gregory,K.J., 1994, Interactions between semi-natural vegetation and hydrogeomorphological processes.
Geomorphology, Vol.13, p.49-69

Gurnell, A.M., Petts, G. E.., 2002, Island-dominated landscapes of large floodplain rivers, a European perspective.
Freshwater Biology, Vol.47, p.581-600

Gurnell, A.M., Petts, G. E.., 2006, Trees as riparian engineers: The Tagliamento river, Italy.
Earth surfaces processes and Landforms, Vol. 31, p. 1558-1574

Hooke, J.M., 1984, Changes in river meanders a review of techniques and results of analyses
Progress in physical geography, Vol. 8, p.473-508

Hupp, C.R., 2000, Hydrology, geomorphology and vegetation of Coastal Plain rivers in the south-eastern USA.
Hydrological processes, Vol.14, p.2991-3010

Hupp, C.R., Osterkamp, W.R., 1985, Bottomland vegetation distribution along Passage creek, Virginia, in relation to fluvial landforms.
Ecology, Vol. 66, p.670-681

Hupp, C.R., Rinaldi, M., 2007, Riparian vegetation in relation to fluvial landforms and channel evolution along selected rivers of Tuscany (central Italy).
Annals of the association of American geographers, Vol.97, No.1, p.12-30

Jahra, F., Yamamoto, H., Hasegawa, F., Kawahara, Y., 2010, Flow-vegetation interaction in a compound channel with localized emergent vegetation.
Proceedings of the 13th Asian congress of fluid mechanics, 17-21 December 2010,Dhaka, Bangladesh

Järvelä, J., 2003, Flow resistance of flexible and stiff vegetation: a flume study with natural plants.
Journal of Hydrology, Vol. 269, p.44-54

Kleinhans, M.G., 2010, Sorting out river patterns.
Progress in physical geography, Vol.34, No.3, p287-326

Kleinhans, M.G., van den Berg, J.R., 2010, River channel and bar patterns explained and predicted by an empirical and a physics-based method.
Earth surface processes and landforms,

Kleinhans, M.G., van Dijk, W.M., van de Lageweg, W.I., Hoendervoogt, R., Markies, H., Schuurman, F., 2010, From nature to lab: scaling self-formed meandering and braided rivers.
Bundesanstalt für Wasserbau

Knight, D.W., Brown, F.A., 2001, Resistance studies of overbank flow in rivers with sediment using the flood channel facility.
Journal of hydraulic research, Vol. 39, No.3

Leopold, L.B., Wolman, M.G., 1957, Braiden, Meandering and Straight.
Geological survey professional paper 282-B.

Mcbride, M., Hession, W.C., Rizzo, D.M., Thompson, D.M., 2007, The influence of riparian vegetation on near-bank turbulence: a flume experiment.
Earth surface processes and landforms, Vol.32, p.2019-2037

Micheli, E.R., Kirchner, J.W., 2002, Effects of wet meadow riparian vegetation on streambank erosion.2.Measurements of vegetated bank strength and consequences for failure mechanics.
Earth surface processes and landforms, Vol.27, p. 687-697

Millar, R.G., 2000, Influence of bank vegetation on alluvial channel patterns.
Water resources research, Vol. 36, No.4, p1109-1118

Naiman, R.J., Fetherson, K.L., McKay, S.J., Chen, J., 1998, Riparian forests.
River ecology and Management

Nanson, G.C., Beach, H.F., 1977, Forest succession and sedimentation on a meandering river floodplain, northeast British Columbia, Canada.
Journal of Biogeography, Vol.4, p.229-251

Nanson, R.A., Flow fields in tightly curving meander bends of low width-depth ratio.
Earth surface processes and landforms, Vol.35, p.119-135.

Osterkamp, W.R., Hupp, C.R., 2010, Fluvial processes and vegetation- Glimpses of the past, the present and perhaps the future.
Geomorphology, Vol.116, p.274-285

Peakall, J., Ashworth ,P.J., Best, J.L., 2007, Meander-bend evolution, alluvial architecture , and the role of cohesion in sinuous river channels: a flume study.
Journal of sedimentary research, Vol.77,

Perona, P., Molnar, P., Couzy, B., Perucca, E., Jiang, Z., Mclelland, S., Würtrich, K., Edemaier, K., Francis, R., Camporeale, C., Gurnell, A., 2012, Biomass selection by floods and related timescales: Part 1. Experimental observations.
Advances in Water resources, Vol. 39, p.85-96

Perrucca, E., Camporeale, C., Ridolfi., L., 2006, Influence of river meandering dynamics on riparian vegetation pattern formation.
Journal of geophysical research, Vol.111

Perrucca, E., Camporeale, C., Ridolfi., L., 2007, Significance of the riparian vegetation dynamics on meandering river morphodynamics.
Water resources research, Vol.34

Pollen, N., Simon, A., 2005, Estimating the mechanical effects of riparian vegetation on stream bank stability using a fiber bundle model.
Water resources research, Vol.41

Pollen-Bankhead, N., Simon, A., 2009, Enhanced application of root reinforcement algorithms for bank-stability modelling.
Earth surface processes, Vol.34, p.470-480

Richardson, K., Carling, P.A., 2006, The hydraulics of a straight bedrock channel: Insights from solute dispersion studies.
Geomorphology, Vol.82, p.98-125

Shiono, K., Muto, Y., Knight, D.W., Hyde., A.F.l., 1998, Energy losses due to secondary flow and turbulence in meandering channels with overbank flow.
Journal of hydraulic research, Vol.37, No.5, p.641-664

Simon, A., Collison,J.C., 2001, Quantifying the mechanical and hydrologic effects of riparian vegetation on streambank stability.
Earth surface processes and landforms, Vol.27, p.527-546

Stella, J.C., Hayden, M.K., Battles, J.J., Piégay, H., Dufour, S., Fremier, A.K., 2011, The role of abandoned channels as refugia for sustaining pioneer riparian forest ecosystems.
Ecosystems

Stephen, U., Gutknecht, D., 2002, Hydraulic resistance of submerged flexible vegetation.
Journal of Hydrology, Vol. 269, p.27-43

Struiksman,N., Olesen, K.W., Flokstra, C., de Vriend, H.J., 1985, Bed deformation in curved alluvial channels.
Journal of Hydraulic research, Vol.23, No.1, p.57-79

Sumner, E.J., Amy, L.A., Talling, P.J, 2008. Deposit structure and processes of sand deposition from decelerating sediment suspensions.
Journal of sedimentary research, Vol. 78, p. 529-547

Tal, M., Gran, K., Murray, A.B, Paola, C., Hicks, D.M., 2003, Riparian vegetation as a primary control on channel characteristics in multi-thread rivers.
Water science and application,

Tal, M., Paola, C., 2007, Dynamic single thread channels maintained by the interaction of flow and vegetation.
Geology, vol.35, No.4, p. 347-350

Tal, M., Paola, C., 2010, Effects of vegetation on channel morphodynamics; results and insights from laboratory experiments.
Earth surface processes and landforms, Vol.35, p1014-1028

Talmon, A.M., Struiksma, N., Van Mierlo, M.C.L.M., 1995, Laboratory measurement's of the direction of sediment transport on transverse alluvial-bed slopes.
Journal of hydraulic research, Vol.33, No.4, p495-517

Teske, R., 2011, Channel- and overbank morphodynamics in an annular flume.
Bachelor thesis Earth sciences Utrecht University

Thiéry, J.M., D'Herbès, J.-M., Valentin, C., 1995, A model simulating the genesis of banded vegetation patterns in Niger.
Journal of Ecology, Vol.83, p.497-507

Townsend, P.A., 2001, Relationships between vegetation patterns and hydroperiod on the Roanoke river floodplain North California.
Plant Ecology, Vol.156, p.43-58

Van Breemen, D., 2011, Interactions between channel pattern, cohesive bank strength hand riparian vegetation.
MSc-thesis Utrecht University

Van Dijk, W.M., van de Lageweg, W.I., Hoendervoogt, R., Kleinhans, M.G., 2010, Incipient meandering and self-formed floodplains in experimens.
Bundestalt für Wasserbau

Van Dijk, W.M., van de Lageweg, W.I., Hoendervoogt, R., Kleinhans, M.G., 2012, Experimental meandering river with chute cutoffs.
Jounal of geophysical research

Van de Lageweg, W.I., 2009, The effect of riparian vegetation on channel pattern.
MSc.-thesis Utrecht University

Van de Lageweg, W.I., van Dijk, W.M., Hoendervoogt, R., Kleinhans, M.G., 2010, Effects of riparian vegetation on experimental channel patterns.
Bundesanstalt für Wasserbau

Van der Nat, D., Trockner, K., Edwards, P.J., Ward, J.V., Gurnell, A.M., 2003, Habitat change in braided floodplains (Tagliamento, NE-Italy).
Freshwater biology, Vol.48, p.1799-1812

Yen, B.C., 2002, Open channel flow resistance.
Journal of Hydraulic engineering January 2002